Claudia Hagedorn

Functional analyses of the human osteoprotegerin gene promoter

-2009-

Biologie

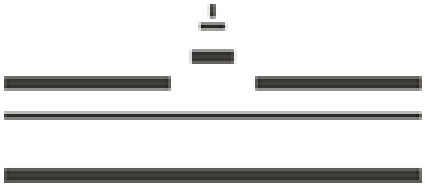

Functional analyses of the human osteoprotegerin gene promoter

Funktionelle Analysen des humanen Osteoprotegerin Genpromotors

Inaugural-Dissertation
zur Erlangung des Doktorgrades
der Naturwissenschaften im Fachbereich Biologie
der Mathematisch-Naturwissenschaftlichen Fakultät
der Westfälischen Wilhelms-Universität Münster

vorgelegt von
Claudia Hagedorn
aus Mühlhausen

2009

Dekan:	Prof. Dr. Christian Klämbt
Erster Gutachter:	Prof. Dr. Bruno Moerschbacher
Zweiter Gutachter:	Prof. Dr. Dr. med. Stefan-Martin Brand-Herrmann
Tag der mündlichen Prüfung:	08.04.2009
Tag der Promotion:	24.04.2009

Und wenn du auch die Kraft hast, einen Berg zu versetzen, so brauchst du noch einen Verstand, der so groß und so ruhig ist wie ein Ozean.

chinesisches Sprichwort

Für meine Eltern

Abbreviations

Acc#	Accession number
AS	Antisense
CAD	Coronary Artery Disease
ChIP	Chromatin Immunoprecipitation
CVD	Cardiovascular Disease
DPE	Downstream Promoter Element
ds	double stranded
ECTIM	Etude CAS-Témoins de l'infarctus du Myocarde
e.g.	for example
Egr1	Early Growth Response 1
EMSA	Electrophoretic Mobility Shift Assay
ERα	Estrogen Receptor α
ERβ	Estrogen Receptor β
GWA	Genome Wide Association Studies
HapMap	Haplotype Map
HEK293T	Human Embryonic Kidney Cells
HPLC	High Pressure Liquid Chromatography
Inr	Initiator Element
LDL	Low Density Lipoprotein
M-CSF	Macrophage Colony-Stimulating Factor
MI	Myocardial Infarction
MolHap	Molecular Haplotype
MolProMD	Münster Molecular Functional Profiling for Mechanism Detection
MONICA	MONitoring Trends and determinants in Cardiovascular disease
NF-1	Nuclear Factor 1
NFκB	Nuclear Factor of κB
NGFN	National Genome Research Network
n.s.	not significant
OD	Optical Density
OPG	Osteoprotegerin
OPG	Osteoprotegerin gene
ox-LDL	oxidized LDL
RANK	Receptor Activator of NFκB
RANKL	Receptor Activator of NFκB Ligand
RP27	Ribosomal Protein 27
RT	Room Temperature
SaOs-2	Osteoblast-like osteosarcoma cell line
SMC	Smooth Muscle Cell
SNP	Single Nucleotide Polymorphism
Sp1	Specificity protein 1
ss	single stranded
SS	Supersense
TBP	TATA-box Binding Protein
TF	Transcription Factor
TFBS	Transcription Factor Binding Site
TNFα	Tumor Necrosis factor α
TNFR	Tumor Necrosis Factor Receptor
TNFRSF	TNFR Superfamily
TSS	Transcription Start Site
U2Os	Human bone osteosarcoma epithelial cell line
VSMC	Vascular Smooth Muscle Cells
WHO	Worlds Health Organization
wt	wild type

Abstract

The clinical progression of atherosclerotic diseases is influenced by environmental and lifestyle factors, and strongly determined by individual genetic predispositions. Osteoprotegerin (OPG) has been reported to be involved in the development of atherosclerotic disease phenotypes, but less is known about its promoter architecture and transcriptional regulation.

Within this study, 1008 bp of the *OPG* 5'-flanking region were identified to be sufficiently active in osteosarcoma cell line SaOs-2 and U2OS. This portion was therefore further analyzed for cell type-specific transcription start sites (TSS). One novel TSS was identified 225 bp upstream the ATG codon, and position of another TSS was corrected in SaOs-2 and U2Os. Sequencing of 1008 bp of the *OPG* promoter portion in 57 patients with cardiovascular disease (CVD) led to the identification of five variants (T-960C, A-946G, G-900A, T-864G, and T-159C). Individual subcloning revealed the existence of three common molecular haplotypes (MolHaps): [T^{-960}-A^{-946}-G^{-900}-T^{-864}; wild type (wt)], [T^{-960}-G^{-946}-G^{-900}-T^{-864}; MolHap2], [C^{-960}-G^{-946}-A^{-900}-G^{-864}; MolHap4], which were analyzed by transient transfection in SaOs-2 and U2Os. The *OPG* full length construct (1008 bp) displayed a moderate transcriptional activity, whereas activities of MolHaps 2 and 4 were significantly reduced (p = 0.0018). Introduction of the -159C allele reduced transcriptional activities of the respective full length constructs (p = 0.0014). To identify *cis*-regulatory regions, serial deletion constructs were generated. Truncation of 84 bp (-1020/-936) resulted in a complete abrogation of transcriptional activity in both cell lines, indicating a *cis*-regulatory region within being essential for transcriptional activity of the *OPG* gene promoter. Introduction of the -159C allele significantly increased activities of the deletion constructs in both cell lines (p = 0.0005). EMSAs and co-transfections revealed specific DNA:protein interactions for the MolHaps with Sp1, NF-1/A1.1, and NF-1/B2. EMSA competition assays and ChIP experiments identified Egr1 interacting exclusively with the -159T allele. Results propose new structural features, the existence of genetically differential functional portions within the *OPG* promoter region, and a transcriptional module composing of Sp1, NF-1, and Egr1 is suggested to be involved in *OPG* gene regulation.

1. Introduction

1.1. Cardiovascular Disease (CVD)

Globally, cardiovascular disease is the leading cause of death for men and women. An estimated 17.5 million people died from cardiovascular disease in 2005, representing 30% of all global human deaths. Of these, 7.6 million were due to heart attacks and 5.7 million to stroke. If current trends continue, by 2015 an estimated 20 million people will die from CVD annually [WHO]. CVD include coronary heart disease (CHD), cerebrovascular disease, hypertension, peripheral artery disease, rheumatic heart disease, congenital heart disease, and heart failure.

1.1.1. Arteriosclerosis

Arteriosclerosis (the pathophysiological basis of CVD) is a systemic proliferative and inflammatory disease of the arterial wall, with particularly noticeable manifestations in the medium and large arteries. It represents a multifactorial disease and is influenced by a variety of genetic, as well as environmental factors, such as hypertension, smoking, diabetes mellitus, vascular injury, etc. Predominantly, it is a clinically silent process, whose acute clinical outcome may be caused by rupture of a single plaque. Artherosclerotic plaques/ lesions (atheromata) are asymmetric thickenings of the innermost layer of the artery, the intima. The earliest lesion in atherogenesis is the fatty streak, an accumulation of lipid-laden macrophages (foam cells). These lesions progress into complex lesions, containing an accumulation of lipids and necrotic cells (Figure 1). Arteriosclerosis describes any hardening or loss of elasticity of medium or larger arteries, while atherosclerosis describes hardening of arteries specifically due to an atheromatous plaque. Therefore, atherosclerosis constitutes a form of arteriosclerosis.

1.1.2. Pathophysiology of Atherosclerosis

Infiltration and retention of low density lipoprotein (LDL), and its modification through oxidation (ox-LDL) or enzymatic attack in the arterial intima initiates an inflammatory response in the artery wall, causing an increased expression of leukocyte adhesion molecules [Skålen et al, 2002; Dai et al, 2004]. The monocyte is the first blood cell to arrive at the scene of endothelial activation [Massberg et al, 2002]. Once attached, chemokines (e.g. macrophage colony-stimulation factor) produced in the underlying intima, stimulate them to migrate through the endothelial junctions into the subendothelial space. Entering the arterial wall and up-take of ox-LDL induces monocytes to differentiate into macrophages.

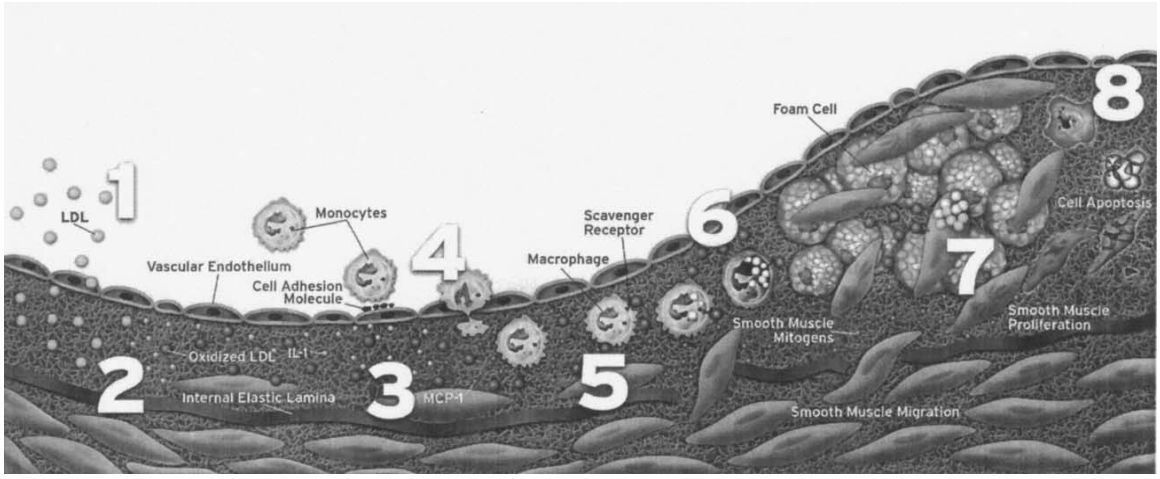

Figure 1 Progression of atherosclerosis over time. (1) Lipoprotein particles, and especially low-density lipoprotein (LDL), enter the arterial wall and undergo modification, including oxidation. (2) These oxidized lipoproteins can incite a cascade of cellular responses that include production of inflammatory mediators such as cytokines. (3) One integral early step in the atherosclerotic process is the expression of adhesion molecules on endothelial cells. (4) Through adhesion molecules, leukocytes attach and ultimately enter the arterial wall, attracted to these sites by chemoattractant cytokines, known as chemokines. (5) Monocytes in the vessel wall take up oxidized lipoproteins, inducing their differentiation into lipid-laden foam cells. (6 and 7) Vascular smooth muscle cells (VSMCs) in the wall respond to many of these as well as other stimuli, with some VSMCs migrating out of the media and into the intima. In the intima and the media, VSMCs also proliferate and elaborate extracellular matrix that contributes to the formation of the early atherosclerotic lesions as well as the fibrous cap seen in later stages of atherosclerosis. (8) Later stages of atherosclerosis involve more complicated plaques [Plutzky, 2003].

This step is critical for the development of atherosclerosis [Smith et al, 1995], and is associated with up-regulation of pattern-recognition receptors, including scavenger receptors. These receptors facilitate the internalization of a broad range of molecules and particles presenting pathogen-like molecular patterns, including ox-LDL [Peiser et al, 2002]. Internalized ox-LDL cannot be mobilized from the cell to a sufficient extend and accumulates in cytosolic droplets. Thus, by harvesting ox-LDL the macrophage transforms into a lipid-laden foam cell, the prototypical cell in atherosclerosis. Immune cells, including T-cells, monocytes and macrophages, patrol various tissues in search of target antigens. A T-cell infiltration is always present in atherosclerotic lesions. Infiltrating T-cells, predominantly CD4+ T-cells, recognize antigens presented as fragments bound to major-histocompatibility-complex (MHC) class II molecules. In human lesions, CD4+ T-cells reactive to ox-LDL were found [Stemme et al, 1995]. Binding of the T-cell antigen receptor to

an antigen, elicited an activation cascade that results in expression of various cytokines, promoting a Th1 response [Frostegård et al, 1999]. Activated T-cells differentiate into Th1 effector cells and produce the macrophage-activating cytokine interferon-γ (INF-γ), which in turn increases the efficiency of antigen presentation and increases expression of tumor necrosis factor-α (TNFα) and interleukin-1 [Hansson, 2001]. Acting synergistically, these cytokines stimulate the production of a series of pro-inflammatory and cytotoxic molecules in macrophages and vascular cells [Szabo et al, 2003]. The process results in proliferation and migration of smooth muscle cells (SMC), which elaborate connective tissue within the inflamed intima and produce the advanced lesions of atherosclerosis [Ross, 1995]. In an advanced atheroma, foam cells and extracellular lipid droplets form the core region, which is surrounded by a cap of SMC and collagen rich matrix [Hansson, 2001]. Within SMC adjacent to atheromata intracellular microcalcifications may form, and lead to extracellular calcium deposits between the muscular wall and the outer portion of the atheromata (intimal calcification). In contrast to intimal calcification, medial calcification occurs in the absence of inflammatory cell infiltration and lipid deposition, but both processes are linked to arterial stiffness [Mackey et al, 2007].

1.1.3. Cardiovascular calcification

The elasticity of the large artery walls plays an important role in hemodynamics. They increase their diameter during systole and decrease during diastole. This “Windkessel effect” lessens blood pressure during systole and facilitates blood flow during diastole. When the elasticity of the large arteries decreases, the systolic pressure, normally diminished by the “Windkessel effect”, is increased and may result in hypertension professing endorgan damage such as renal insufficiency, stroke, and other atherosclerosis related diseases. Stiffening of the arterial walls increases with age and/or by vascular calcification. Most individuals >60 years of age display enlarged deposits of calcium in their major arteries [Allison et al, 2004], leading to reduced arterial elasticity. Cardiovascular calcification is a strong indicator for inflammatory disease, usually atherosclerosis, and its extend is directly related to the overall burden of atherosclerosis [Rumberger et al, 1995].

For most of the 20th century, vascular calcification has been regarded as a passive, unregulated, degenerative process occurring within advanced atherosclerotic plaques. The concept of regulated ossification as the mechanism responsible for vascular calcification emerged in the past decade. The first evidence for regulation of vascular calcification was brought by Tanimura et al, who found structures involved in osteogenesis in human calcified aortas [Tanimura et al, 1983]. Giachelli et al examined vascular calcification at the molecular level, showing expression of a bone matrix protein in vascular smooth muscle cells (VSMC)

[Giachelli et al, 1991]. Primary VSMCs express bone matrix proteins when treated with β-glycerophosphate (which serves as a phosphate donor), in the presence of alkaline phosphatase *in vitro* [Shioi et al, 1995]. As VSMC undergo osteogenic differentiation, they lose expression of smooth muscle cell markers, indicating a de-differentiation process [Steitz et al, 2001]. Approximately 15% of carotid atherosclerotic plaque specimens and calcified valve tissues display ossification [Hunt et al, 2002; Mohler et al, 2001]. Calcium phosphate (hydroxyapatite, $Ca_3[\text{-}PO_4]_2\text{-}xCa[OH]_2$), which contains 40% calcium by weight, precipitates in diseased coronary arteries by a mechanism similar to that found in active bone formation and remodeling. Bone formation is characterized by tightly regulated osteoblast production of an extracellular matrix (osteoid) that is the substrate for passive crystallization, leading to hydroxyapatite formation. Bone formation actually fixes circulating calcium in its mineral form, removing it from the bloodstream. Conversely, resorption actively unfixes it, thereby increasing circulating calcium levels. In bone, mineral is resorbed by osteoclasts, which derive from the monocytic line of hematopoetic cells. Macrophages exposed to particulate calcium mineral have been reported to undergo osteoclastic differentiation [Merkel et al, 1999]. Thus, atherosclerotic plaques, by being rich in monocytes and macrophages, are an abundant source of preosteoclasts. Maturation of preosteoclasts (e.g. peripheral blood mononuclear cells) to osteoclasts is mainly directed by two cytokines: monocyte colony-stimulating factor (M-CSF) and the ligand for receptor activator of NF-κB (RANKL). Many key regulators of bone formation and bone structural proteins are also expressed in atherosclerotic plaques, including bone morphogenetic protein-2 (BMP-2) [Bostrom et al,1993], osteopontin (OPN) [Giachelli et al, 1993; Ikeda et al, 1993], matrix Gla protein (MGP) [Shanahan et al, 1994], and osteoprotegerin (OPG) [Dhore et al, 2001].

1.2. Osteoprotegerin (OPG) as a candidate for calcification risk

1.2.1. TNF receptor superfamily (TNFRSF)

The tumor necrosis factor (TNF) superfamily is a group of cytokines with important functions in immunity, inflammation, differentiation, control of cell proliferation, and apoptosis. With TNFα as founding member, their biological effects are exerted through members of the TNF receptor superfamily (TNFRSF). This superfamily includes both membrane-bound and soluble receptors. The mammalian TNFR family members are type I membrane proteins and characterized by the presence of cysteine-rich domains (CRD), which are the hallmark of the family (Figure 2). CRD pseudo-repeats are characterized by intra-chain disulphids generated by highly conserved cysteine residues within the receptor chains [Smith et al, 1994]. In general, each receptor contains varying numbers of CRD, from B-cell activating factor receptor (BAFFR) with only a partial CRD, to TNFR I and TNFR II with the most common

structure of 3 CRD, and up to 6 CRD found in CD30. Upon receptor stimulation, some members of the TNFRSF are cleaved from the cell surface (e.g. TNFR II), while others are directly expressed as soluble forms lacking the transmembrane domain (e.g. OPG). In general, receptor activation by TNF family members causes recruitment of several intracellular adaptor proteins, which activate several signaling pathways.

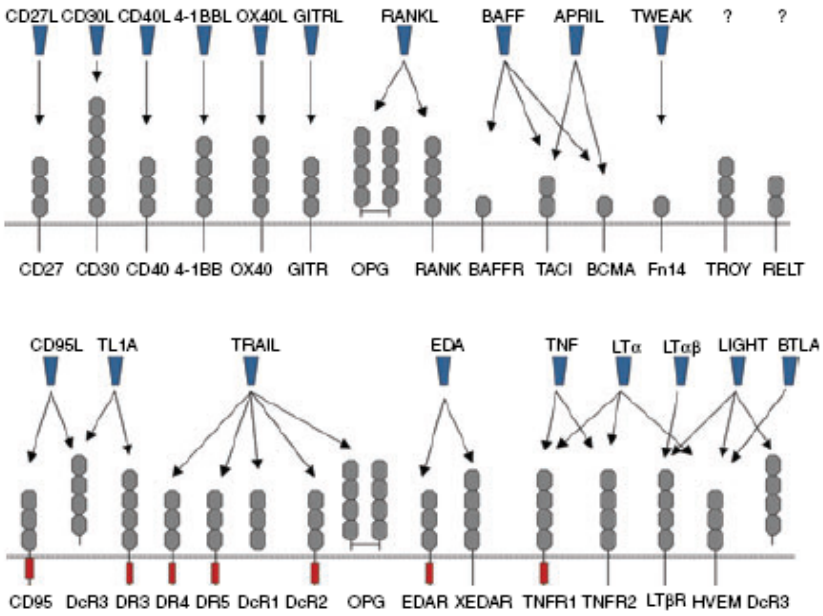

Figure 2 The TNF/TNFR superfamily. The TNF related ligands are marked in blue, arrows indicate interactions with their receptors. The ectodomains of TNFR superfamily are shown in grey with the appropriate number of CRD. Death domains within the cytoplasmatic domain are indicated red [Hehlgans and Pfeffer, 2005].

Based on their intracellular sequences, TNFRSF members can be classified into three major groups. The first group, including FAS, TNFR I, TNF-related apoptosis inducing ligand receptor 1 (TRAIL-R1), TRAIL-R2, TRAIL-R4, and TNF-like receptor apoptosis mediating protein (TRAMP), contains so called death domains in their cytoplasmatic domains (Figure 2). Activation of these members leads to recruitment of intracellular, death domain containing adaptors, such as FAS-associated death domain (FADD) and TNFR-associated death domain (TRADD). These proteins activate the caspase cascade which subsequently leads to apoptosis. TRADD in turn can also interact with TNFR-associated factor (TRAF)-2 and receptor interacting protein (RIP), thus activating the nuclear factor κB (NFκB) and Jun N-terminal kinase (JNK) pathways, which protect cells from apoptosis (Figure 3) [Stanger et al, 1995; Hsu et al, 1996]. The second group contains TRAF-interacting motifs (TIM) in their cytoplasmatic domain, and includes amongst others TNFR II, receptor activator of NFκB

(RANK), CD27, CD30, and CD40. Activation of TIM leads to recruitment of TRAF family members and activation of signaling cascades like NFκB, JNK, p38, extracellular signal-related kinase (ERK), and phosphoinositide 3-kinase (PI3K) [Dempsey et al, 2003]. The third group, including TRAIL-R3 and OPG, does not contain signaling motifs and competes with the other two receptor groups for binding of their corresponding ligands.

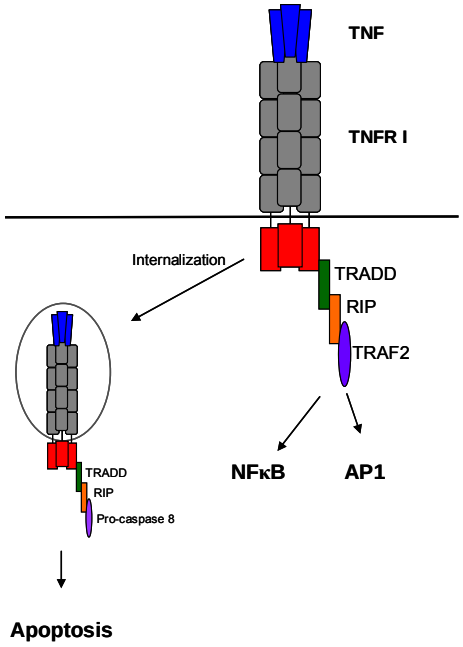

Figure 3 Signal transduction of TNFR I. After binding of TNF, TNFR I recruits TRADD as a platform adaptor and assembles alternative signaling complexes. One involves TRAF2, which links ligand induced signaling to activation of NFκB and AP-1. Another signaling complex leads to internalization of TNFR I. During endocytosis, FADD and caspase 8 are recruited to form the death signaling complex [adapted from Hehlgans and Pfeffer, 2005].

1.2.2. OPG – gene and protein

OPG was isolated independently by two laboratories [Simonet et al, 1997; Tsuda et al, 1997], and synonyms such as osteoclastogenesis inhibitory factor (OCIF) or TNF receptor related molecule (TR1) have been coined. According to the American Society for Bone and Mineral Research Committee, the term osteoprotegerin (OPG) is now recommended. The human OPG represents a single copy gene located on chromosome 8 (8q24). It spans 29 kb and consists of 5 exons, 4 introns, and is transcribed into four transcripts (2.4 kb, 3.0 kb, 4.2 kb, and 6.5 kb). The 2.4 kb transcript represents the major transcript and originates from transcriptional initiation from a TATA box ~30 bp upstream the transcription start site. The 3.0 kb transcript is derived form the alternative use of transcription start sites, while the 4.2 kb and 6.5 kb transcripts result from alternative splicing events [Morinaga et al, 1998].

High OPG mRNA levels were detected in lung, liver, heart, kidney, spleen, thymus, ovary, colon, thyroid, spinal cord, lymphnode, and bone [Simonet et al, 1997; Yasuda et al, 1998]. Expression of OPG mRNA and protein in osteoblastic lineage cells is increased by cytokines, including IL-1β and TNF-α, by the osteoblast-differentiating factors 1a, vitamin D3 and bone morphogenetic protein 2 (BMP2) [Hofbauer et al, 1998], by the antiresorptive hormones estrogen [Hofbauer et al, 1999] and TGF-β [Takai et al, 1998; Murikami et al, 1998]. In contrast, mRNA and protein level are downregulated by glucocorticoids [Vidal et al, 1998] and prostaglandin E2 (PG-E2) [Brändström et al, 1998].

OPG is a member of the TNFRSF and represents a secretory basic glycoprotein, existing either in a 60 kDa monomeric form or a 120 kDa disulfide-linked homodimeric form. Yamaguchi and colleagues characterized the structural domains of the OPG protein. The N-terminal portion of the protein, containing domains 1-4, has structural similarity to the extracellular CRD domains of the TNFRSF proteins and mediates inhibition of osteoclastogenesis. The C-terminal portion contains domains 5 and 6, which are death domain homologous regions (DDH), having a high potential for mediating cytotoxic signals. Domain 7 contains a heparin-binding site. A cysteine residue (Cys-400) within this domain was found to be responsible for dimer formation [Yamaguchi et al, 1998] (Figure 4).

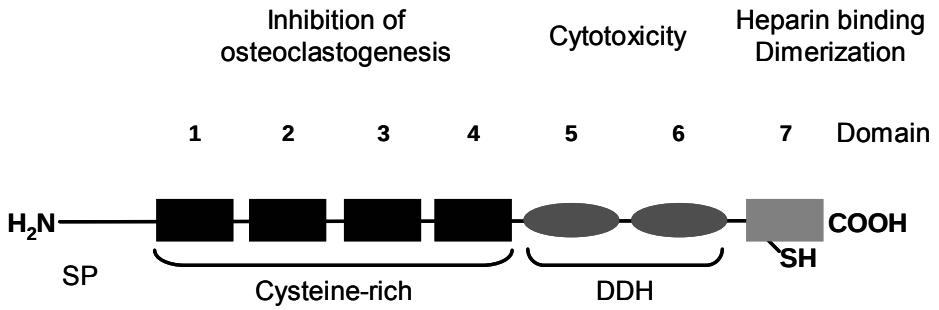

Figure 4 Structure-function relationship of the OPG protein. OPG domains and their biochemical and functional properties are indicated. N_2H indicates amino-terminus; COOH, carboxyterminus; SP, signal peptide; DDH, death-domain homologous regions [adapted from Schoppet et al, 2002].

1.2.3. OPG and vascular calcification

OPG was first identified as a key regulator of osteoclastogenesis. Osteoclast formation requires the presence of RANKL and M-CSF. These membrane-bound proteins, expressed by osteoblasts/stromal cells, are necessary for osteoclastogenesis, and widely involved in the differentiation of monocyte/macrophage derived cells. M-CSF acts through its receptor on the osteoclast, a transmembrane tyrosine kinase-receptor, leading to secondary

messenger activation of tyrosine kinase Src. RANKL is a member of the TNF superfamily and activates NFκB through binding to its receptor RANK. By binding of RANKL to RANK, and in the presence of M-CSF, RANKL promotes differentiation of osteoclast precursor cells to mature osteoclasts, their activation, survival, and adherence to bone surface [Matsuzaki et al, 1998; Burgess et al, 1999]. OPG, expressed by osteoblasts, acts as a soluble decoy receptor by binding and neutralizing RANKL, thus suppressing osteoclastogenesis, osteoclast activity, and inducing osteoclast apoptosis (Figure 5) [Ross, 2000; Khosla, 2001; Schoppet et al, 2002]. Besides its key role in regulation of osteoclastogenesis, OPG has been reported to be involved in atherosclerosis and vascular calcification. Several observational studies show that OPG serum levels correlate positively with the severity and progression of CAD, atherosclerosis, and vascular calcification (Figure 6). Jono et al reported increased OPG serum level in patients with clinically significant stenosis of the coronary arteries, and a significant association of OPG serum level with the presence of CAD [Jono et al, 2002].

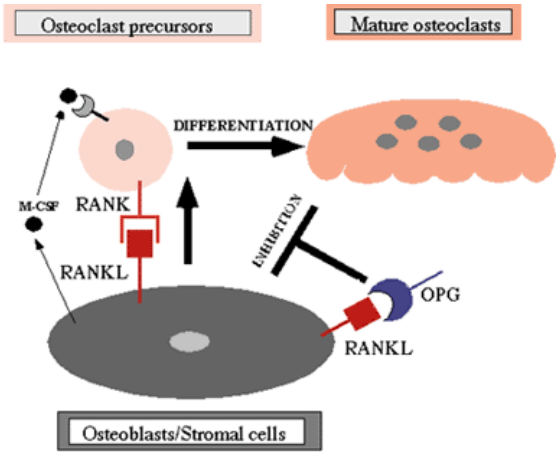

Figure 5 **Regulation of osteoclastogenesis.** Factors from osteoblasts/stromal cells interact with receptors on hematopoietic osteoclast precursor cells. An excess of OPG suppresses bone resorption [adapted from Medscape General Medicine™].

In multivariate analyses, Kiechl and colleagues reported a significant association of OPG with severity and 10-year progression of carotid atherosclerosis, and that elevated OPG serum level were a risk factor for vascular mortality [Kiechl et al, 2004]. Associations of elevated OPG serum level with diabetes, cardiovascular mortality [Browner et al, 2001], development of diabetic vascular complications [Rasmussen et al, 2006], and progression of vascular calcification have also been reported [Nitta et al, 2004]. Actually, Olesen and colleagues found a downregulation of OPG secretion during accelerated calcification *in vitro*, while differences in the expression of OPG mRNA were not detectable [Olesen et al, 2007].

However, animal models suggest that OPG may protect against vascular calcification. Bucay and colleagues reported that OPG-deficient ($OPG^{-/-}$) mice developed medial calcification of the aorta and renal arteries, while no atherosclerotic plaques were detectable [Bucay et al, 1998]. In *ldlr*$^{-/-}$ mice, fed an atherogenic diet, development of atherosclerotic lesions, vascular calcification, and increased OPG serum level was detected. Accessorily treatment of these mice with recombinant OPG resulted in reduced vascular calcification without affecting atherosclerotic lesion number and size [Morony et al, 2007].

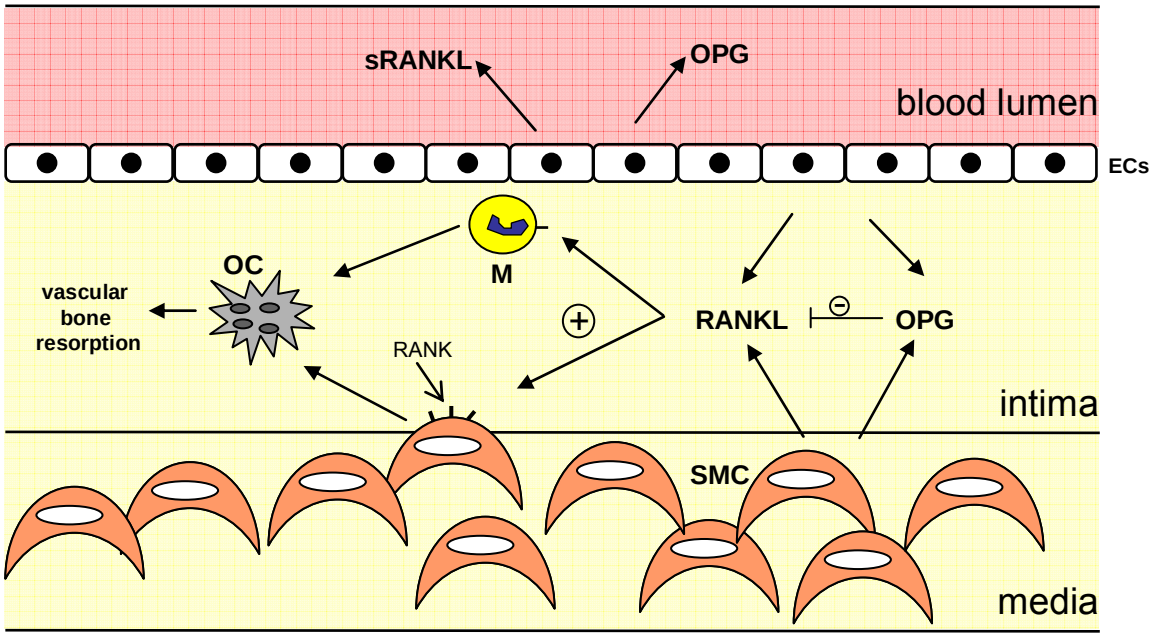

Figure 6 Potential role of OPG in vascular calcification. Soluble RANKL (sRANKL) and OPG are secreted in the atherosclerotic plaque and in the blood stream mainly by smooth muscle cells (SMCs) and endothelial cells (ECs). RANKL promotes differentiation of osteoclast precursors (mainly monocytes/macrophages [M] and SMCs) into osteoclasts (OC) leading to vascular bone resorption. OPG neutralizes the action of RANKL [adapted from Montecucco et al, 2007].

Bennett and colleagues examined atherosclerotic lesion areas and aortic calcium content in $OPG^{-/-}$.$apoE^{-/-}$ mice at 20, 40, and 60 weeks of age, and found an increase in lesion areas in 40 and 60 weeks old mice. Older mice (60 weeks of age) had also an increase in the area of calcification of the lesions. $OPG^{+/+}$.$apoE^{-/-}$ mice served as control, and displayed less atherosclerotic plaque progression [Bennett et al, 2006]. Since OPG-deficient mice, which have no measurable serum OPG, develop arterial calcification of the media and large vessels that is preventable by restoration of the *OPG* gene, elevated OPG levels are associated with increased, rather than decreased, risk of cardiovascular disease in human. One possible explanation for this discrepancy is that elevated OPG serum levels are rather a

response than a cause of vascular calcification. Another hypothesis assumes that the increased OPG serum levels are a result from decreased clearance of OPG [Browner at al, 2001].

Besides the associations found for OPG serum levels, associations of single nucleotide polymorphisms (SNPs) within the *OPG* gene, and CAD have also been reported. Soufi and colleagues examined SNPs in the *OPG* gene in a study population, in whom OPG serum levels, established CAD risk factors, and coronary findings had been determined. They found a particular SNP, T 950C (Acc# AB008822), in the *OPG* promoter region, whose minor allele (TC or CC) was associated with a significantly increased risk of CAD and increased OPG serum levels in Caucasian men [Soufi et al, 2004]. Another group assessed intima-media thickness (IMT) of the common coronary arteries in a Swedish cohort of apparently healthy individuals (n= 59), and found that 950C homozygosity was allele associated with an increased IMT and significantly lower forearm blood flow, as compared with the other genotypes (TC or TT) [Brändström et al, 2002].

1.3. Gene expression control

In general, a gene consists of exon and intron sequences, as well as promoter regions for concerting transcriptional activities. Only about 30% of the human genome consists of gene regions, of which approximately 90% are intronic and 10% are exonic regions. In total, only 2-3% of the human genome encode proteins. One of the major findings of the Human Genome Project (HUGO) was that the human genome contains far less protein coding genes than expected, and that the molecular basis of its plasticity and diversity resides in the availability of multiple alternative promoters in the majority of human genes. Each coding gene requires at least one promoter, which regulates its transcriptional performance depending on tissue and physiological specificities. A promoter is located within the 5'-flanking region upstream of the first exon of a transcribed gene sequence. In case of alternative promoters, from which transcription is driven from alternative TSS, the promoter may also be located intronically. For most of the human genes the exact and comprehensive localization of promoter regions remains unknown [Eckhardt et al, 2006].

1.3.1. Levels of transcriptional control

The concept of eukaryotic transcription consists of five control levels (Figure 7): (a) release of DNA from nucleosomal packaging and susceptibility of *cis*-active regulatory elements, (b) assembly of the basal transcription machinery at specific sites (TATA-box or TATA-less promoter elements [e.g. initiator element (Inr), downstream promoter element (DPE)]), (c)

binding of regulatory proteins which interact with the basal transcription machinery (transcription factors (TF), repressors, balancers), (d) recruitment of co-regulating proteins, which interact with both, TF and basal transcription machinery without interacting with the DNA itself ("bridging-proteins", e.g. CBP, p300), and (e) secondary or epigenetic activation/inactivation by histone acetylation or methylation respectively, and natural transcript knock-down by micro RNA (miRNA) interference [Lin et al, 2008]. Another recently described important level of control is the combination of transcription and splicing by a complex of up to 147 proteins ("mRNA factory") and the splicosome [Kornblihtt, 2006].

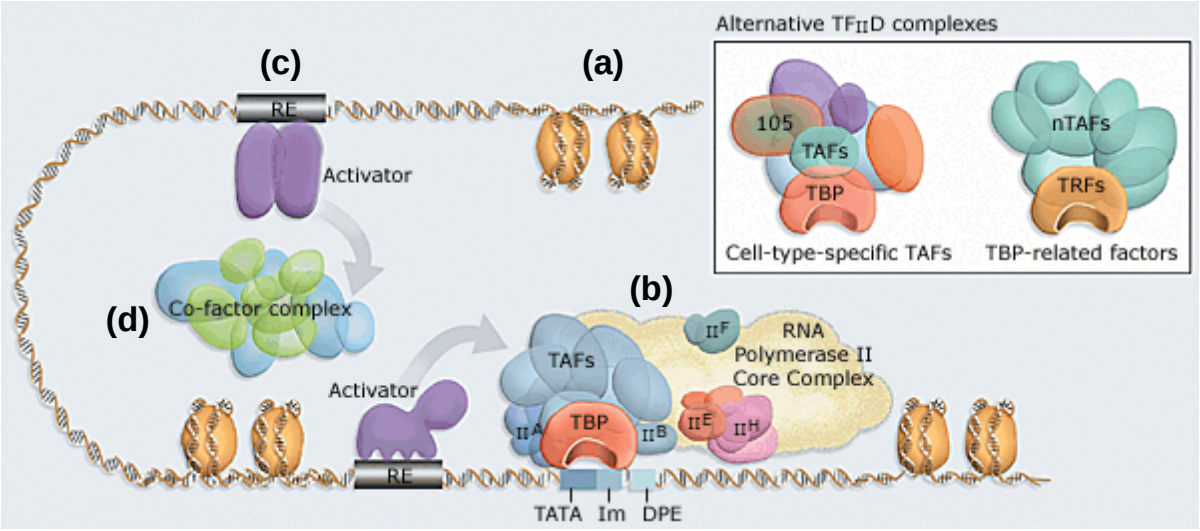

Figure 7 Control levels of eukaryotic transcription. (a) DNA release from the nucleosome. (b) TATA-binding protein (TBP) and TBP associated factors (TAFs) form the TFIID complex and, together with RNA polymerase II and other general TFs the basal transcription machinery. (c) TFs bind to upstream regulatory elements, having either activating or repressive functions. (d) Co-factors serve as bridges between bound TFs and the RNA polymerase II machinery. All cells use an elaborate transcription apparatus to express genes; TATA-less promoters use alternative versions of TBP (box) [adapted from R. Tjian, Howard Hughes Medical Institute homepage].

1.3.1.1. Basal transcription machinery

The term "promoter" typically refers to the "core promoter" and its adjacent sequences. The core promoter surrounds the TSS and comprises 70-80 bp that contain elements like TATA-box or initator elements (Inr). This minimal region is required for assembly of the basal transcription machinery and initiation of transcription. The "proximal promoter" describes the region extending upstream of the core promoter and comprises *cis*-active elements, which present repressor or enhancer elements, serving as transcription factor binding sites (TFBS). Interaction of bound TFs with the basal transcription machinery is mediated by co-activator proteins [Heintzman and Ren, 2006]. The basal transcription machinery consists of six

proteins: RNA polymerase II (pol II) and five general transcription factors, known as TFIIB, -D, -E, -F, and -H. The core promoter recognition complex TFIID consists of the TATA-box binding subunit (TBP) and 8-12 TBP associated factors (TAFs). It bends promoter DNA around pol II and TFIIB, whose N-terminal domain brings DNA to the polymerase surface. TFIIE enters the complex and recruits TFIIH, whose ATPase/helicase subunit introduces negative superhelical tension in the DNA. The emerging transient bubble is captured by TFIIF. DNA can now descend into the active center of pol II, which is capable of unwinding DNA, synthesizing RNA, and rewinding DNA, but it is incapable of recognizing a promoter and initiating transcription. TFs bound to *cis*-active elements interact with bridging-proteins, which in turn interact with the basal transcription machinery. The assembly of this complex leads to the initiation of transcription [Kornberg, 2007]. However, a TATA-box is only present in ca. 12% of mRNA genes in humans [Bajic et al, 2004] and in about 30% of promoters of *Drosophila* [Ohler et al, 2002]. TATA-less promoters commonly contain a combination of Inr, downstream promoter elements (DPE), and GC-rich regions, often containing binding sites for the activating TF Sp1. True TATA-less promoters have no intrinsic specificity for TFIID recruitment, therefore certain activators such as Sp1 are proposed, when bound to a GC-box, to recruit the TFIID complex via a tethering factor physically associated with TBP [Pugh and Tijan, 1991].

1.3.2. Mechanisms of transcriptional regulation

1.3.2.1. Epigenetic regulation of gene expression

Epigenetics can be defined as functional events in the genome physiology that are not encoded by the DNA itself. Post-translational modifications of histone proteins in chromatin and methylation of DNA are two of the major epigenetic modifications. In its transcriptional inactive state, DNA is coiled round a set of eight histones in the nucleosome and further condensed to chromatin. Nucleosomes serve as general transcription repressors, assuring the transcriptional inactivity of all packaged genes in eukaryotic cells. They can rapidly be removed and reassembled in the activated state, making promoter DNA transiently available for interaction with the transcription machinery. At this level, dominant mechanisms of transcriptional regulation are DNA methylation and histone acetylation.

In complex organisms that contain a large number of tissue-specific genes, mechanisms to permanently turn off transcription of genes, not required in a particular cell-type, are mandatory. In fact, 40% of mammalian genes contain CpG sites in their upstream region, and approximately 60-90% of all CpG sites in the genome are methylated, predominantly intergenic regions [Bird, 2002]. High levels of methylated CpG dinucleotides correlate with transcriptional inactivity and nuclease resistance. Changes in the affinity of histones to

methylated DNA, or changes in the composition of chromatin could explain the inaccessibility of chromatin containing methylated DNA to nucleases. Chromatin compositional changes are suggested by the replacement of normal nucleosomal components by methylated CpG dinucleotide binding proteins, which may have repressor domains recruiting other proteins that might alter chromatin structure [Wolffe, 1998].

Alterations in core histone acetylation status might have a causal role in determining the influence of chromatin on transcriptional activity: transcriptional co-activators that direct histone acetylation have been identified, while co-repressors have been discovered to direct deacetylation. Each core histone has two domains: a histone fold domain involved in histone-histone interactions and DNA wrapping, and one N-terminal domain outside of the nucleosome, where it can interact with other regulatory proteins. These N-terminal domains are lysine rich and targets for acetylation. A dramatic increase in the accessibility of DNA to transcription factors depends on acetylation of the N-terminal domains [Wolffe, 1998]. The mechanism by which histone acetylation controls gene activity is unclear, but one plausible idea is that acetylation disrupts internucleosomal contacts, resulting in a less compact form of chromatin being more accessible to the transcriptional machinery [Jenuwein and Allis, 2001].

1.3.2.2. Regulatory elements

The assembly of the basal transcription machinery is all that is required for initiating transcription in any gene. However, the transcription levels achieved by the core promoter are minimal, and upstream factors and elements are required to modify transcription rates. Additional transcriptional regulators are *cis*-active elements that are usually located within the upstream region and described as enhancer (increasing transcriptional activity), silencer (decreasing transcriptional activity), or response elements.

In case of enhancers, their regulatory character is independent of orientation and flexible with respect to the distance from the gene to be regulated. Binding of activators to this enhancer region recruits transcription factors, which are ubiquitous, tissue-specific, or differentiation-dependent. Promoter-enhancer communication over large distances requires usage of facilitating mechanisms. As a result of enhancer action, a promoter binding protein can be recruited, enhancer-promoter interaction may result in a change of activity of an already promoter-bound protein, or interactions with promoter-bound proteins may cause recruitment of other factors required for transcription initiation. Several models have been proposed explaining promoter-enhancer interactions over large distances (Figure 8): (A) Interaction of an enhancer-bound activator with a promoter-bound protein is facilitated by looping of the intervening DNA (DNA looping model). (B) In the tracking model, the enhancer

is used as a loading platform for a DNA tracking protein. Since the tracking protein is leaving the loading site (enhancer), the protein may be loaded again and thus accumulating in the vicinity of the promoter. (C) The spread-looping model suggests that binding of an activator protein to the enhancer induces binding-polymerization of a protein to the DNA. A series of small loops is formed during polymerization and the array of proteins may reach the target promoter [Dorsett, 1999].

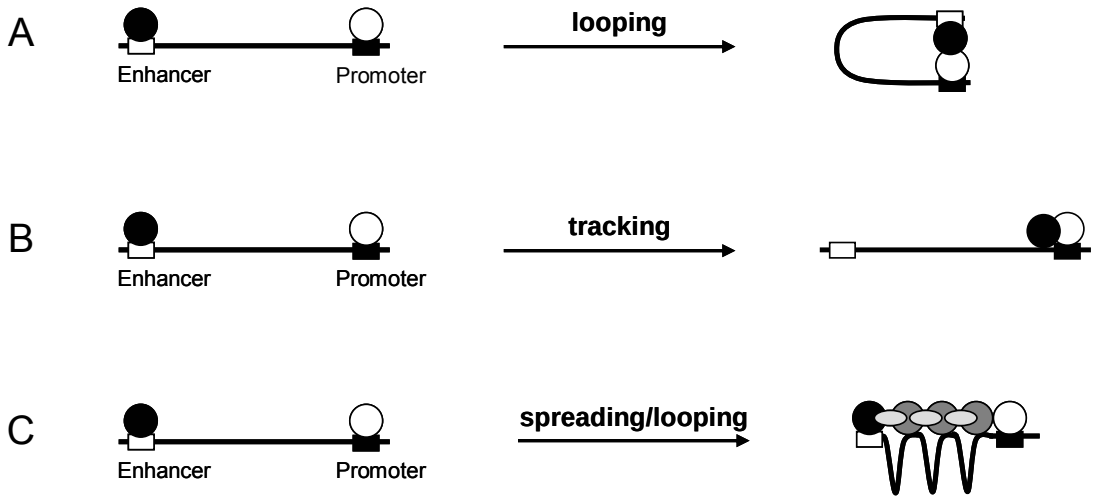

Figure 8 Models for enhancer-promoter interaction over distances. The enhancer- and promoter-bound proteins are indicated in white and black circles, respectively. DNA binding sites are indicated by rectangles. (A) Looping. (B) Tracking. (C) Spreading/looping. Activator bound to the enhancer induces highly cooperative binding of a protein (grey circle) to several, closely spaced DNA-binding sites. Spreading is accompanied by DNA looping [adapted from Bondarenko et al, 2003].

Silencers direct an active transcriptional repression and have been located at various positions: upstream the promoter region, intronically, and exon- or 3'-UTR [Ogbourne and Antalis, 1998]. Enhancers and silencers act bi-directionally over long distances and control spatial and temporal patterns of transcription. Their widespread occurrence and universal actions require mechanisms to prevent inappropriate regulator interactions, so that long-term control prevails. Insulators represent a novel class of DNA sequences that constrain regulatory interactions within eukaryotic genomes and restrict enhancer and silencer function. Insulators are operationally defined by two functional properties. After binding of the corresponding protein, they firstly protect gene expression from positive and negative chromatin effects, caused when transgenes are integrated randomly within a genome. Secondly, insulators block enhancer-activated transcription, when located between enhancer and corresponding promoter, but not when the insulator is positioned upstream of the enhancer [Geyer and Corces, 1992; Scott and Geyer, 1995; Rosemann et al, 1993].

Response elements modulate transcription rates in response to external stimuli, e.g. specific hormones (e.g. estrogene response element, ERE) or intracellular second messengers (e.g. cAMP response element, CRE).

1.3.2.3. Alternative promoters

In mammalian genomes, alternative splicing is a key mechanism to enlarge transcript and protein diversity. A variety of exon combinations enables tissue- and differentiation specific gene splicing control form a single gene locus. The mRNA isoforms are usually transcribed by alternative promoters by inclusion of alternative first exons. Alternative leader exons can affect gene expression in diverse ways, including temporal expression of a gene, tissue- or cell type-specific expression, stability of mRNA, translational efficiency, and the structure of the N-terminus of the protein encoded by the gene. Differences in N-termini of proteins can lead to alterations in protein levels, functions, and localizations [Ayoubi and Van De Ven, 1996]. This alternative usage depends probably on cell-type and tissue specificity, as well as on differentiation status. It is mainly defined as an alternative usage of alternative sequences with alternative TSS.

The usage of alternative promoters becomes more and more evident, suggesting the existence of 3.1 promoters per gene on average [Cheong et al, 2006]. In addition to alternative promoter usage and TSS, the assembly of alternative TF modules also differently regulates transcription.

1.3.2.4. Modularity of transcription factor assembly

Early studies led to the identification of multiple eukaryotic RNA polymerases and mapping of promoter and enhancer sequences, including the core promoter elements (i.e. TATA, Inr, DPE), proximal basal level enhancer elements (i.e. GC box, CCAAT), and distal gene-specific, signal-responsive elements, such as hormone responsive elements (HRE). Genetic approaches in yeast and *Drosophila*, and purification of transcription factors from mammalian cells revealed the existence of large families of sequence-specific activator proteins, i.e. Sp1, activator proteins (AP1), or CCAAT enhancer-binding proteins (C/EBP) as well as a host of accessory factors like TATA-binding protein (TBP) and general transcription factors (i.e. TFIIA, TFIIB, TFIID, TFIIE, TFIIF, and TFIIH) necessary for a functional RNA pol II complex.

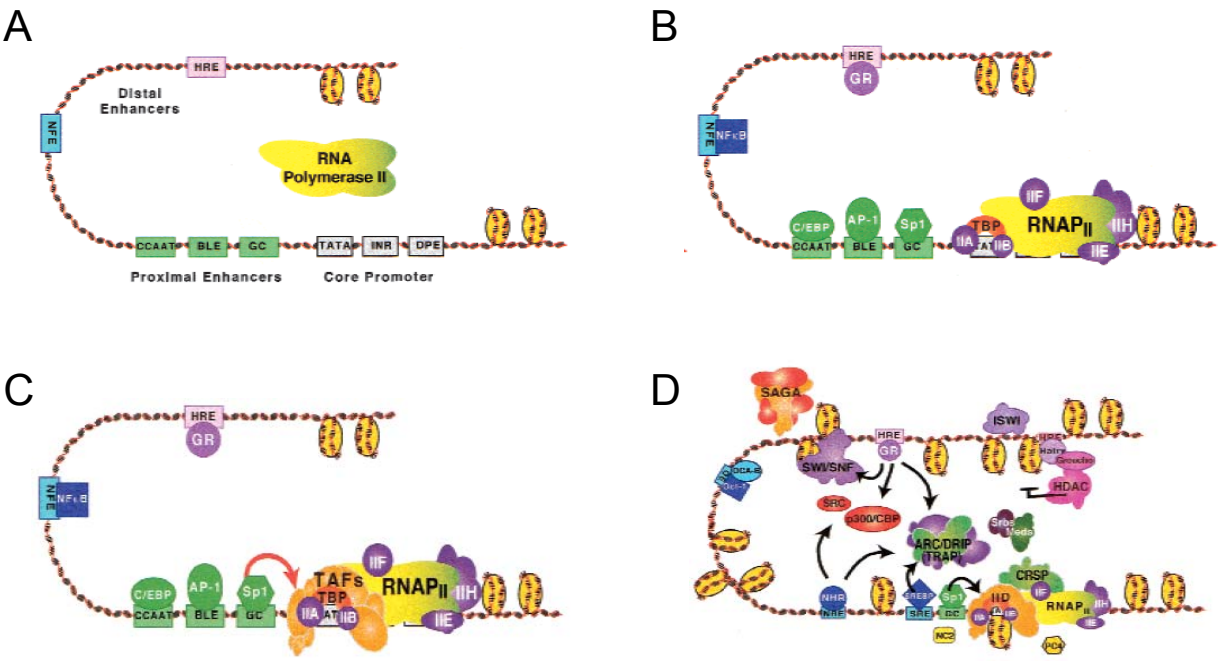

Figure 9 Fundamental elements of eukaryotic transcriptional control. (A) Identification of RNA polymerases (yellow/green), core promoter elements (grey), proximal basal level enhancer elements (green), gene-specific, signal-responsive distal enhancer elements (i.e. nuclear factor element [NFE], blue; hormone responsive element [HRE], purple). (B) Sequence-specific DNA-binding transcription factors were isolated biochemically, including specificity-protein 1 (Sp1, green), activator-proteins (AP1, green), CCAAT enhancer-binding proteins (C/EBP, green), steroid receptors (i.e. glucocorticoid [GR], purple), tissue-specific TFs (NF-κB, blue), components of the core machinery, including TATA-binding protein (TBP, red), and general TFs (purple). (C) Discovery of TBP associated factor (TAF) subunits (orange). (D) Identification of co-activators and co-repressors mediating between the core machinery and sequence-specific elements [adapted from Lemon and Tjian, 2000].

As the presence of TBP alone is insufficient for transcriptional activation, discovery of TBP-associated factors (TAFs) revealed the requirement of co-activators to mediate activator responsiveness. Many co-activators and co-repressors were subsequently found to be required for mediating signals between sequence-specific TFs and the core machinery. It is now evident that one regulator can partner and function with multiple types of co-activators and co-repressors, and vice versa (Figure 9). TF work in complexes that are represented on sequence level as sets of TFBS. A physical TFBS can be found every 10-15 bp within the genome. A functional TFBS requires a cellular context, which is defined by availability of the respective binding protein, and a genomic context. Although the respective TF is available in a certain cell type, the biological function may require additional binding sites, forming a transcriptional module. A transcriptional module consists of at least two TFBS, in certain distance relationship and strand orientation. They are present in promoters and enhancers,

and can shift within a promoter. Signals are integrated via the interacting TF. With this promiscuity, transcriptional models represent the basic elements of regulatory pathways and networks (Figure 10). Most genes are regulated by missing different types of activators and repressors in a coordinated way. Since biological systems are dynamic, TFs only transiently associate with their cognate binding site and co-regulators [McNally et al, 2000; for review Lemon and Tjian, 2000]. Gene transcription and the associated complex-forming events are of eminent importance, and should be tightly regulated to ensure appropriate and correct mRNA expression. Variations within regulatory sequences, such as single nucleotide polymorphisms – SNPs, may alter TFBS and/or the affinity of DNA:protein interactions, probably affecting gene transcription and protein content.

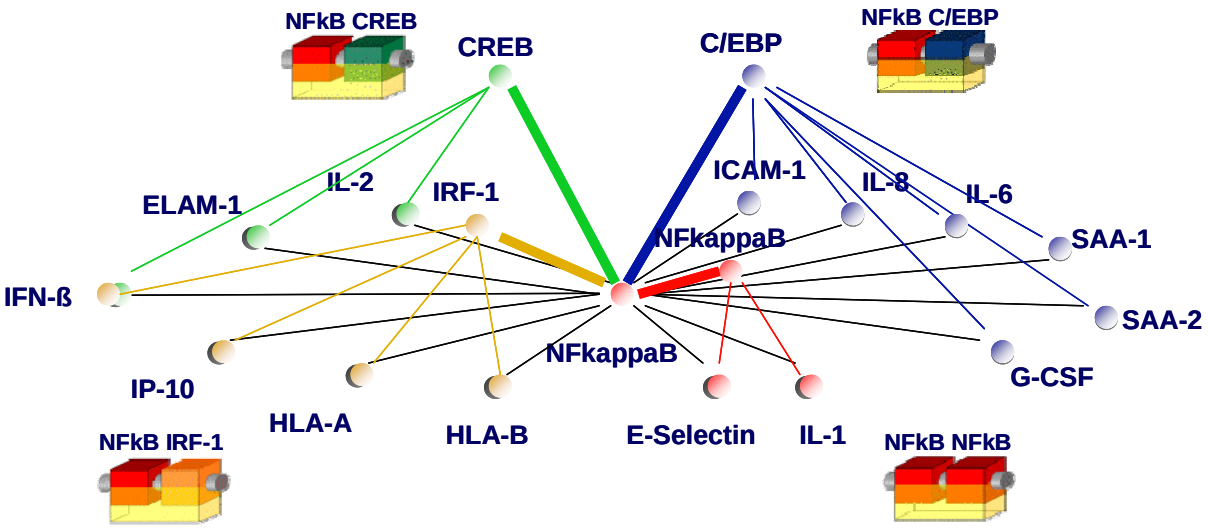

Figure 10 Transcriptional modules define target genes of pathways. Target genes of NFκB (black lines) are regulated by several pathways via different interaction partners (different modules) of NFκB: CREB (green lines), C/EBP (blue lines), IRF-1 (yellow lines), NFκB (red lines) [adapted from Genomatix].

1.4. Linkage and association studies

Common forms of CVD are known to be multifactorial and influenced by several genes. Two main types of studies are used to identify the genetic cause of a complex disease: linkage studies and gene association studies (Figure 11) [Arnett et al, 2007].

Linkage analyses use phenotypic and genetic data from families for identifying genomic regions that might contain genes possibly influencing a phenotypic trait. Thereby, analyses

are initiated without any a priori assumptions. Families are genotyped for polymorphic marker at known locations across the genome. The marker data together with phenotype data and pedigree data are entered into biostatistical algorithms calculating a degree of similarity, how a marker correlates with phenotypic resemblance among family members. Once chromosomal regions have been discovered through linkage analyses, gene maps are reviewed near the region of significant linkage, and potential causal genes are positionally identified. Linkage analyses have been successful in identifying the genetic basis of rare disorders, but are less useful in identifying common genetic variants that generally have moderate effects.

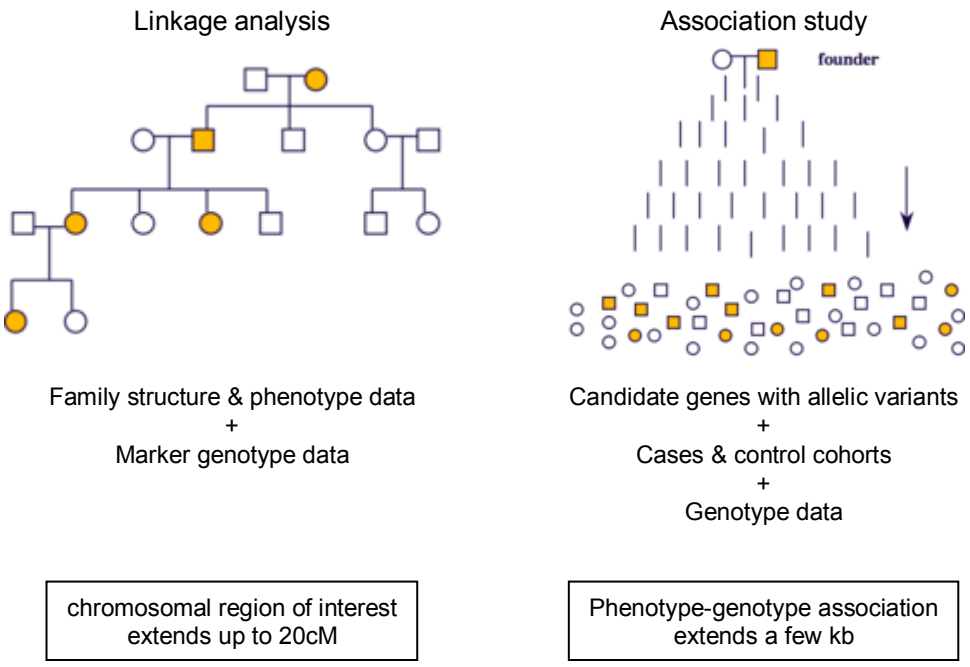

Figure 11 Schematic representation of linkage analyses and association studies. Linkage analyses identify chromosomal regions using family structure, and phenotype data (left panel). Association studies are hypothesis driven and result in phenotype-genotype association data using case-control-study populations (right panel) [adapted from www.goldenhelix.com].

For complex disease, such as CVD, high resolution whole-genome association studies, typing hundreds of thousands of variants, provide an excellent power to detect genotype-phenotype relations, markedly exceeding the power of linkage analyses. Association-studies are based on SNPs and/or haplotypes (a haplotype describes a combination of alleles on the same chromosome that are inherited together and are statistically related), and are designed to compare allele/haplotype frequencies between case and control groups. The statistical difference in frequencies between cases and controls provides evidence whether an allele/haplotype is associated with the trait.

Candidate genes are mostly selected basing its known biological function, significant findings in a linkage-study, or both.

However, a genetic association is not necessarily genetic causation. A genetic variant associated with a trait may be causal, or associated with the causal variant within the same or another gene (linkage disequilibrium). Both, genome-wide linkage studies and association studies, often fail to disclose a specific functional effect of the detected variant(s). Consequently, a reliable molecular profiling of genetic variation and a better knowledge of the molecular/functional structure of the locus of interest is mandatory. Functional analyses of the candidate genes target protein function, structure, stability, and its expression. Dysregulation in protein transcription due to genetic variants within the promoter region might affect its appropriate expression in response to physiological necessities with pathophysiological consequences. Therefore, functional analyses do not include exclusively the coding region of a gene, but also the 5'-flanking region harboring the regulatory elements of a gene.

1.5. Aim and design of the study

Vascular calcification is a strong indicator for inflammatory disease, commonly atherosclerosis. *OPG* was chosen as a candidate gene because of its emerging role in atherosclerosis and vascular calcification [Bucay et al, 1998]. Genetic predispositions are entailed by the functionality of genetic variants and individual haplotype patterns. One genetic variant within the regulatory region of *OPG* was identified and associated with elevated OPG serum levels and an increased risk of CAD [Soufi et al, 2004].

Genetic variants that possibly affect transcriptional regulation of *OPG* might have an influence on OPG expression balance and its cytokine-activity. Within this study, genetic variants within the regulatory region of the OPG gene were to identify and comprehensively characterized. For this purpose, a sufficiently active promoter portion needed to be identified in two OPG endogenously expressing osteosarcoma cell lines SaOs-2 and U2Os. *Cis*-regulatory elements within the sufficiently active promoter portion should be identified by serial 5'-deletion. Further, haplotype constellations within the *OPG* regulatory region were to identify by scanning genomic DNA from patients with essential hypertension and/or MI (MolProMD cohort). The impact of the detected variants on DNA:protein interactions should be analyzed, since alterations in TFBS may influence the affinity of interaction of a certain TF for its cognate DNA binding site. Therefore, modified DNA sequences harboring the variant or haplotype of interest were to characterize by allele-specific response in electrophoretic

mobility shift assays (EMSA). To identify transcription factors presumably participated in DNA:protein interactions, *in silico* analyses should be performed and predicted factors were to confirm by co-transfection analyses and EMSA competition assays.

In a parallel asset, functional effects of the genetic variants on transcriptional activity of the *OPG* gene were to examine in an appropriate cell system. Variants should be analyzed in the context of the sufficiently active promoter region, as well as in the 5'-truncated deletion constructs by use of reporter gene assays. Reporter gene assays allow to determine and quantify transcriptional activity of a chosen promoter region, which is cloned into a promoter-less luciferase reporter gene vector; expression of the luciferase gene is exclusively driven by the cloned promoter portion. Transcriptional influences of the detected variants were compared to the wild type sequence. A concept of a transcription factor module involved in transcriptional regulation of *OPG* should be proposed.

2. Material

2.1. Chemicals

Acidic acid, 96%	Roth, Karlsruhe
Acrylamide, 40% (AA)	Merck, Darmstadt
Agarose	Biozym, Hess. Oldendorf
Ammonium peroxydisulfate (APS)	Roth, Karlsruhe
Bacto™ Agar	Becton Dickinson, Heidelberg
Bacto™ Tryptone	Becton Dickinson, Heidelberg
Bacto™ Yeast Extract	Becton Dickinson, Heidelberg
Betaine	Sigma, Steinheim
Bisacrylamide, 2% (BAA)	Merck, Darmstadt
„Blocking reagent“	Roche Diagnostics, Mannheim
Boridic acid	Roth, Karlsruhe
Bromphenole blue	Sigma, Steinheim
Caseine	Sigma, Steinheim
Chloroform	Fluka Riedel-de Haën, Seelze
Coomassie Brilliant Blue R-250	Roth, Karlsruhe
Dimethylsulfoxide (DMSO)	Roth, Karlsruhe
dNTPs (dATP, dCTP, dGTP, dTTP)	Rapidozym, Berlin
1,4-Dithiothreitol (DTT)	Roth, Karlsruhe
17β-Estradiol (E2)	Sigma Aldrich, Schnelldorf
Ethanol	Merck, Darmstadt
Ethidium bromide	Roth, Karlsruhe
Ethylenediamine-tetraacetic acid (EDTA)	Roth, Karlsruhe
Ethyleneglycol-tetraacetic acid (EGTA)	Roth, Karlsruhe
Ficoll	Fluka Riedel-de Haën, Seelze
Formaldehyde, 37%	Roth, Karlsruhe
Formamide	AppliChem, Darmstadt
Glycerol, 87%	Roth, Karlsruhe

β-Glycerophosphate	Sigma Aldrich, Schnelldorf
Glycine	Roth, Karlsruhe
HEPES (4-(2-hydroxyethyl)-1-piperazineethanesulfonic acid)	Roth, Karlsruhe
Imidazole	Roth, Karlsruhe
Isoamylalcohol	Merck, Darmstadt
Isopropylalcohol	Merck, Darmstadt
L-Glutamine	Roth, Karlsruhe
Lithium chloride	Merck, Darmstadt
Magnesium chloride hexahydrate	Roth, Karlsruhe
Maleic acid	Roth, Karlsruhe
β-Mercaptoethanol	Serva, Heidelberg
Methanol	Roth, Karlsruhe
N', N', N', N'-Tetramethylendiamine (Temed)	Roth, Karlsruhe
Nitric acid	Roth, Karlsruhe
Nonidet P-40 (IGEPAL-C630)	Sigma Aldrich, Schnelldorf
Phenylmethylsulphonyl fluoride (PMSF)	Roth, Karlsruhe
Poly(dI•dC)/Poly(dA•dT)	Amersham Biosciences, Piscataway, USA
Polyethylene glycol 4000 (PEG 4000)	Roth, Karlsruhe
Polyvinylpyrrolidone (PVP-10)	Sigma, Steinheim
Potassium chloride	Merck, Darmstadt
Protease Inhibitor cocktail with EDTA (Complete)	Roche Diagnostics, Mannheim
Sodium carbonate	Merck, Darmstadt
Sodium chloride	Roth, Karlsruhe
Sodium dodecyl sulfate (SDS)	Roth, Karlsruhe
Sodium fluoride	Serva, Heidelberg
Sodium hydroxide	Roth, Karlsruhe
Sodium molybdate	Roth, Karlsruhe
Sodium orthovanadate	Sigma Aldrich, Schnelldorf
Sodium pyrophosphate	Sigma Aldrich, Schnelldorf
Sodium pyruvate	Sigma, Steinheim
Spermidine	Fluka Riedel-deHaën, Seelze
Tumor necrosis factor α (TNFα)	Cell Signaling, Frankfurt
Tris-(hydroxymethyl)-aminomethane (Tris-base)	Roth, Karlsruhe

Triton X-100	Roth, Karlsruhe
Tween-20	Roth, Karlsruhe
Xylene xyanole	Roth, Karlsruhe

2.2. Other solutions and reagents

2.2.1. Sera and media

Fetal bovine serum (conditioned)	PAA, Pasching
Fetal bovine serum, iron supplemented	Cell Concepts, Umkirch
Dulbecco's modified eagle's medium (DMEM)	Sigma, Steinheim
Dulbecco's phosphate buffered saline (PBS)	Sigma, Steinheim

2.2.2. DNA ladder and protein marker

Precision Plus Protein Dual Color Standard Plus	BioRad, Munich
50 bp DNA ladder	Invitrogen, Karlsruhe
100 bp DNA ladder	Invitrogen, Karlsruhe
1 kb DNA ladder	Invitrogen, Karlsruhe

2.2.3. Enzymes and antibiotics

Trypsine-EDTA (0.05%)	Gibco, Karlsruhe
Ampicillin	Roth, Karlsruhe
Penicillin/Streptomycine solution	Sigma Chemie, Steinheim
Spectinomycine	Sigma, Steinheim

2.3. Consumables and kits

5'/3' RACE Kit, 2nd Generation	Roche, Mannheim
BCA Protein Assay Kit	Thermo Fischer, Bonn
Biotin 3' End labeling Kit	Thermo Fischer, Bonn
Chemiluminescent Nucleic Acid Detection Module	Thermo Fischer, Bonn
CL-XPosure™ Film	Thermo Fischer, Bonn
Effectene	Qiagen, Hilden
Egr1 EMSA Kit	Panomics, Heidelberg
First Strand cDNA Synthesis Kit	Fermentas, St. Leon-Rot
High Pure PCR Product Purification Kit	Roche Diagnostics, Mannheim

Immobilon-P Transfer Membrane (PVDF)	Millipore, Bedford, USA
LightShift Chemiluminescent EMSA Kit	Thermo Fischer, Bonn
Lipofectamine™ 2000	Invitrogen, Karlsruhe
Luciferase Assay System	Promega, Mannheim
Magnetic Protein-G beads	Invitrogen, Karlsruhe
Passive Lysis Buffer (5x)	Promega, Mannheim
Platinum® SYBR® Green qPCR SuperMix-UDG with ROX	Invitrogen, Karlsruhe
PureLink™ HiPure Plasmid DNA Purification Kit	Invitrogen, Karlsruhe
QIAamp® DNA Blood Mini Kit	Qiagen, Hilden
QIAprep® Spin Miniprep Kit	Qiagen, Hilden
QIAquick® Gel Extraction Kit	Qiagen, Hilden
QuikChange®Multi Site-directed Mutagenesis Kit	Stratagene, Amsterdam, The Netherlands
TRIzol® Reagent	Invitrogen, Karlsruhe
Whatman® Paper 3MM Chr.	Biometra, Göttingen
Pipette tips 0.1 µl-1000 µl	Sarstedt, Nürnbrecht
Reaction tubes 0.2 ml-2 ml	Eppendorf, Hamburg Biozym, Hess. Oldendorf
15 ml/50 ml tubes	Greiner, Kremsmünster Nunc, Wiesbaden
Petri dishes	Sarstedt, Nürnbrecht
Plastics for cell culture	Greiner, Kremsmünster
PCR plates, microtiter plates	Abgene, Hamburg

2.4. DNA modifying enzymes

Exonuclease I	Fermentas, St. Leon-Rot
GoTaq® DNA Polymerase	Promega, Mannheim
Herculase II DNA Polymerase	Stratagene, Amsterdam, The Netherlands
High Fidelity PCR Enzyme Mix	Fermentas, St. Leon-Rot
Restriction endonucleases	Fermentas, St. Leon-Rot
Shrimp Alkaline Phosphatase	Fermentas, St. Leon-Rot
T4 DNA Ligase	Fermentas, St. Leon-Rot

2.5. Antibodies

primary

Antibody	*Host*	*Manufacturer*
anti-OPG (ab14049)	mouse	Abcam, Cambridge, UK
anti-MAPK2 (6G11)	mouse	Nanotools, Teningen
anti-Egr1 (#4154)	rabbit	Cell Signaling, Frankfurt
anti-Sp1 (MAB10126)	rabbit	Upstate (Milipore), Schwalbach
anti-NF-1 (sc-5567X)	rabbit	Santa Cruz, Heidelberg
anti-ERα	rabbit	Chemicon (Milipore), Schwalbach
anti-ERβ	rabbit	Upstate (Milipore), Schwalbach

secondary

Antibody	*Host*	*Manufacturer*
anti-rabbit IgG (#7074)	goat	Cell Signaling, Frankfurt
anti-mouse IgG (RPN4201)	sheep	Amersham Biosciences, Piscataway, USA

Secondary antibodies were horseradish peroxidase-conjugated.

2.6. Plasmids and vectors

Cloning vectors

Vector	*Type*	*Manufacturer*
pCR®II TOPO® cloning vector	cloning vector	Invitrogen, Karlsruhe
pCR®8/GW/TOPO® cloning vector	cloning vector	Invitrogen, Karlsruhe
pGL3basic	reporter gene vector	Promega, Mannheim
ptk81-luc3	reporter gene vector	Dr. Tadashi Kimura, Kobe, Japan

Control vectors

Vector	*Type*	*Manufacturer*
pGL3control	reporter gene vector	Promega, Mannheim
pTA/luc	reporter gene vector	Clontech, Saint-Germain-en-Laye, France
pNFκB-TA/luc	reporter gene vector for NFkB	Clontech, Saint-Germain-en-Laye, France

pERE2-tk/luc	reporter gene vector for estrogen receptor (ER)	Dr. Gwendal Lazennec, Montpellier, France

Expression vectors

Vector	***Type***	***Manufacturer***
pCH0	expression vector	Dr. Rich Gronostajski, Buffalo, USA
pCH-NF1-A1.1	expression vector (NF1-A1.1)	Dr. Rich Gronostajski, Buffalo, USA
pCH-NF1-B2	expression vector (NF1-B2)	Dr. Rich Gronostajski, Buffalo, USA
pCH-NF1-C2	expression vector (NF1-C2)	Dr. Rich Gronostajski, Buffalo, USA
pCH-NF1-X2	expression vector (NF1-X2)	Dr. Rich Gronostajski, Buffalo, USA
pGFP	reporter gene vector	Amaxa, Cologne
pEgr1/EGFP	expression vector (Egr1)	Dr. Kerstin Duning, Münster
pRc/CMV	expression vector	Dr. Dimitris Kardassis, Heraklion, Greece
pSp1/CMV	expression vector (Sp1)	Dr. Dimitris Kardassis, Heraklion, Greece

All following vectors were generated within the course of this study (see 3.1.9, and Figure 23).

OPG promoter portion constructs

pOPG-159T/luc	reporter gene construct, 275 bp of *OPG* 5'-flanking region, according to Acc#.: AB008822
pOPG-159C/luc	reporter gene construct, 275 bp of *OPG* 5'-flanking region, bearing variant -159C, according to Acc#.: AB008822

pOPG-wt/luc	reporter gene construct, 249 bp of *OPG* 5'-flanking region, according to Acc#.: AB008822
pOPG-MolHap2/luc	reporter gene construct, 249 bp of *OPG* 5'-flanking region, bearing variant -946G, according to Acc#.: AB008822
pOPG-MolHap4/luc	reporter gene construct, 249 bp of *OPG* 5'-flanking region, bearing variants -960C, -946G, -900A, -961G, according to Acc#.: AB008822

OPG deletion constructs

pOPG-Del1/luc	reporter gene construct, 1008 bp of *OPG* 5'-flanking region, according to Acc#.: AB008822
pOPG-Del1-159C/luc	reporter gene construct, 1008 bp of *OPG* 5'-flanking region, bearing variant -159C, according to Acc#.: AB008822
pOPG-D1H2/luc	reporter gene construct, 1008 bp of *OPG* 5'-flanking region, bearing variant -946G, according to Acc#.: AB008822
pOPG-D1H2-159C/luc	reporter gene construct, 1008 bp of *OPG* 5'-flanking region, bearing variants -946G, -159C, according to Acc#.: AB008822

pOPG-D1H4/luc	reporter gene construct, 1008 bp of *OPG* 5'-flanking region, bearing variants -960C, -946G, -900A, -864G, according to Acc#.: AB008822
pOPG-D1H4-159C/luc	reporter gene construct, 1008 bp of *OPG* 5'-flanking region, bearing variants -960C, -946G, -900A, -864G, -159C, according to Acc#.: AB008822
pOPG-Del2/luc	reporter gene construct, 924 bp of *OPG* 5'-flanking region, according to Acc#.: AB008822
pOPG-Del2-159C/luc	reporter gene construct, 924 bp of *OPG* 5'-flanking region, bearing variant -159C, according to Acc#.: AB008822
pOPG-D2H4/luc	reporter gene construct, 924 bp of *OPG* 5'-flanking region, bearing variants -900A, -864G, according to Acc#.: AB008822
pOPG-D2H4-159C/luc	reporter gene construct, 924 bp of *OPG* 5'-flanking region, bearing variants -900A, -864G, -159C, according to Acc#.: AB008822
pOPG-Del3/luc	reporter gene construct, 665 bp of *OPG* 5'-flanking region, according to Acc#.: AB008822

pOPG-Del3-159C/luc	reporter gene construct, 665 bp of *OPG* 5'-flanking region, bearing variant -159C, according to Acc#.: AB008822
pOPG-Del4/luc	reporter gene construct, 275 bp of *OPG* 5'-flanking region, according to Acc#.: AB008822

2.7. Bacteria (E.coli)

Strain	***Genotype***	***Reference***
DH5α (K12)	F^- φ80lacZΔM15 Δ(lacZYA-argF) U169 recA1 endA1 hsdR17(r_k^-, m_k^+) phoA supE44 thi-1 gyrA96 relA1 λ^-	Invitrogen, Karlsruhe
Mach1™	derivatives of E.coli W strains ΔrecA1398 endA1 tonA Φ80ΔlacM15 ΔlacX74 hsdR(r_K^- m_K^+)	Invitrogen, Karlsruhe

2.8. Eucaryotic cells

Line	***Origin***	***Reference***
SaOs-2	Human osteogenic sarcoma	DSMZ no.: ACC 243
U2Os	Human osteosarcoma	ATCC no.: HTB-96
HEK293T	Human embryonic kidney	ATCC no.: CRL-11268
MCF-7	Human breast adenocarcinoma	DSMZ no.: ACC 115

2.9. Hardware and equipment

Instrument	***Type***	***Manufacturer***
Autoclave	FVS-2	Fedegari, Albuzzano, Italy
	Systec VX-75	Systec, Wettenberg
Cell Counter	Casy® Model TT	Innovatis, Bielefeld
CO_2-Incubator (eukaryotic cells)	MCO-18AIC	Sanyo, Munich
Developing machine	Optimax	Protec, Oberstenfeld

Gel electrophoresis chamber (Acrylamid)	Mini PROTEAN®	BioRad, Munich
	NuPage Novex MiniCell	Invitrogen, Karlsruhe
Gel electrophoresis chamber (Agarose)	StarPhoresis	Starlab, Ahrensburg
Gel Imaging	AlphaImagerEC	Alpha Innotech Corp, San Leandro, USA
Sterile Hood (bacteria)	BSD4	Gelaire, Sydney, Australia
Sterile Hood (eukaryotic cells)	HS 12	Heraeus, Hanau
Luminometer	Sirius V12	Berthold Detection Systems, Pforzheim
Microbiological incubator	B 6120	Heraeus, Hanau
Microscope	Axiovert 40 CFL	Zeiss, Jena
pH-Meter	Calimatic 766	Knick, Dülmen
Photometer	Nanophotometer	Kisker, Steinfurt
Scales	Sartorius excellence	Sartorius, Göttingen
Sequence detection system	7500 ABIprism	Applied Biosystems, Foster City, USA
Shaker	GFL 3006	GFL, Großburgwedel
Shaker (bacteria)	Incubator Shaker Series 25	New Brunswick Scientific, Nürtingen
Tank Blot Chamber	Mini Trans-Blot® Cell	BioRad, Munich
Thermocycler	PTC-225, PTC-240	MJ Research, Miami, USA
	DNA Engine Tetrad (2)	
Thermomixer	Thermomixer compact	Eppendorf, Hamburg
UV-table	Transilluminator	Intas, Göttingen
Power Supply	PowerPackBasic	BioRad, Munich
Vortexer	VortexGenie2	Bender&Hobein, Zurich, Switzerland
	BioVortex V1	Kisker, Steinfurt
Waterbath	GFL 1083	GFL, Großburgwedel
Centrifuges	Multifuge 3SR	Heraeus, Hanau
	Centrifuge 5415C	Eppendorf, Hamburg
	Centrifuge 5417R	Eppendorf, Hamburg
	Centrifuge 5810R	Eppendorf, Hamburg

3. Methods

3.1. Molecular biological methods

All standard molecular biological methods were performed as described by Sambrook and Russell [Sambrook and Russell, 2001], or according to manufacturers' application guidelines. Modifications are indicated where applicable.

3.1.1. Preparation of genomic DNA

Genomic DNA was extracted from white blood cells using the QIAamp® DNA Blood Mini Kit according to manufacturers' instructions (Qiagen). Briefly, 200 µL of human whole blood (EDTA-treated) were mixed with 20 µL Qiagen Protease (Proteinase K) and 200 µL buffer AL (binding buffer) and incubated at 56°C for 10 min. These lysate buffering conditions allow for optimal DNA-binding to the silica-gel membrane of the spin columns. After two washing steps, DNA was eluted from the spin column with either dH_2O or 10% (v/v) buffer AE (Qiagen).

3.1.2. Preparation of total RNA

Crude RNA was extracted using TRIzol® Reagent (Invitrogen) following the manufacturers' instructions. Briefly, confluent cells in a 75 cm^2 culture dish were washed twice with Dulbecco's phosphate buffered saline (PBS; w/o Mg^{2+}, Ca^{2+}) and directly lysed by adding 1 mL of TRIzol® Reagent. After 5 min incubation, addition of 200 µL chloroform, followed by centrifugation separated the probes into an aqueous and an organic phase. The aqueous phase was transferred into a fresh tube, and RNA was recovered by precipitation with isopropyl alcohol in the presence of 2.5 M lithium chloride, and washed with 75% (v/v) ethanol. The RNA pellet was dried and resolved in DEPC treated H_2O (RNase free).

3.1.3. Preparation of plasmid DNA

The method describes the purification of plasmid DNA from bacterial cells, following modified protocols of the originally described procedure [Birnboim and Doly, 1979]. For the isolation of plasmid DNA from E.coli cultures, the PureLink™ HiPure Plasmid DNA Purification Kit (Invitrogen) was used. Cells were spun down, resuspended in resuspension buffer containing RNase A, and lysed with lysis buffer. Precipitation buffer was added and the lysates centrifuged. Probes were routinely cleared from bacterial endotoxins by an additional incubation step with Endotoxin Removal Buffer A and washing with Endotoxin Removal

Buffer B. Afterwards the cleared lysate was loaded onto a pre-packed anion exchange column. Plasmid DNA was eluted with elution buffer, desalted and concentrated by an alcohol precipitation step.

For Maxi- or Mini- preparation, 100 mL or 2 mL of an overnight culture were used and plasmids eluted in 200 μL or 50 μL TE-buffer, respectively.

Endotoxin Removal Buffer A
50 mM MOPS, pH 7.0
750 mM sodium chloride
10% (w/v) Triton X-100
10% (v/v) isopropyl alcohol

Endotoxin Removal Buffer B
100 mM sodium acetate, pH 5.0
750 mM sodium chloride
1% (w/v) Triton X-100

TE-buffer
10 mM Tris-HCl, pH 8.0
1 mM EDTA

3.1.4. Photometric measurement of nucleic acid concentration

Concentration and purity of nucleic acids was measured photometrically using a nanophotometer (Implen). An optical density (OD) of 1 at 260 nm represents a concentration of 50 μg/mL of DNA or 40 μg/mL of RNA. The particular elution or storage buffers served as blank. The E_{260}/E_{280} ratio reveals the degree of purity, with 1.9 found in pure DNA preparations, and >2.0 in RNA solutions.

3.1.5. Standard Polymerase Chain Reaction (PCR)

The PCR was first introduced in 1986 by Mullis et al and describes an enzymatic amplification of DNA fragments *in vitro* with two specific oligonucleotides (primer) using a thermo resistant DNA polymerase (e.g. from *Thermus aquaticus* (*Taq*)) [Mullis et al, 1986]. All oligonucleotides used in single applications are listed in the appendix.

Standard PCR reaction

1x *Taq* polymerase buffer
0.6 U DNA *Taq* polymerase
200 μM of each dNTP
10 μM of each primer
5 ng of genomic DNA
nuclease free water to 25 μL

Standard PCR program

Initial denaturation	95°C, 5 min	
Denaturation	95°C, 1 min	
Annealing*	x°C, 45 sec	33 cycles
Elongation	72°C, 90 sec	
Terminal elongation	72°C, 10 min	

*Annealing temperatures depended on primer sequence and were calculated as [Tm – 3°C].

Four modifications were applied when necessary:
- "Hot start PCR": Thermocycler was pre-heated to 95°C before placing the reaction tubes into.

- "Touch down PCR": To address problematic sequences, annealing temperatures were gradually decreased. The annealing temperature was set 5-10°C over the primer annealing temperature and reduced by 2°C every second cycle until the correct annealing temperature was reached, and applied for the remaining number of cycles. This procedure allows for an enrichment of specific PCR products over any non-specific products [Don et al, 1991].

- "Nested PCR": Use for very weak amplification signals. Amplicons from the first PCR run undergo a second run with a second set of primers located within the first amplified fragment. The higher amount of template in the second PCR run should ensure higher amplification results and specificity.

- “Real time PCR”: This technique is used to amplify and simultaneously quantify the targeted DNA sequence. It enables both detection and quantification (as absolute number of copies or relative amount when normalized) of a specific sequence in a DNA sample. The procedure follows the general principle of polymerase chain reaction; its key feature is that the amplified DNA is quantified as it accumulates in the reaction in *real time* after each amplification cycle. Quantification occurs with the use of fluorescent dyes that intercalate with double-stranded DNA.

3.1.5.1. Reverse Transcriptase PCR (RT-PCR)

Generation of cDNA was performed with First Strand cDNA Synthesis Kit (Fermentas). One µg total RNA was mixed with oligo(dT) primers and incubated with Moloney Murine Leukemia Virus (M-MuLV) reverse transcriptase for one hour at 37°C. The reaction was heat inactivated at 70°C for 10 min. To detect endogenous expression of OPG, cDNA was used as template for amplification with specific primers (see appendix) in a semi-quantitative hot start PCR. Intactness and purity of the cDNA was routinely controlled by diagnostic PCR for human Ribosomal Protein 27 (hRP27).

3.1.5.2. Rapid amplification of 5’ cDNA ends (RACE)

RACE represents an appropriate method for identification and characterization of 5’ ends from RNA message. RACE PCR was performed as described previously [Frohman et al, 1988], using the 5’/3’ RACE kit (Roche). This technique differs from conventional PCR in that it requires knowledge of only a small region of sequence within the target RNA. Briefly, RNA was extracted from SaOs-2 and U2Os cells and first strand cDNA was generated using an *OPG* specific antisense primer, followed by d(A)tailing of the 3’ end using terminal desoxynucleotidyl transferase (TdT). With the use of an homopolymeric d(T)-anchor primer, complementary to the 3’ poly(A) tail, and an antisense primer located within the gene, the second strand was synthesized and sequenced (for primer sequences see appendix).

First strand cDNA synthesis

4 μL Synthesis buffer
2 μL dNTP mixture
1 μg total RNA
1 μL cDNA synthesis primer
1 μL Reverse Transcriptase
ad ddH_2O to 20 μL

Synthesis reaction

55°C	60 min
85°C	5 min

Poly(A) tailing

2.5 μL reaction buffer
19 μL purified cDNA sample
2.5 μL dATP (2 mM)
incubate 3 min at 95°C,
add 1 μL TDT (80 U/μL)
incubate for 30 min at 37°C,
heat inactivate for 10 min at 70°C

PCR amplification of d(A)-tailed cDNA

5 μL d(A)-tailed cDNA
1 μL d(T) anchor primer
1 μL antisense primer
1 μL dNTP mixture
0.5 μL *Taq* polymerase
appropriate amount of reaction buffer
ad ddH_2O to 50 μL

PCR reaction

Initial denaturation	94°C, 2 min	
Denaturation	94°C, 15 sec	
Annealing*	x°C, 30 sec	10 cycles
Elongation	72°C, 40 sec	
Denaturation	94°C, 15 sec	
Annealing*	x°C, 30 sec	25 cycles
Elongation**	72°C, 40 sec	
Final Elongation	72°C, 7 min	

*Annealing temperatures depended on primer sequence and were calculated as [Tm – 3°C].
**Each successive cycle was elongated by additional 20 sec (e.g. for cycle no. 10 is 40 sec, for cycle no. 11 is 60 sec, for cycle no. 12 is 80 sec etc.).

3.1.6. DNA/RNA modifying reactions

3.1.6.1. Restriction endonucleases

For restriction reactions with endonucleases up to 1 μg of DNA and 1 unit of the appropriate endonuclease were used. H_2O and 10x reaction buffer were added to a total volume of 20 μL, incubated for 1 hour at 37°C (depending on the optimal temperature of the used enzyme), and heat-inactivated at 70°C for 10 min.

3.1.6.2. Dephosphorylation of DNA

Restriction with one endonuclease results in compatible ends, which are able to religate. Dephosphorylation of 5' ends of linearized plasmid DNA disables religation and was performed using Shrimp Alkaline Phosphatase (SAP). One unit of SAP, the appropriate amount of 10x reaction buffer, and dH_2O were added to the digestion reaction (see 3.1.6.1) to a total volume of 25 μL. Reaction mixtures were incubated at 37°C for 30 min and heat-inactivated for 10 min at 65°C. Efficiency of dephosphorylation was controlled by religation and transformation (see 3.3.1.3).

3.1.6.3. 3'-end labeling of single-stranded oligonucleotides and subsequent annealing

Single-stranded oligonucleotides (30 bp) for EMSA experiments were synthesized at a minimum coupling efficiency of >98.5% and purified twice by high pressure liquid chromatography (HPLC) (IBA, Göttingen). These single-stranded probes, as well as double-stranded PCR products, were 3'-biotinylated with biotin-16-ddUTP (Roche) using a TdT. Per reaction, 5 pmol of each probe were labeled in a reaction mix containing 2 mM $CoCl_2$, 500 pmol biotin-16-ddUTP, and 60 U TdT at 37°C for 30 min. Excess biotin molecules were removed via phase separation with chloroform. The following centrifugation step (2 min at high speed) separated the solution into an organic and aqueous phase, the latter containing the labeled probe. PCR products were purified via column-wash using High Pure PCR Product Purification Kit (Roche).

Since double-stranded blunt or recessed 3' termini are poor substrates for TdT, oligonucleotides were labeled prior to annealing. For PCR fragments, *Taq* polymerase was used, which adds a protruding adenosine to the 3' end. To generate double-stranded oligonucleotides, 20 fmol of each primer were mixed in 100 mM NaCl, heated at 95°C for 5 min, and then slowly cooled down to room temperature (RT) over night. To generate double-stranded, but unlabeled oligonucleotides, 2 pmol of each unlabeled primer were used for annealing reaction. Annealing was controlled routinely by gel electrophoresis.

3.1.7. Agarose gel electrophoresis

In an electric field, DNA migrates because of its negatively charged phosphate backbone. Agarose concentrations of 1% to 3% were applied in 1x TAE buffer, depending on fragment sizes.

50x TAE	***6x Loading buffer***
2 M Tris base	0.02% (w/v) bromphenole blue
50 mM EDTA	0.02% (w/v) xylene xyanole
adjust to pH 8.0	30% (v/v) glycerol
with acetic acid	20 mM Tris-HCl, pH 7.6
	2 mM EDTA

For visualizing DNA double-strands, 0.05 μg/mL ethidium bromide (EtBr) was added to the gel solution.

3.1.8. Site-directed mutagenesis

In vitro site-directed mutagenesis is a valuable technique for modifying vector sequences to facilitate cloning and expression strategies. Within this work, site directed mutagenesis was used for introducing genetic variants into the respective reporter gene vectors (QuikChange®Multi Site-directed Mutagenesis Kit, Stratagene). Allelic variants -960C, -900A, and -864G were introduced into the deletion constructs pOPG-Del1/luc and pOPG-Del2/luc as follows: Mutant strand synthesis was performed by denaturation of input DNA, followed by annealing and extension of the mutagenic primers (see appendix), and ligation of nicks. In a subsequent step, methylated and hemimethylated DNA was digested with *Dpn*I (1 hrs, 37°C), and mutated single-strand DNA was transformed into Mach1™ competent cells.

Standard Reaction (templates > 5 kb)	***Standard mutagenesis PCR program***	
2.5 μL QuikChange®Multi reaction buffer	Initial denaturation	95°C, 5 min
0.5 μL Quik Solution		
100 ng template DNA	Denaturation	95°C, 1 min
100 ng of each mutagenic primer	Annealing	55°C, 1 min
1 μL dNTP mix	Elongation	65°C, 12 min
1 μL QuikChange® Multi enzyme blend		(1 min per 1 kb)
	30 cycles	

3.1.9. Construction of reporter gene plasmids

Promoter fragments were generated using genomic DNA from a volunteer, bearing the respective variants, as template (oligonucleotide sequences see appendix). One fragment included the TATA-box of the *OPG* promoter and a proximal variant (constructs pOPG-159T/luc, pOPG-159C/luc), the other harboring four distal variants, representing three molecular haplotypes (constructs pOPG-wt/luc, pOPG-MolHap2/luc, pOPG-MolHap4/luc). For the latter a 249 bp fragment was amplified using sense primers located -1020 bp upstream the major TSS (defined in Accession number AB008822), linked to a *Sac*I site, and antisense primers located -772 bp upstream the TSS, linked to a *Nhe*I site. The TATA-box harboring fragment (275 bp) was generated using sense primers at position -287 bp upstream the TSS linked to a *Sac*I site, and antisense primers at position -13 bp upstream the TSS linked to a *Bgl*II site. For deletion constructs the same antisense primer was used, sense primers (linked to a *Sac*I site) were positioned at -1020 bp for the pOPG-Del1/luc construct (1008 bp), at -936 bp for the pOPG-Del2/luc construct (924 bp), at -677 bp for the pOPG-Del3/luc construct (665 bp), and at -287 bp for the pOPG-Del4/luc construct (275 bp). For generation of deletion constructs, genomic DNA with the wild type sequence was used. Further, three additional deletion constructs were generated, each harboring distinct allelic variants: (I) pOPG-D1H2/luc, being congruent with pOPG-Del1/luc, but harboring the -946G allele, (II) pOPG-D1H4/luc, being congruent with pOPG-Del1/luc, but harboring alleles -960C, -946G, -900A, and -864G, and (III) pOPG-D2H4/luc, being congruent with pOPG-Del2/luc, but harboring alleles -900A and -864G. Introduction of the respective SNPs was performed via site-directed mutagenesis using vectors pOPG-Del1/luc and pOPG-Del2/luc as template DNA (see 3.1.8). Each of the mentioned deletion constructs was generated harboring either the -159T or -159C allele.

For transient transfection assays the generated PCR fragments were linked to the promoter-less luciferase reporter gene vector pGL3basic (Promega). Therefore, purified PCR fragments were cloned into the pCR®II TOPO® cloning vector and transformed in competent DH5α bacterial cells (see 3.3.1.3). After plasmid preparation and purification, TOPO-constructs were double digested with the respective restriction endonucleases (see 3.1.6.1). Inserts were purified and subcloned in 5'-3' orientation into the respective sites of the luciferase reporter gene vector pGL3basic (Promega) in a 1:3 ratio in favor of the insert. For ligation, 1 U of T4 DNA ligase (Fermentas), the appropriate amount of 10x T4 reaction buffer and dH_2O to a total volume of 20 µL was used. All reporter constructs were directly sequenced (see 3.1.11) to ensure sequence accuracy and identity.

Standard pCR®II TOPO® cloning reaction

1 µL salt solution (1.2 M NaCl, 0.06 M $MgCl_2$)

1 µL pCR®II TOPO cloning vector (10 ng/µL)

4 µL purified insert

To control reporter gene vector religation, a standard ligation mixture was prepared, without adding the purified insert, and transformed into bacterial cells DH5α (see 3.3.1.3).

The isolated 249 bp promoter fragments (-1020/-772) were cloned into the reporter gene vector ptk81-luc3 (a kind gift of Dr. T. Kimura) using the Gateway® cloning system (Invitrogen). The ptk81-luc3 represents a "self-made" reporter gene vector based on pGL3basic (Promega). A 132 bp fragment of the thymidine kinase promoter (-81/+52, V00470) was cloned in 5'-3' direction into pGL3basic. The resulting reporter gene vector ptk81-luc3 allows for the assembly of the basic transcription machinery, but lacks enhancer performance (Figure 13).

The Gateway® cloning technique is based on site-specific recombination properties of bacteriophage λ [Landy et al, 1989]. These events occur by recombination at specific attachment sequences on phage DNA (*attP*) and bacteria DNA (*attB*). The recombination process begins, when several molecules of the phage-coded integrase and the bacterial integration host factor (IHF) bind tightly to *attP*. The complex then couples with *attB* in the bacterial chromosome, followed by strand exchange and thereby generating flanking two-hybrid *att* sites (*attL* and *attR*) (BR reaction). The reaction can be reversed by addition of the phage-encoded Xis enzyme (LR reaction). Purified PCR fragments were cloned into the entry vector pCR®8/GW/TOPO®, where the fragment is flanked by *attL* sequences, and transformed in competent Mach1™ bacterial cells (see 3.3.1.3). After plasmid preparation, the entry clone was mixed *in vitro* with the destination vector ptk81-luc3 that carries *attR*

sites. Addition of the LR® Clonase enzyme mix (Invitrogen) results in an expression clone carrying the 249 bp promoter fragment (Figure 12).

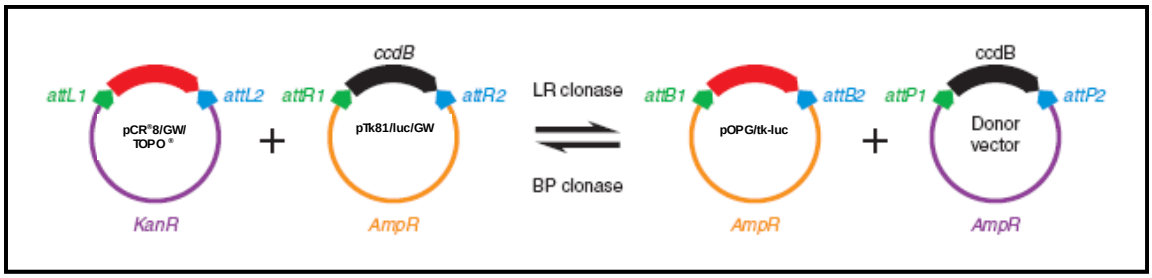

Figure 12 Gateway assisted subcloning. Schematic representation of the four Gateway vectors and enzymes involved in cloning reactions. The red arrows represent the fragment of interest. [adapted from Katzen, 2007].

Standard pCR®8/GW/TOPO® cloning reaction

1 µL salt solution (1.2 M NaCl, 0.06 M $MgCl_2$)
1 µL pCR®8/GW/TOPO cloning vector (10 ng/µL)
4 µL purified insert
incubation for 5 min at RT,
transformation in competent
Mach1™ bacterial cells

LR® clonase reaction

100 ng entry vector
150 ng destination vector
2 µL LR clonase
add 8 µLTE-buffer
incubation for 1 hr at 25°C
add 1 µL Proteinase K
incubation for 10 min at
37°C

3.1.10. Purification of DNA fragments

Purification of DNA fragments for subsequent applications, like ligation or sequencing, was performed either by gel extraction, column wash or enzymatic reaction.

Gel extraction was performed using QIAquick® Gel Extraction Kit (Qiagen). After agarose gel electrophoresis, the DNA fragments were excised from the gel, mixed with buffer QG and heated 10 min at 50°C for dissolving the gel slice. After applying the sample onto the silica membrane of the column, the column was washed two times and DNA was eluted in dH_2O.

For purifying PCR products for further enzymatic reactions or sequencing, the High Pure PCR Product Purification Kit (Roche) was used. PCR reactions were mixed with binding buffer and load onto a column. After two washing steps, the DNA was eluted in dH_2O.

A rapid one-step PCR clean-up for subsequent sequencing reactions was performed with the ExoSAP-it protocol. A mixture of exonuclease I and shrimp alkaline phosphatase (SAP) (both Fermentas) was used to digest small single-stranded fragments (e.g. primers) and to remove dNTP's.

ExoSAP-it mixture

20 U exonuclease I
10 U shrimp alkaline phosphatase (SAP)
ad dH_2O to 100 μL

Purification protocol

1 μL of ExoSAP-it mix was used for 5 μL PCR products, incubated at 37°C for 30 min, and heat-inactivated for 15 min at 80°C.

3.1.11. Sequencing

Samples were sequenced (both strains) for detection and localization of genetic variants, and to ascertain correctness of DNA fragments and plasmid constructs using an automated ABI 3730 fluorescence sequencer with big dye terminator chemistry (PE Applied Biosystems) (oligonucleotide sequences see appendix).

Standard sequencing reaction

5-50 ng purified PCR fragment or 120 ng plasmid DNA
1.6 μM primer
5x BigDye buffer
1 μL BigDye 3.1
ad dH_2O to 10 μL

Probes were sequenced using the sequencing service of the University Hospital of Münster.

3.1.12. Electrophoretic Mobility Shift Assay (EMSA)

An Electrophoretic Mobility Shift Assay (EMSA) is a common technique to investigate DNA:protein interactions. This assay offers the possibility to determine whether a nuclear protein extract is capable of binding to a given DNA sequence. A mobility shift assay involves the electrophoretic separation of the DNA:protein complexes in a native PAGE. The

velocity at which molecules and molecule-complexes move through the gel is determined by their size and charge. A control lane contains a single band representing the unbound DNA probe. Assuming that a protein is capable of binding to the given sequence, the lane in which protein is present will contain a "shifted" band, representing a larger, less mobile DNA:protein complex.

EMSAs were performed using the LightShift Chemiluminescent EMSA Kit (Thermo Fisher). Per reaction, 5 μg nuclear protein extracts were incubated in binding buffer with 500 ng pre-sheared poly dI●dC:dA●dT (1:2) as non-specific competitor, 250 mM Betaine, 5 mM $MgCl_2$ and a 200-fold molar excess of unlabeled oligonucleotide as specific competitor for 15 min at RT. After addition of the labeled OPG probe (see 3.1.6.3), reactions were incubated for another 45 min on ice, then submitted to a 6% native PAGE (0.5x TBE; 100 V), and blotted onto PVDF membranes (see 3.2.6) (0.5x TBE; 100 V; 60 min). Subsequently, DNA probes were cross-linked to the membrane by UV-light (312 nm) for 10 min.

4x binding buffer
20 mM $MgCl_2$
240 mM KCl
40 mM HEPES/KOH, pH 7.9
5 mM spermidine
16% (w/v) Ficoll

6% PAGE
2 mL AA/BA, 30%
1 mL 5x TBE
83.7 μL APS, 10%
3.7 μL TEMED
ad dH_2O to 10 mL

5x TBE
45 mM Tris base
45 mM boridic acid
10 mM EDTA

After blotting, bands were visualized by Chemiluminescent Nucleic Acid Detection Kit (Thermo Fischer). First, membranes were blocked in blocking buffer containing streptavidin-horseradish peroxidase conjugate. After four washing steps, membranes were incubated in substrate equilibration buffer, and subsequently incubated for 5 min in substrate working solution, consisting of luminol/enhancer solution and stable peroxidase solution, followed by exposure to CL-X Posure Film (Thermo Fischer) for 30 sec to 5 min.

3.1.13. Chromatin Immunoprecipitation Assay (ChIP)

Chromatin Immunoprecipitation (ChIP) assays are used to evaluate the association of proteins with specific DNA regions. The technique involves crosslinking of proteins with

DNA, fragmentation and preparation of soluble chromatin followed by immunoprecipitation with an antibody recognizing the protein of interest. The segment of the genome associated with the protein is then identified by PCR amplification of the DNA in the immunoprecipitates. ChIP was performed as described previously [Boyd et al, 1998; Liu et al, 2000]. About 10^8 cells were fixed by adding formaldehyde to a final concentration of 1% (v/v) and incubated by modest shaking for 30 min at RT. After that cells were washed twice with cold PBS (Sigma). The pellet was then resuspended, lysed, and nuclei were isolated and sonicated until the chromatin had an average length of 500-1500 bp. After centrifugation the supernatant was incubated with 3 μg of antibody against Sp1 (Upstate), NF-1 (St. Cruz), and Egr1 (Cell Signalling) over night at 4°C for immunoprecipitation. The next day 10 μL of magnetic Protein-G beads (Invitrogen) were added and further incubated at 4°C for 1-3 hrs. After extensive washing the antibody/transcription factor/DNA complex was eluted from the beads, subsequently formaldehyde crosslinks were reversed and proteins were digested with proteinase K at 67°C over night. The DNA was extracted by phenol/chloroform/isoamyl alcohol, washed with 75% (v/v) ethanol, resuspended in water, and used for PCR.

3.2. Protein biochemical methods

3.2.1. Extraction of crude proteins

Crude protein extracts from cells were harvested by scraping the cells in lysis buffer. Nuclei and debris were removed by centrifugation at 4°C for 5 min at 12.000xg, pre-heated 4x SDS-PAGE sample buffer was added immediately to the supernatants and heated to 95°C for 5 min prior to aliquoting and freezing.

Lysis buffer

20 mM imidazole, pH 6.8
100 mM KCl
1 mM $MgCl_2$
10 mM EGTA
0.2% (v/v) Triton X-100
10 mM NaF
1 mM sodium vanadate
1 mM sodium molybdate
10 mM sodium pyrophosphate
25 mM β-glycerophosphate

4x SDS sample buffer

200 mM Tris-HCl, pH 6.8
8% (w/v) SDS
0.4% (w/v) bromphenol blue
40% (v/v) Glycerol

3.2.2. Extraction of nuclear proteins

Nuclear protein extracts were harvested by a modified procedure of the protocol published by Schreiber et al [Schreiber et al, 1989]. Briefly, 10^7 cells were washed twice with cold PBS. After scraping and transfer into centrifugation tubes, cells were spun down for 2 min at 5000xg at 4 ºC. Pellets were resuspended in a “low salt” buffer and allowed to swell on ice for 15 min. After addition of detergent NP-40 and another centrifugation step, the supernatant containing the cytosolic protein fraction was removed from the pellet. This was resuspended in a “high salt” buffer. After 30 min of incubation, the cellular debris was spun down, the nuclear protein fraction aliquoted, snap frozen, and kept at –70°C.

"low salt" buffer
10 mM HEPES, pH 7.9
10 mM KCl
1 mM DTT
1.5 mM $MgCl_2$
protease inhibitor cocktail (complete)

"high salt" buffer
20 mM HEPES, pH 7.9
0.2 mM EDTA
1 mM DTT
420 mM NaCl
1.5 mM $MgCl_2$
0.5 mM PMSF
25% (v/v) Glycerol
protease inhibitor cocktail
(complete, w/o EDTA)

3.2.3. Measurement of protein content

The protein content of nuclear extracts was measured using the BCA™ Protein Assay Kit (Thermo Fischer). A series of dilutions with known concentrations was prepared from bovine serum albumine (BSA), serving as standard protein. Protein concentrations were detected photometrically and calculated with reference to the standard curve.

3.2.4. SDS-Polyacrylamid Gel Electrophoresis (PAGE)

Intactness of nuclear protein extracts was routinely ascertained by PAGE and Coomassie blue staining. Therefore, 5 μg of each probe were mixed with 4x SDS sample buffer and loaded onto a 10% SDS gel as described by Rittenhouse and Marcus [Rittenhouse and Marcus, 1984].

SDS is an anionic detergent which denatures secondary and non-disulfid-linked tertiary structures, applying a negative charge to each protein in relation to its mass and thereby creating a nearly uniform negative charge along the length of the polypeptide. The distance of the migration in the gel can therefore be assumed to be directly proportional to the size of the protein.

Stacking gel (4%)

560 µL AA/BA, 30%
675 µL 0.5 M Tris-HCl, pH 6.8
675 µL 0.5 M imidazole, pH 6.8
75 µL SDS, 10%
5 µL TEMED
40 µL APS, 10%
ad dH_2O to 4.2 mL

Run at 80 V, approximately for 30 min

Running gel (10%)

2.5 mL AA/BA, 30%
1.9 mL 1.5 M Tris-HCl, pH 8.8
75 µL SDS, 10%
5 µL TEMED
25 µL APS, 10%
ad dH_2O to 7.5 mL

Run at 130 V, duration depending on protein sizes

1x SDS running buffer

25 mM Tris base
192 mM glycine
1% (w/v) SDS

3.2.5. Coomassie blue staining

Protein bands were visualized by incubation of the gel in Coomassie blue staining solution, followed by two destaining steps of 30 min each.

Coomassie staining solution

0.25% (w/v) Coomassie™ Brilliant Blue R-250
45% (v/v) methanol
10% (v/v) acetic acid

Destaining solution I

45% (v/v) methanol
10% (v/v) acetic acid

Destaining solution II

5% (v/v) methanol
5% (v/v) acetic acid

3.2.6. Western Blot (tank blot)

From each cell extract, 10 µL were subjected to a 10% SDS-PAGE as described before [Rittenhouse and Marcus, 1984], and blotted onto a PVDF membrane following the Towbin tank blot protocol [Towbin et al, 1979]. Briefly, a PVDF membrane was activated in methanol and placed onto the gel, covered with two sheets of whatman-paper on each site. Air bubbles were removed carefully. The “sandwich” was put into a gel holder cassette with fiber

pads on each site, and placed vertically into the blotting buffer tank. Blots were run for 1 hr at 100 V at RT, but using cooling units.

1x Blotting buffer

25 mM Tris base
192 mM glycine
10% (v/v) methanol

After blotting, membranes were allowed to dry completely over night and re-activated in methanol the next day. Blocking of non-specific binding sites was performed by hybridizing the membranes in blocking solution for 30 min at RT. Proteins of interest were detected by immunodetection using specific antibodies (see 2.5) at a dilution of 1:1000 for 1 hrs at RT with gentle agitation. Secondary antibodies were given at a dilution of 1:10.000. The samples' even-loading was ascertained by immunodetection of Mitogen Activated Protein Kinase 2 (MAPK2) (Nanotools).

Blocking solution

0.5% (w/v) casein
1% (w/v) PEG-4000
1% (w/v) PVP-10
0.1% (v/v) Tween-20
in 2x PBS

Washing solution (1x TBS-T)

100 mM Tris base
1.5 mM NaCl
0.03% (v/v) Tween-20
adjust to pH 7.4

3.3. Cell biological and microbiological methods

3.3.1. Prokaryotic cells

3.3.1.1. E.coli

Bacteria were cultured at 37°C either in liquid medium (lysogeny broth (LB)-medium) or plated on agar plates. Antibiotics were added for specific selection of transformed bacteria. For long term storage 15% (v/v) glycerol was added to an over night liquid culture and stored at –80°C.

LB-Medium

10 g Bactotryptone
10 g Sodium chloride
5 g Yeast extract
ad dH_2O to 1000 mL, pH 7.0

Autoclave at 121°C for 20 min

LB-Agar

15 g Bacto agar in 1000 mL LB-Medium

Autoclave at 121°C,
cool down to 56°C,
add appropriate antibiotics
(e.g. 100 μg/mL ampicilline)

3.3.1.2. Generation of competent cells

Competent bacterial cells were generated as follows: 200 mL of LB-medium were inoculated with *E.coli* cells and grown to an OD_{600} 0.5-0.6. After 20 min of incubation in an ice bath with gentle agitation, cells were harvested at 4000xg for 15 min (4°C), pellets resuspended in 10 mL $MnCl_2$-transform buffer, and kept on ice for 10 min, followed by another centrifugation step (3000xg, 10 min, 4°C). Finally, pellets were resuspended in 7.4 ml $MnCl_2$-transform buffer and mixed gently, followed by dropwise addition of 560 μL DMSO. Aliquots of 100 μL were snap frozen in liquid nitrogen and kept at –80°C. All equipment was properly chilled prior to processing the bacteria.

$MnCl_2$-transform buffer

10 mM HEPES, pH 6.8
15 mM $CaCl_2$
20 mM KCl
55 mM $MnCl_2$

3.3.1.3. Transformation

An aliquot of competent cells (100 μL) was thawed on ice, mixed with 4-6 μL of ligation reaction or 20 ng plasmid DNA, kept on ice for 25 min, heat-shocked at 42°C for 45 sec, and briefly cooled on ice for 2 min. Five-hundred μL LB-medium were added and cells gently shook for 35 min at 37°C. Thereof, 150 μL were plated onto antibiotic agar plate and incubated over night at 37°C.

3.3.2. Eukaryotic cells

3.3.2.1. Cell culture

The human osteoblast-like osteosarcoma cell lines SaOs-2 and U2Os, the human embryonic kidney cell line HEK293T, and the breast cancer cell line MCF-7 were maintained in Dulbecco's Modified Eagle Medium without phenol red with 10% (v/v) fetal calf serum (PAA), 100 U/mL penicillin, 100 μg/mL streptomycin, 2 mM/mL L-Glutamine (all GIBCO), and 1 mM sodium pyruvate (Sigma). For cultivation of HEK293T iron-supplemented fetal calf serum was used (Cell Concepts). In case, cells were stimulated with 10^{-8}M 17β-Estradiol (E2, Sigma), and/or 2 ng/mL recombinant tumor necrosis factor-α (TNFα; Calbiochem). When reaching confluence, cells were detached from surface by trypsination for 2 min and splitted at appropriate ratios for further cultivation.

3.3.2.2. Storage

For long term storage, cells were washed twice with PBS, trypsinated, and transferred to fresh medium. After centrifugation, cells were placed on ice and resuspended in fetal calf serum (FCS) containing 10% (v/v) DMSO. Cells were stored at –80°C and transferred to liquid nitrogen the next day.

Thawing cells was performed as quickly as possible, in a waterbath at 37°C. To remove DMSO from the freezing medium, cells were washed with PBS and transferred into pre-warmed medium after centrifugation.

3.3.2.3. Transient transfection

The osteoblast-like cell lines SaOs-2 and U2Os were transfected using Effectene transfection reagent (Qiagen). Per reaction 50.000 cells/well were plated in 24-well plates and transfected the next day. For both, SaOs-2 and U2Os, 0.2 μg DNA and 1.6 μL Enhancer solution were diluted in 60 μL buffer EC, and incubated for 5 min at RT. Subsequently, 4 μL

Effectene reagent was added, mixed gently, and incubated for 10 min at RT. After addition of 350 µL medium, cells were transfected with 415 µL transfection reagent for 10 hrs.

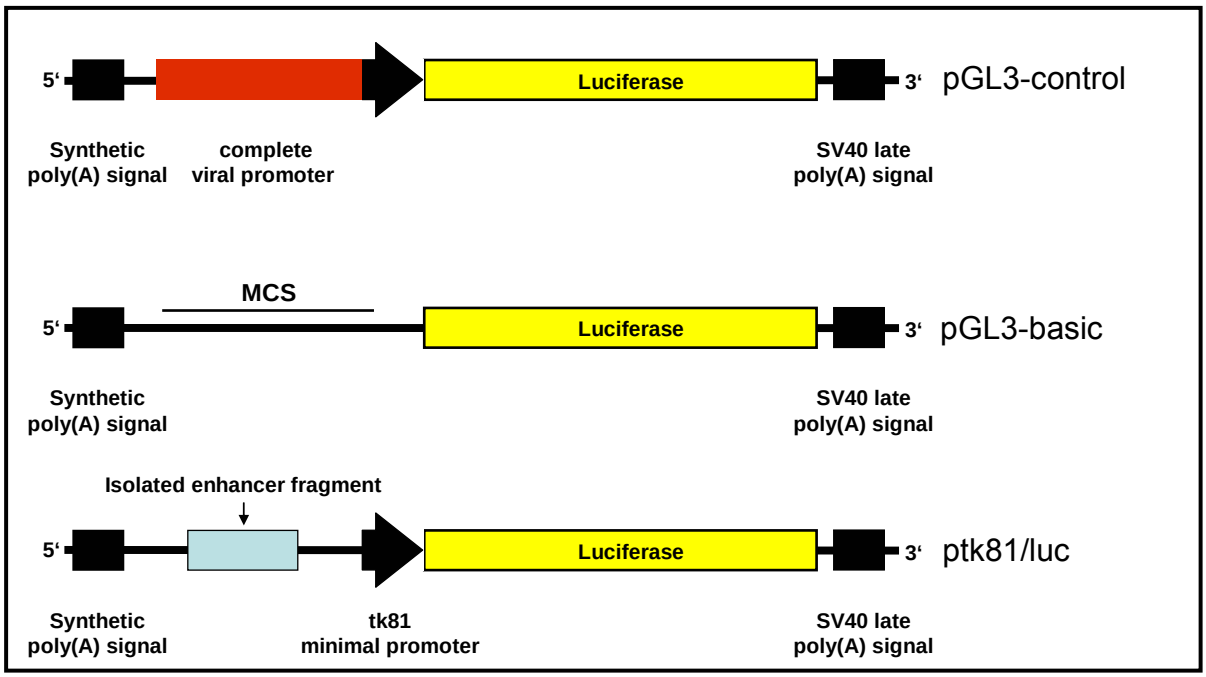

Figure 13 Schematic presentation of used reporter gene vectors. Construction of reporter gene vectors, containing either a strong viral promoter (pGL3control), a minimal promoter (ptk81-luc3), or no promoter (pGL3basic) was making it feasible to clone any promoter portion in front of the luciferase gene for detecting its transcriptional activity. With kind permission of R. Telgmann.

Cell lines HEK293T, EA.hy 926, and MCF-7 were transfected using Lipofectamine 2000 (Invitrogen). Cells were plated at a density of 100.000 cells per well in 24-well plates and transfected the next day. In brief, 0.8 µg DNA were diluted in 50 µL serum-free DMEM. Per reaction, 2 µL Lipofetamine 2000 were diluted in 50 µL serum-free DMEM and incubated for 5 min at room temperature. Subsequently, DNA dilution was added dropwise to Lipofectamine 2000 dilution, and incubated for 20 min at room temperature. Cells were exposed to the transfection reagent for 6 hrs. For both transfection procedures, cells were harvested 24 hrs post transfection with 100 µL Passive Lysis buffer (Promega), and luciferase activity was determined using a Sirius single-tube luminometer (Berthold detection systems). The cell lysate/luciferase substrate ratio was routinely 20 µL/75 µL.

Transfection of the truncated promoter constructs (deletion constructs) was performed in equimolar amounts of reporter vectors using the inert vector p0GH (Nichols Institute) for adjustment of DNA content. The pGL3control vector (Figure 13), in which transcription is driven by a powerful viral promoter served as positive control, the ptk81-luc3 vector, containing a minimal viral promoter but lacking enhancer performance, and the promoter-

less pGL3basic served as negative controls (Promega). Transfection experiments were repeated at least three times, in triplicates for each plasmid.

3.3.2.4. Cotransfection

In cotransfection experiments, a transient overexpression of a certain protein (e.g. transcription factor) is forced upon cells to analyze its possible effects on transcription of the cotransfected reporter gene. Therefore, an expression vector carrying the cDNA of distinct proteins was cotransfected with the reporter gene vector in a ratio of 3:1. In this study expression vectors for family members of the NF-1 family of transcription factors (pCH-A1.1, pCH-B2, pCH-X2, and pCH-C2 [a kind gift of Dr. Rich Gronostajski, Buffalo, USA]), Sp1, or Egr1 (a kind gift of Dr. Kerstin Duning, Münster, Germany) were used.

3.4. Study populations

The current investigation was based on the Münster Molecular Functional Profiling for Mechanism Detection (MolProMD) study. The Münster MolProMD Study is a prospective study of patients with CVD (MI, essential hypertension) and families, aimed at studying molecular genetic mechanism of CVD. The study was approved by the ethics committee of the Medical Faculty, Westfälische Wilhelms-University of Münster and written informed consent was obtained from all study subjects.

3.5. In silico binding analyses of putative TFBS

To analyze whether a polymorphic site potentially affects TFBS, a sequence flanking either side of the genetic variant was submitted to computational comparison using the AliBaba2.1 net-based and up-to-date TFBS search tool (http://www.gene-regulation.com/pub/databases.html) and the TRANSFAC7.0 database. Pairsim and minimal matrix conditions as well as factor type were adjusted and analyzed by cross checking with a different search engine (match; http://www.gene-regulation.com/cgi-bin/pub/programs/match/bin/match.cgi). AliBaba2.1 is a program for predicting binding sites of TFBS in an unknown DNA sequence. Therefore it uses the binding sites collected in TRANSFAC database and is currently the most specific tool for predicting TFBS. It pairwise aligns the known sites to the unknown sequence, forms small sets of sites by their position and their according class of factor, and constructs matrices from these sets representing the prediction [Grabe, 2002].

3.6. Statistical methods

P-values were calculated using the scientific analysis and presentation computer program "Graph Pad Prism 4.0/5.0". Significance was calculated by unpaired, two-tailed t test [C.I.=95%]; the significance levels were set at ***$p \leq 0.001$, **$p \leq 0.01$, and *$p \leq 0.05$.

4. Results

4.1. Identification of OPG gene variants and molecular promoter haplotypes (MolHaps)

In initial studies, the 5'-flanking region, exons, introns, and the 3'-flanking region of the *OPG* gene were scanned for alterations in genomic DNA from 95 patients of the ECTIM study. ECTIM (Etude Cas-Témoins de l'Infarctus du Myocarde) is a study of patients with MI from regions covered by the World Health Organization's Monitoring Trends and Determinants in Cardiovascular Disease (MONICA) registers and of control subjects (cases [n=988, mean±SD age 55.8±8.1 years, 26.2% women], controls (n=949, mean±SD age 56.6±8.3, 27.0% women]) [Cambien et al, 1992]. Altogether, 9 SNPs were identified, three of which were located in intronic regions (C1217T, Ins/Del/ct 6533/34, A8731C), two polymorphisms were found in exonic regions (one non-synonymous SNP in exon 1 [K3N], one synonymous SNP in exon 4 [A+832G]), and four SNPs located in the *OPG* gene promoter region (one proximal variant [T-159C] and three distal variants [A-946G, G-900A, T-864G]) (Figure 14).

Of the 5'-flanking region of the *OPG* gene, a portion of 275 bp bearing the T-159C (-287/-13) variant and a portion of 249 bp covering SNPs A-946G, G-900A, T-864G (-1020/-772) were amplified in an additional set of genomic DNA of 57 patients with MI and/or essential hypertension (MolProMD study). All polymorphisms of the 5'-flanking region, detected in the ECTIM study, were also found in patients of the MolProMD study. Further, polymorphism T-960C was identified exclusively in probes of the MolProMD study. All polymorphisms had previously been identified [Arko et al, 2002; Rhee et al, 2006; Langdahl et al, 2002; Brändström et al, 2002; Soufi et al, 2004].

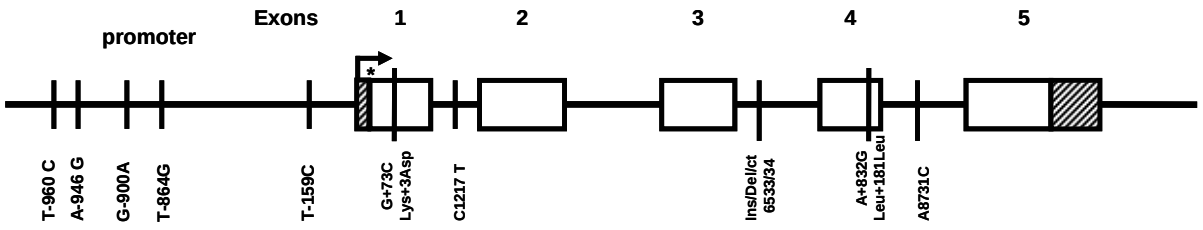

Figure 14 Schematic representation of the *OPG* gene architecture. The promoter, the 3'- and 5'-untranslated regions (dashed bars), the exons (blank bars), the major transcription start site (arrow), and the translation termination codon (asterisk) are indicated. Identified SNPs are indicated, for rs numbers see appendix, Table 1.

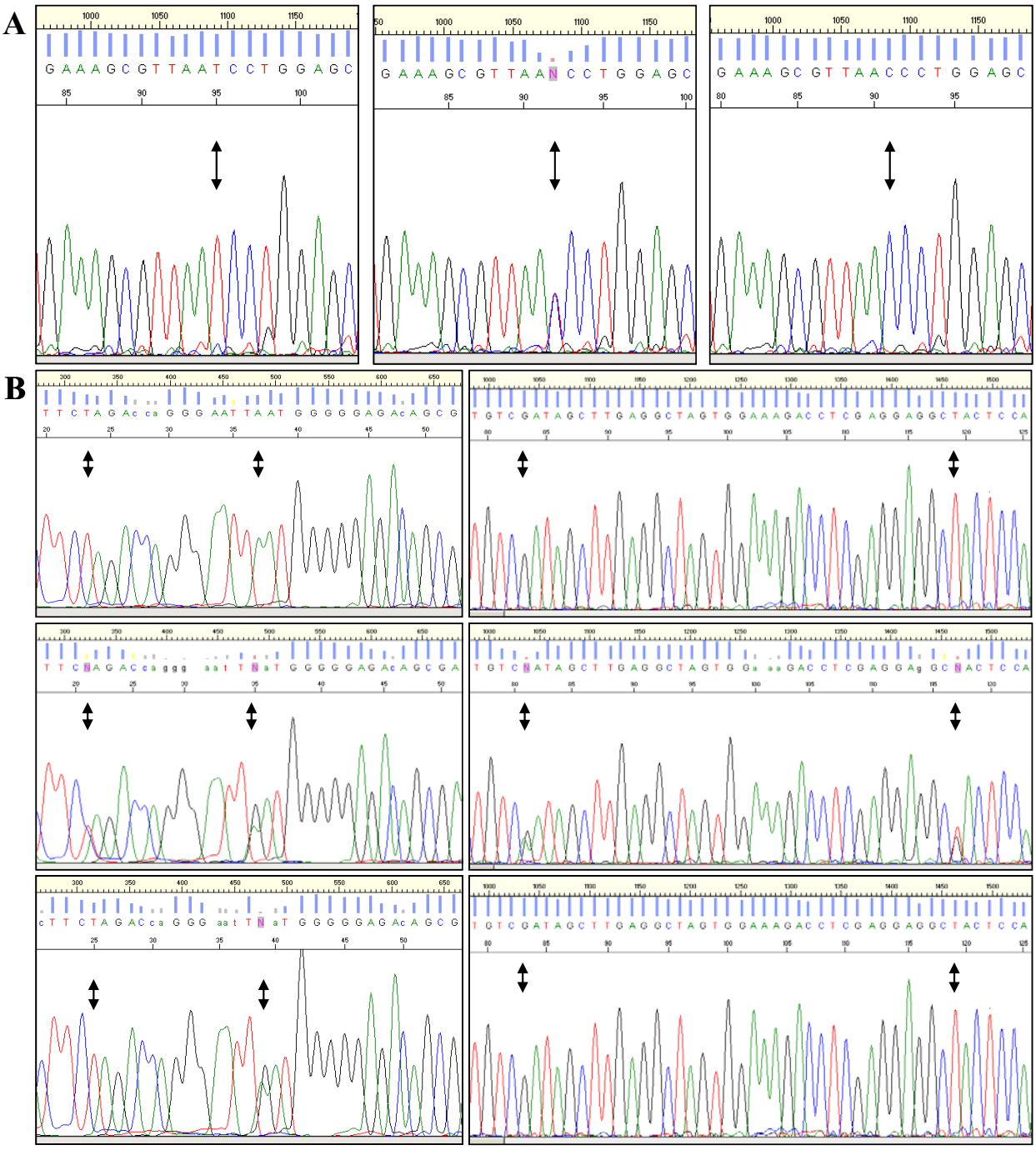

Figure 15 Sequence analyses of genomic DNA of 57 MolProMD patients. (A) Alleles TT, TC, and CC for -159; (B) homozygotic and heterozygotic occurrence for SNPs T-960C, A-946G, G-900A, T-864G.

The proximal polymorphism T-159C was found to be the most frequent variant occurring in 72.72% of the patients (CC [18.18%], TC [54.54%]). The homozygous wild type allele (TT) was found in 27.27% (Figure 15*A*). The distal SNPs T-960C, A-946G, G-900A, T-864G were found to be transmitted either homozygously for the common alleles (-960T, -946A, -900G, -864T) or heterozygously (-960TC, -946AG, -900GA, -864TG). Further, while alleles -946A and -946G were observed to be transmitted with the major alleles -960T, -900G, and -864T,

alleles -960TC, -900GA, -864TG where only transmitted in the presence of each other, and in the presence of -946A and -946G (Figure 15*B*).

To identify molecular promoter haplotypes (MolHaps) harboring SNPs T-960C, A-946G, G-900A, and T-864G, genomic DNA from 57 patients of the MolProMD study were screened. A 249 bp fragment (-1020/-772 portion of the *OPG* promoter) was amplified, subcloned, and sequenced in both directions. Three common molecular haplotypes were identified: OPG-MolHap1 (wt) bearing no variant and representing the most frequent haplotype (78.9%); OPG-MolHap2 [T^{-960}- G^{-946}- G^{-900}- T^{-864}] occurring in 12.3% of the MolProMD patients, and OPG-MolHap4 [C^{-960}- G^{-946}- A^{-900}- G^{-864}] being the least frequent haplotype with 8.8% of occurrence. Noteworthy, as described above, alleles -960C, -900A, and -864G were always transmitted in the same haplotypic background (Figure 16).

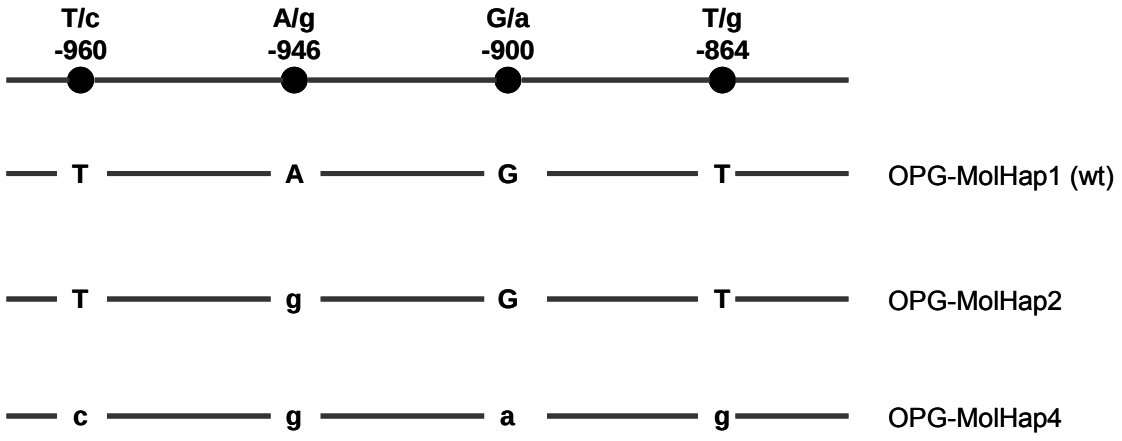

Figure 16 Molecular haplotypes of the human *OPG* promoter region. Haplotypes OPG-MolHap1 (wt), OPG-MolHap2 and OPG-MolHap4 were subcloned (-1020/-772 portion of the human OPG promoter) into the reporter gene vector ptk81-luc3, which harbors a minimal viral promoter.

4.2. In silico analysis of putative TFBS in the OPG promoter

Analyses of the molecular promoter haplotypes OPG-wt, OPG-MolHap2, and OPG-MolHap4 with the net-based program Alibaba 2.1 predicted several putative TFBS, some of which were altered in the presence of respective nucleotide substitutions. OPG-wt, OPG-MolHap2 [T^{-960}, G^{-946}, G^{-900}, T^{-864}] and OPG-MolHap4 [C^{-960}, G^{-946}, A^{-900}, G^{-864}] showed a sequence similarity for NF-κB, a beta scaffold transcription factor with minor groove contact harboring a Rel homology region. For both, OPG-MolHap2 and OPG-MolHap4, the -946A allele represents a putative binding site for transcription factor Sp1 (specificity protein 1), belonging to the family of ubiquitous factors bearing a Cys2His2 zinc finger domain (Figure 17*A*). This

binding pattern is lost for the minor -946G allele. Further, the -960C allele of OPG-MolHap4 is a putative binding sequence for the family of NF-1 transcription factors, which is lost for the -960T allele (Figure 17*B*). Members of the NF-1 family are transcription factors originally identified as essential for DNA replication by adenoviruses [Nagata et al, 1982]. They play important roles in mammary gland function and development [Jones et al, 1987]. In contrast, alleles -900A and -864G did not alter predicted binding motifs when compared to major alleles.

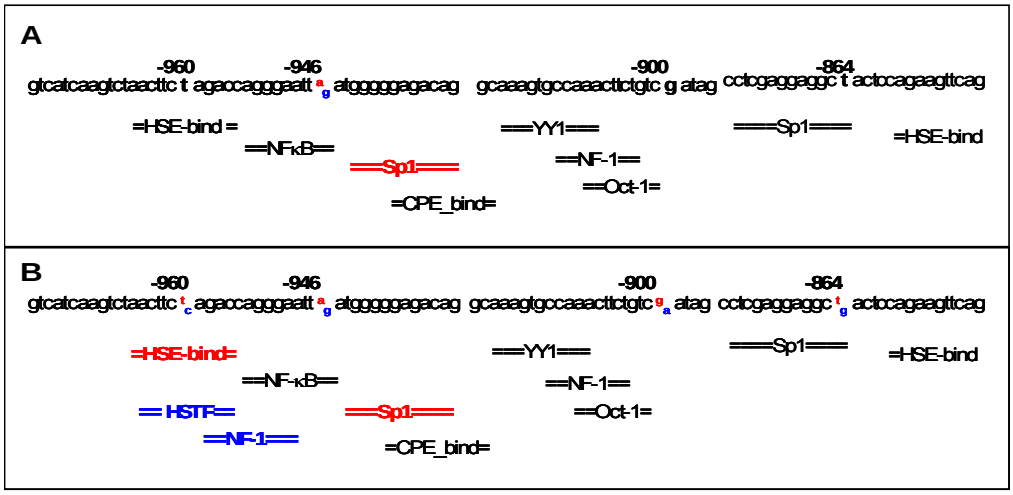

Figure 17 Transcription factor binding sites (TFBS). (A) TFBS for OPG-MolHap2 (B) for OPG-MolHap4. Analyses were performed using AliBaba 2.1. Major alleles are marked in red, minor alleles are in blue. Potential transcription factors are marked in red and blue, accordingly. Factors binding both, major and minor alleles, are marked in black.

The genomic area flanking T-159C predicted several putative and partly overlapping TFBS, but no physical TFBS was predicted for the position of the variant itself (Figure 18). Interestingly, 68 bp upstream of T-159C two “clusters” of TFBS with repetitive binding sites of Sp1, AP-2, and early growth response-1 (Egr1) occur. Members of the Egr family of transcription factors contain three repetitive zinc finger DNA binding domains.

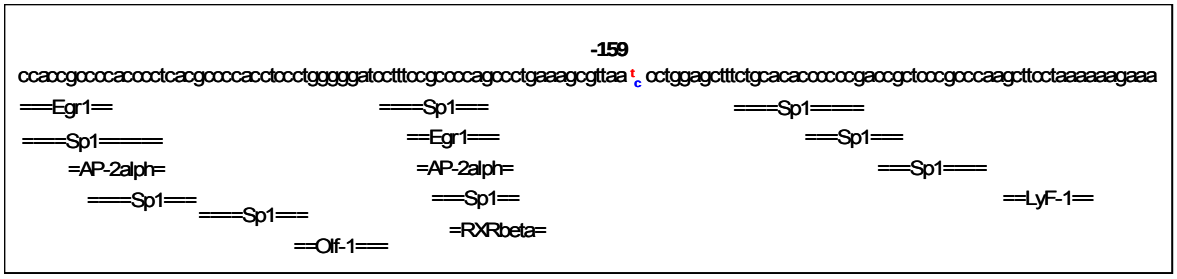

Figure 18 Transcription factor binding sites (TFBS) in sequence flanking SNP T-159C. Analyses were performed using AliBaba 2.1. Major allele is marked in red, minor allele in in blue. Potential transcription factors are marked in red and blue, accordingly. Factors binding both, major and minor allele, are marked in black. Allele-specific TFBS were not predicted.

4.3. Endogenous OPG expression

Since it has been shown that OPG mRNA and protein levels are regulated, among other factors, by 17β-Estradiol and TNFα [Hofbauer et al, 1998; Hofbauer et al, 1999], cells were stimulated with TNFα (2 ng/mL, 6 hrs), 17β-Estradiol (10^{-8}M, 24 hrs), or both. To detect endogenous OPG expression at both transcript and protein level, semi-quantitative PCR using a specific intron-spanning primer set for the *OPG* coding region, and Western Blot analyses were performed using a specific antibody against OPG. OPG mRNA expression was evenly detectable in both SaOs-2 and U2Os cells with and without stimulation. Likewise, OPG protein was detectable in both cell lines under all stimulatory regimes (Figure 19). No differences in OPG mRNA and immunoreactive protein expression were detectable after stimulation with TNFα, 17β-Estradiol, and both. Therefore, all following experiments were performed under basic conditions.

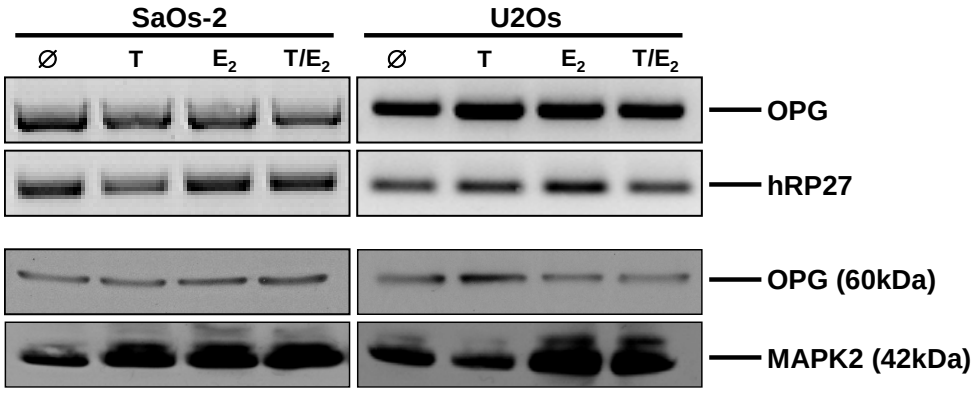

Figure 19 Endogenous OPG expression. Endogenous OPG mRNA and protein expression in SaOs-2 and U2Os cells stimulated with TNFα (T; 2 ng/mL, 6 hrs), 17β-Estradiol (E2; 10^{-8}M, 24 hrs), and both TNFα and 17β-Estradiol (T/E2). Semi-quantitative PCR was performed with a specific primer set for OPG and hRP27 (upper panel), the latter serving as control for the PCR experiment. OPG protein was detected using a specific antibody (lower panel).

Bioactivity of TNFα and 17β-Estradiol was tested in dose-response assays by reporter gene assay with plasmids harboring TNFα responsive elements (pNFκB-TA/luc) and estrogen responsive elements (pERE2-tk/luc) linked to the luciferase gene. HEK293T und MCF-7 cells were used as reference cell lines, respectively. Stimulation with 2 ng/mL TNFα (6 hrs) resulted in a significant increase of pNFκB-TA/luc activity in both cell lines (SaOs-2: 3.45-fold induction over basic conditions, p=0.0012; HEK293T: 8.82-fold induction over basic condition, p<0.0001). Increasing TNFα concentration did not alter pNFκB-TA/luc activity (Figure 20*A*). Stimulation of estrogen receptor (ER) α and β positive MCF-7 breast cancer cells with 17β-Estradiol (24 hrs) resulted in a classical ER-mediated dose-response curve of the activity of pERE2-tk/luc, with 10^{-9}M being the optimal concentration (2.4-fold induction over basal conditions, p=0.0017). In contrast, SaOs-2 did not respond to 17β-Estradiol stimulation (Figure 20*B*), probably due to the absence of ERα in this cell line (Figure 20*C*) [Hillebrand et al, 2009].

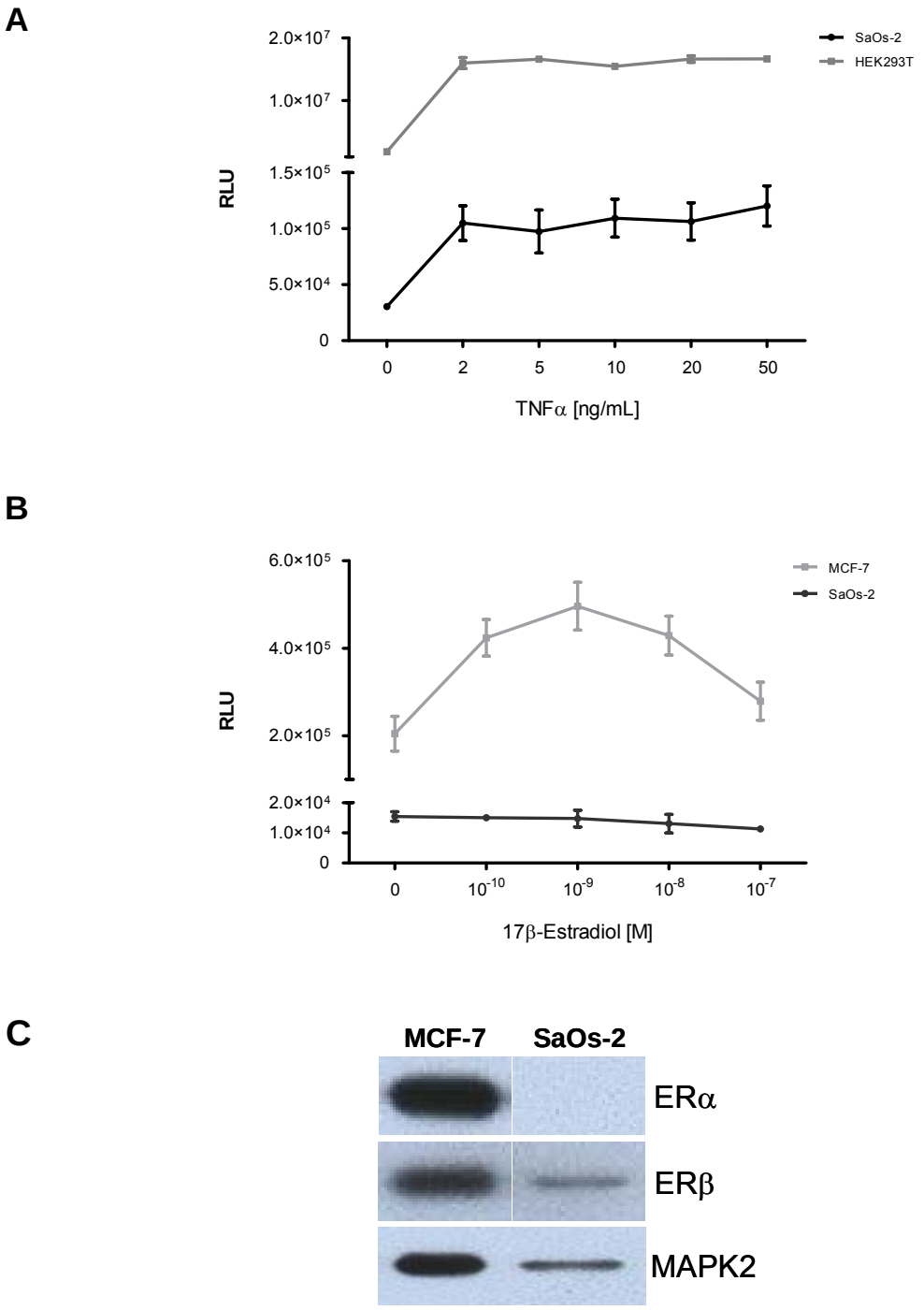

Figure 20 Dose-response curves for TNFα and 17β-Estradiol. (A) Dose-response curve for TNFα in SaOs-2 and HEK293T. Both responded to TNFα stimulation (6 hrs). (B) Dose-response curve for 17β-Estradiol (24 hrs) in SaOs-2 and MCF-7 cells, the latter displayed a classical dose-response curve, while SaOs-2 did not respond to any 17β-Estradiol concentration. (C) Detection of immunoreactive ERα (upper panel) and ERβ (middle panel) in MCF-7 and SaOs-2 cells. Samples' even loading was ascertained using a specific antibody against MAPK2 (lower panel).

4.4. Alternative transcription start sites (TSS) of the OPG gene

Preference for TSS is often tissue- and cell type-specific, therefore the focus was set on SaOs-2 and U2Os cells to determine osteosarcoma-typical TSS. The *OPG* gene is transcribed into four transcripts (2.4 kb, 3.0 kb, 4.2 kb, and 6.5 kb in length). The 4.2 kb and 6.5 kb transcripts result from alternative splice-events in intron 2, while the 2.4 kb and 3.0 kb transcripts result from the alternative usage of transcription start sites (TSS, Figure 21*A*) [Morinaga et al, 1998]. Using RACE, we identified two TSS in both cell lines. TSS1 is located 64 bp upstream of the ATG codon (position 1109 in Acc# AB008822), while TSS2 is located 225 bp upstream of the ATG codon (position 948 in Acc# AB008822). We confirmed these results by diacritic PCR with specific primers, located directly at the respective TSS. In SaOs-2, both TSS were utilized equally, while in U2Os transcription is mainly driven from TSS1. Further, we defined a third TSS (TSS3, 667 bp upstream of the ATG codon, position 506 in Acc# AB008822) by diacritic PCR in both cell lines. TSS3 is utilized as frequent as TSS1 in both cell lines, and has already been described by Morinaga and colleagues (Figure 21*B*) [Morinaga et al, 1998]. Transcription from TSS1 and TSS2 results in the 2.4 kb transcript, while transcription started at TSS3 results in the 3.0 kb transcript. As TSS1 is usually described as major TSS, positions of SNPs are indicated relative to this site.

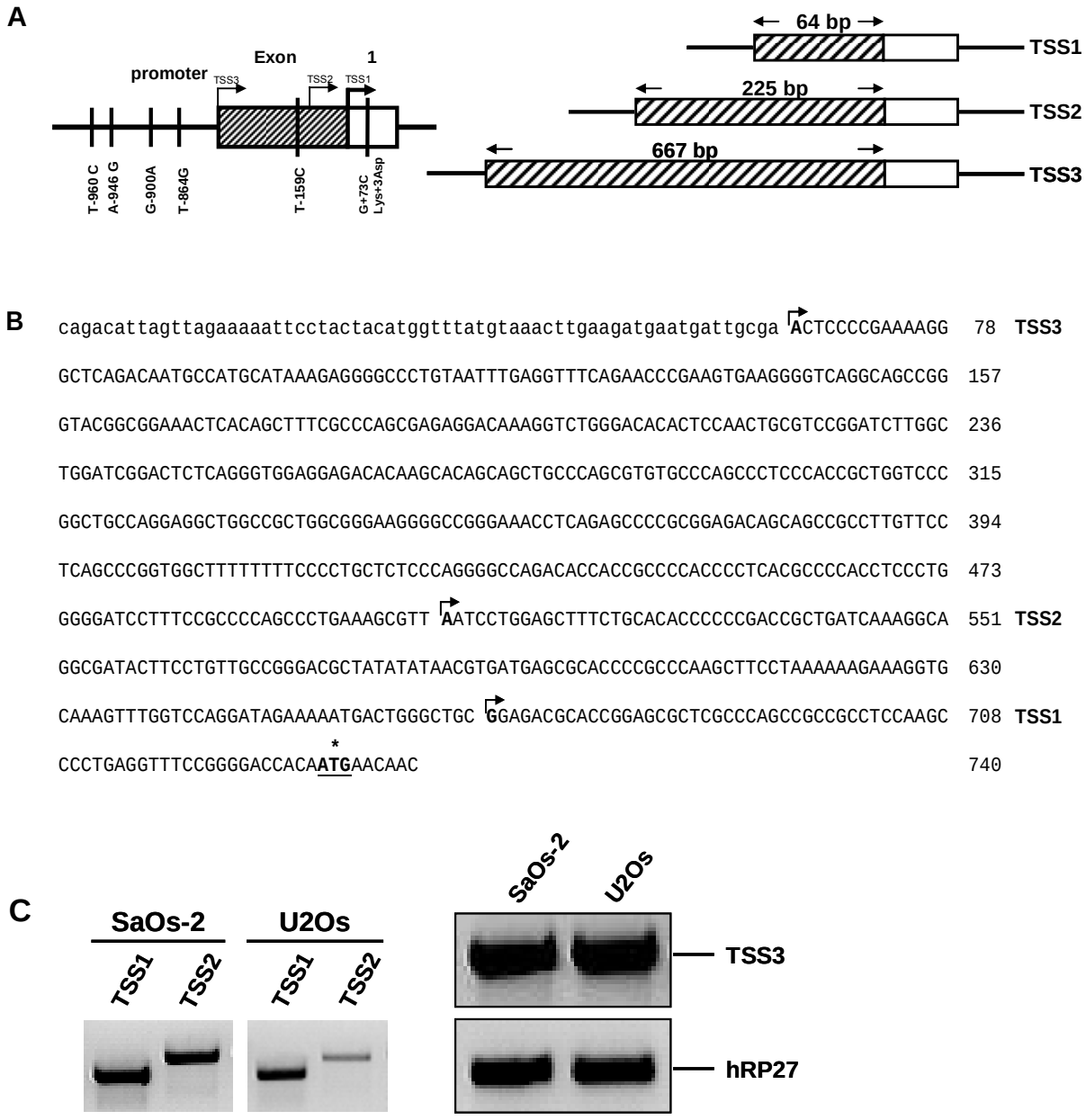

Figure 21 Alternative TSS of the OPG gene. (A) Schematic representation of the alternative TSS of the *OPG* gene. The 5'UTR (dashed box), coding region (blank box), and TSS (right-tangled arrows) are indicated. (B) 740 bp of the *OPG* sequence (bp 442-1181, Acc# AB008822). 5'-flanking region (lower case), exon 1 (upper case), alternative TSS 1-3 (bold, arrows), and the ATG codon (underlined, asterisk) are indicated. (C) Diacritic PCR for verification of the detected TSS. In SaOs-2 all detected TSS are used equally, while in U2Os TSS2 is used less frequent.

4.5. OPG promoter constructs

For characterization of the *OPG* promoter region and identification of regulatory sequences by deletion constructs, the focus was set on analyzing the detected promoter variants. A sufficiently active promoter portion (1008 bp) of the *OPG* gene in osteosarcoma cell lines is termed full length construct for this study. Serial deletion constructs were generated (Figure 23*A*) and the detected variants were analyzed in the context of both, the full length constructs (Figure 23*B*) and the deletion constructs (Figure 23*C*). According to the identified haplotypes (4.1), 249 bp (-1020/-772) flanking OPG-wt, MolHap2, and MolHap4 were linked into reporter gene vector ptk81-luc3 (Figure 22*A*). In addition, 275 bp flanking T-159C were linked to reporter gene vector pGL3basic (Figure 22*B*).

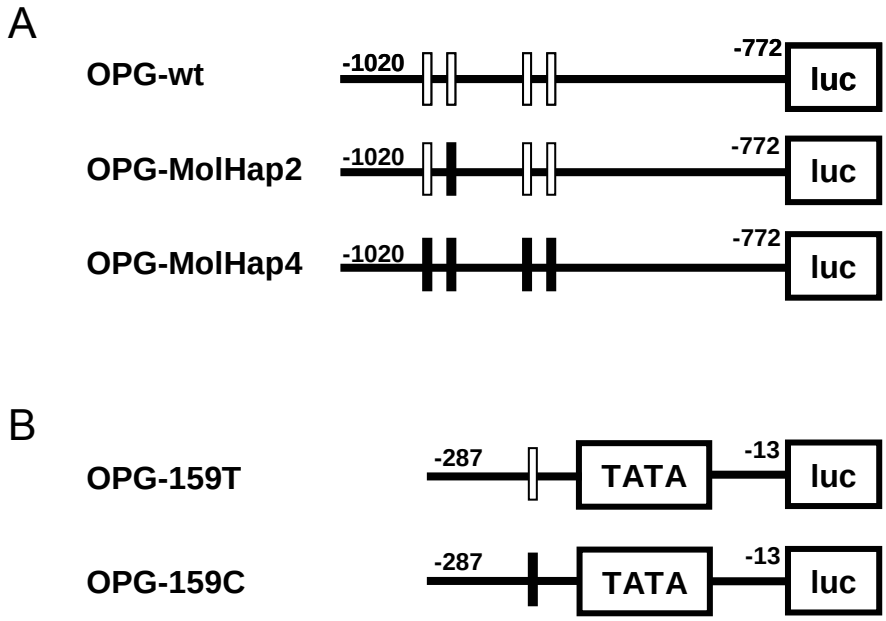

Figure 22 Reporter gene constructs of *OPG* MolHaps and -159. (A) Sequences flanking the identified molecular haplotypes (-1020/-772) were linked to reporter gene vector ptk81-luc3, harboring a minimal promoter. (B) 275 bp spanning T-159C were linked to promoter-less reporter gene vector pGL3basic. Common alleles (with boxes) and less frequent alleles (black boxes) are indicated.

4.6. Reporter gene assays

4.6.1. OPG promoter analyses with full length constructs

The identified SNPs were introduced in the context of the commonly occurring MolHaps into the full length constructs (-1020/-13), and transient transfection assays in SaOs-2 and U2Os cells were performed.

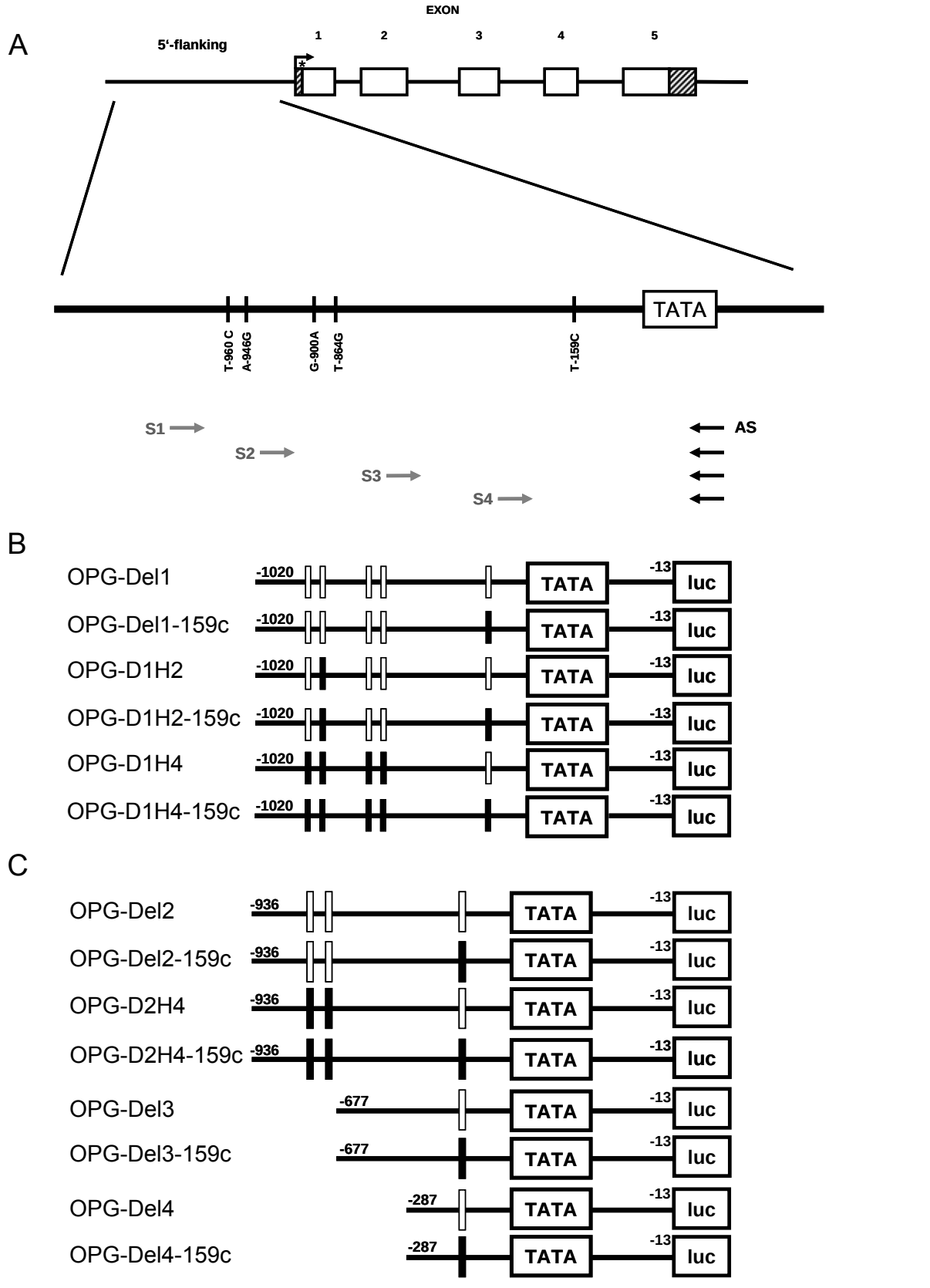

Figure 23 Schematic presentation of *OPG* 5'-flanking region. (A) Design of deletion constructs, positions of antisense (AS) and respective sense primers (S1–S4) are indicated. (B) Detected variants in haplotypic constellation in the context of the full length construct, and (C) in the context of the 5'-truncated constructs. Common alleles (white boxes) and less frequent alleles (black boxes) are indicated.

In both cell lines, the wt full length construct (OPG-Del1) was sufficiently active, and transcriptional activity was significantly decreased for both MolHap2 (OPG-D1H2 [SaOs-2: 0.63-fold activity over wt, p=0.0014; U2Os: 0.69-fold activity over wt, p=0.0018]), and MolHap4 (OPG-D1H4 [SaOs-2: 0.43-fold activity over wt, p<0.0001; U2Os: 0.59-fold activity over wt, p=0.0011]). Transcriptional activity was further significantly decreased for OPG-wt and MolHap2, when the -159C allele was introduced into the respective full length constructs (OPG-Del1-159c [SaOs-2: 0.53-fold activity over OPG-Del1, p<0.0001; U2Os: 0.71-fold activity over OPG-Del1, p=0.0014], OPG-D1H2-159c [SaOs-2: 0.65-fold activity over OPG-D1H2, p=0.0058; U2Os: 0.71-fold activity over OPG-D1H2, p=0.0029]). Presence of the -159C allele in the MolHap4 full length construct resulted in a slight, but not significant decrease of transcriptional activity (OPG-D1H4-159c [SaOs-2: p=0.2749; U2Os: p=0.9989]) (Figure 24).

4.6.2. Serial deletion analyses

To define regions involved in the transcriptional activity of the *OPG* promoter, deletion constructs of the *OPG* 5'-flanking region were generated (Figure 23*A*). Reporter vector pOPG-Del1/luc represents the full length construct (1008 bp) with "wild type" sequence [T^{-960}- A^{-946}- G^{-900}- T^{-864}- T^{-159}]. All following constructs were 5'-truncated, each harboring "wild type" sequences: pOPG-Del2/luc (924 bp [G^{-900}- T^{-864}- T^{-159}]), pOPG-Del3/luc (665 bp [T^{-159}]), and pOPG-Del4/luc (275 bp [T^{-159}]). As shown in Figure 25, pOPG-Del1/luc displayed a sufficient transcriptional activity in both cell lines. Truncation of 84 bp (-1020/-936) resulted in a complete abrogation of transcriptional activity (pOPG-Del2/luc, p<0.0001), indicating a *cis*-active element within. Further, truncated constructs pOPG-Del3/luc (-936/-677) and pOPG-Del4/luc (-677/-287) did not restore and transcriptional activities remained silent at the level of empty vector pGL3basic.

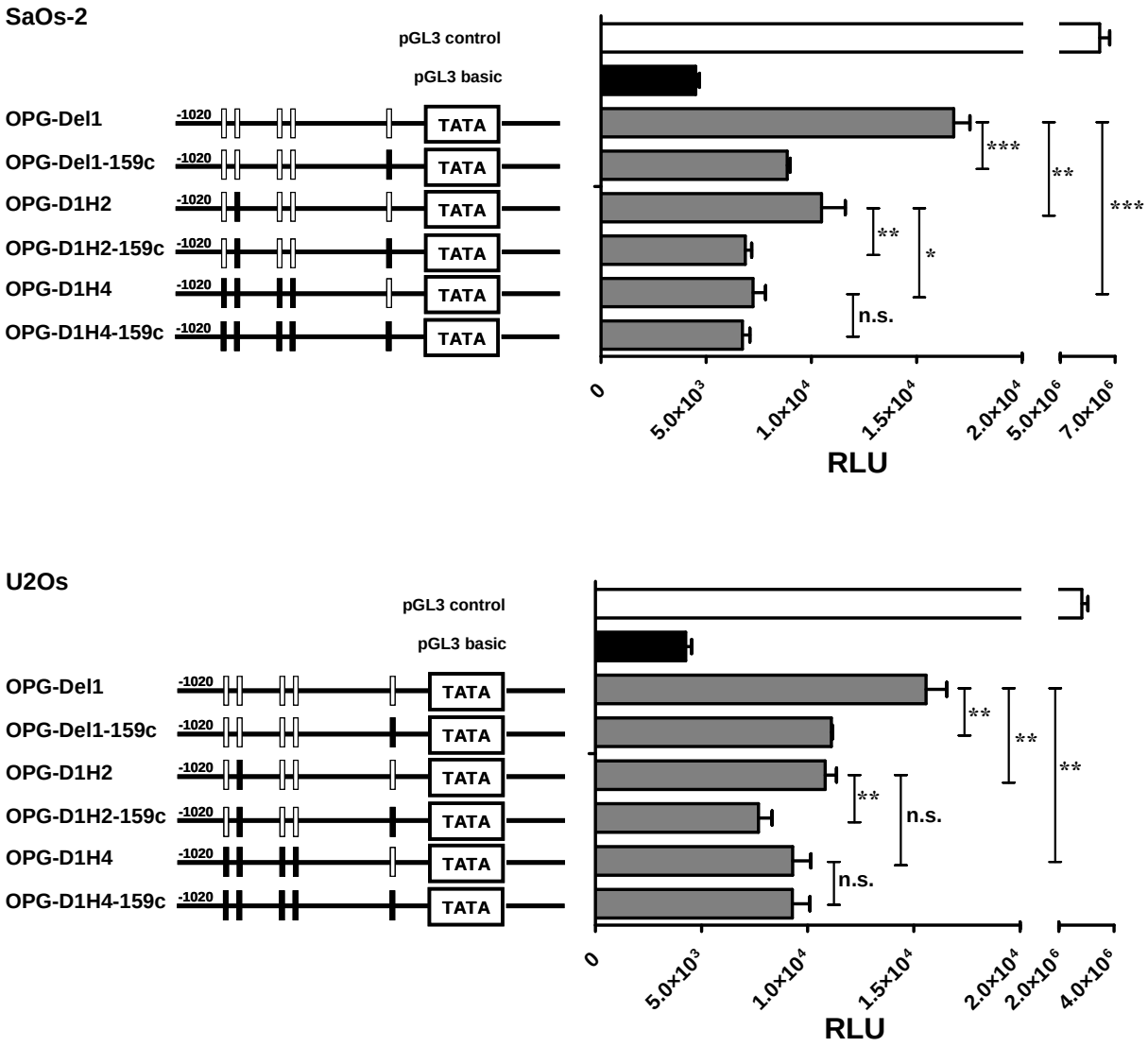

Figure 24 Transient transfection assays with full length reporter gene constructs harboring the identified SNPs in the context of the MolHaps. Common alleles (white boxes) and less frequent alleles (black boxes) are indicated at the corresponding promoter positions. In both, U2Os and SaOs-2, presence of the -159C allele reduced the transcriptional activities of the MolHaps, for OPG-wt (OPG-Del1) and MolHap2 (OPG-D1H2) to a significant extend (***, $p \leq 0.001$; **, $p \leq 0.01$; *, $p \leq 0.05$; *ns*, not significant).

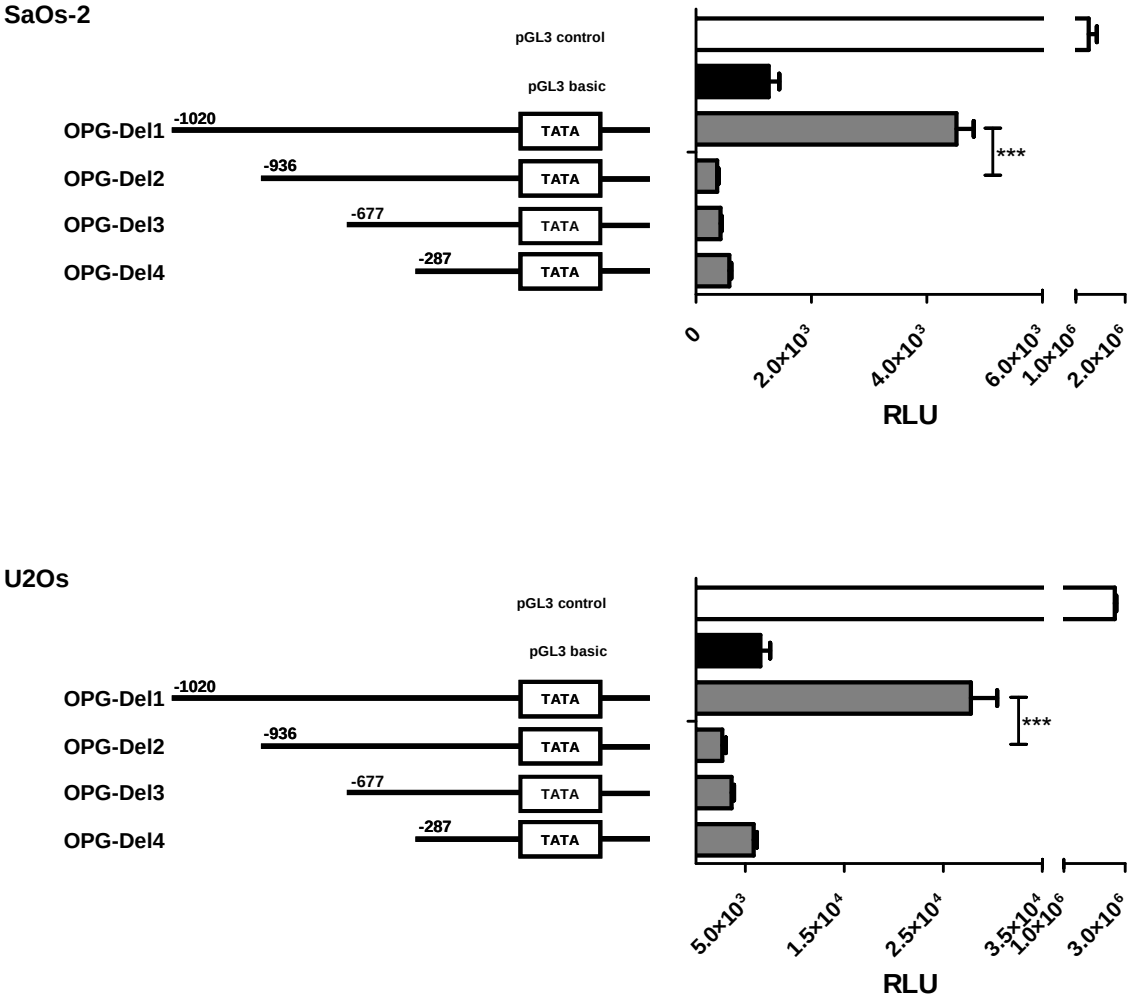

Figure 25 Transcriptional activities of *OPG* promoter deletion constructs. SaOs-2 and U2Os cells were transfected with *OPG* deletion constructs. The full length construct (OPG-Del1) displayed a sufficient transcriptional activity, whereas activities of remaining constructs were below of that of the full length construct ($p<0.0001$ for both cell lines) (***, $p\leq0.001$; **, $p\leq0.01$; *, $p\leq0.05$; *ns*, not significant).

Truncation of the full length construct by 84 bp (-1020/-936) resulted in significantly decreased transcriptional activity in both cell lines (OPG-Del2, $p<0.0001$). Introduction of the -159C allele increased activity (OPG-Del2-159c [SaOs-2: 3.9-fold activity over OPG-Del2, $p=0.0005$; U2Os: 1.76-fold activity over OPG-Del2, $p<0.0001$]). Likewise, transcriptional activities were significantly increased in both cell lines for OPG-Del3 (OPG-Del3-159c [SaOs-2: 5.6-fold activity over OPG-Del3, $p<0.0001$; U2Os: 6.2-fold activity over OPG-Del3, $p<0.0001$]), and OPG-Del4 (OPG-Del4-149c [SaOs-2: 5.9-fold activity over OPG-Del4, $p<0.0001$; U2Os: 4.4-fold activity over OPG-Del4, $p<0.0001$]), when the -159C allele was introduced into the respective constructs (Figure 26 and Figure 27), indicating a repressive effect of the -159C allele on *OPG* gene transcription.

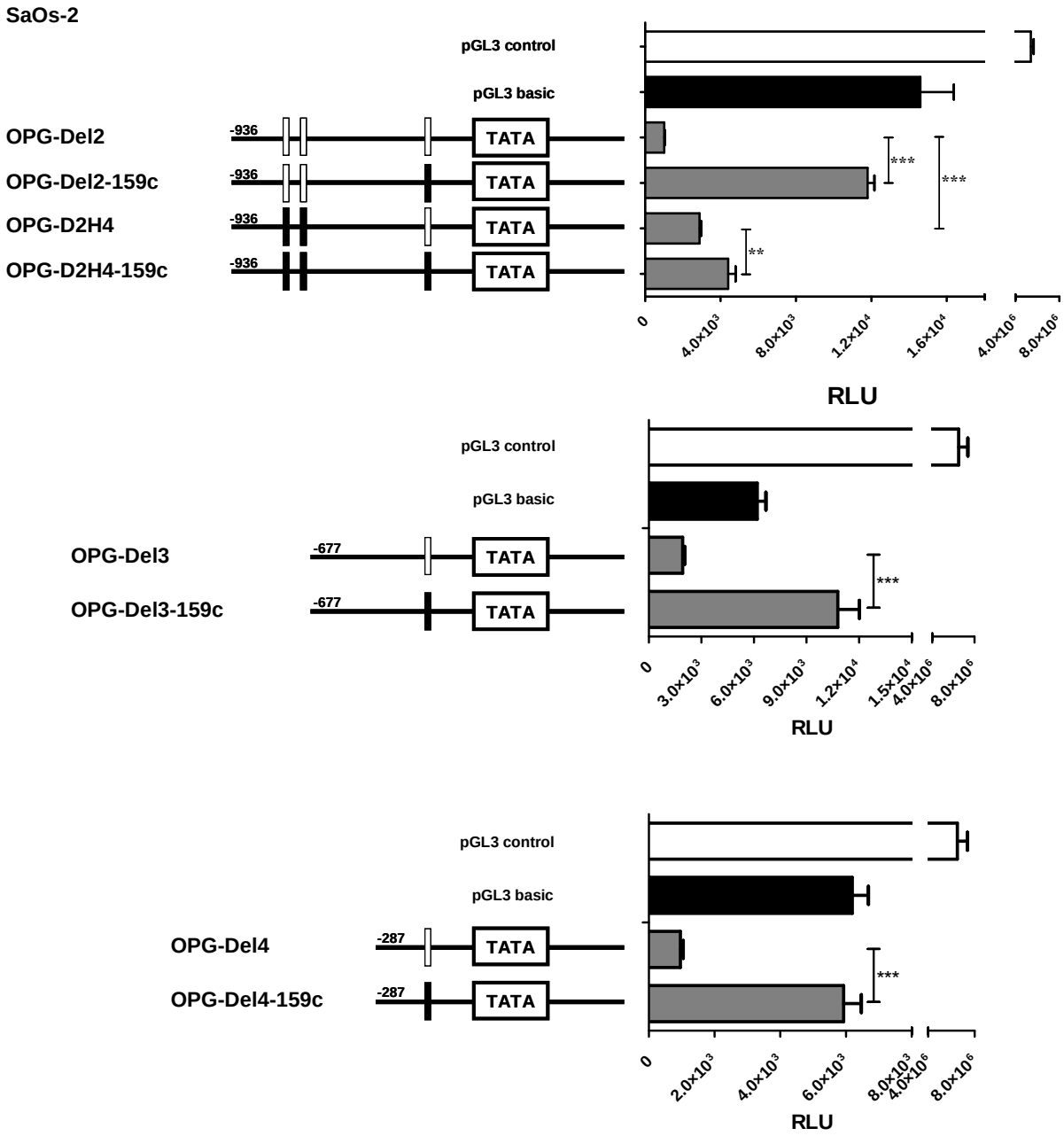

Figure 26 The -159C allele increases transcriptional activity of *OPG* in the context of the promoter deletion constructs. Transient transfection assays with deletion constructs harboring the identified SNPs in context of the MolHaps. Common alleles (white boxes) and less frequent alleles (black boxes) are indicated at the corresponding promoter positions. In SaOs-2, and in contrast to the full length promoter constructs, transcriptional activities of the deletion constructs (OPG-Del2, OPG-Del3, OPG-Del4) were significantly increased, when the -159C allele was introduced into the constructs (***, $p \leq 0.001$; **, $p \leq 0.01$; *, $p \leq 0.05$; *ns*, not significant).

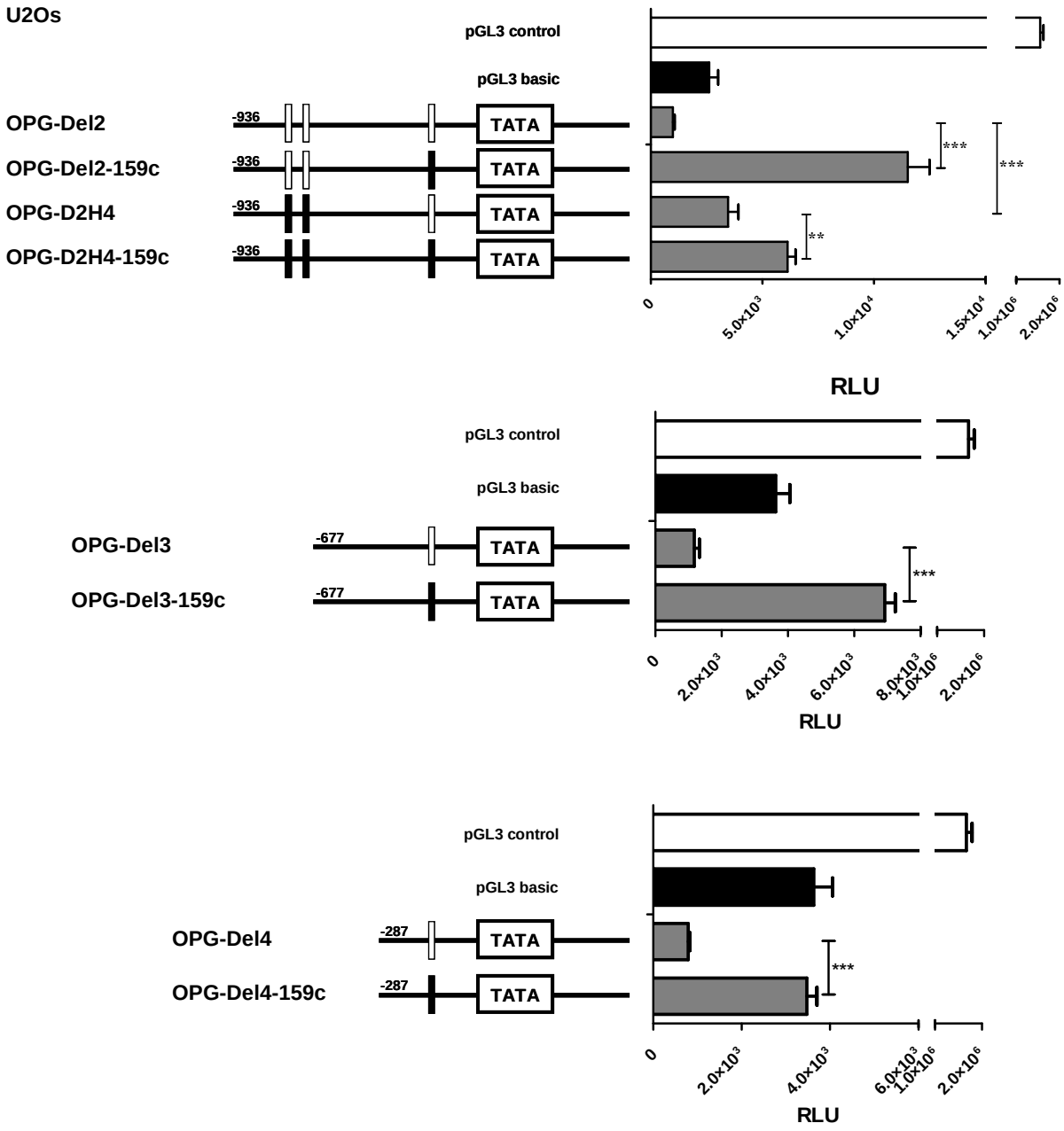

Figure 27 The -159C allele increases transcriptional activity of *OPG* in the context of the promoter deletion constructs. Transient transfection assays with deletion constructs harboring the identified SNPs in context of the MolHaps. Common alleles (white boxes) and less frequent alleles (black boxes) are indicated at the corresponding promoter positions. In U2Os, and in contrast to the full length promoter constructs, transcriptional activities of the deletion constructs (OPG-Del2, OPG-Del3, OPG-Del4) were significantly increased, when the -159C allele was introduced into the constructs (***, $p \leq 0.001$; **, $p \leq 0.01$; *, $p \leq 0.05$; *ns*, not significant).

4.6.3. OPG promoter analyses with MolHaps and T-159C separately

To investigate the transcriptional activity of the three MolHaps and T-159C separately, the -1020/-772 portion of the human *OPG* 5'-flanking region was linked to the reporter gene vector ptk81-luc3, which contains a minimal promoter allowing for the assembly of the transcriptional machinery, with only very little remnant activity. As shown in Figure 28*A*, in both cell lines, the OPG-wt displayed poor transcriptional activity, being as active as the mock vector ptk81-luc3. As seen in the context of the full length constructs, a highly significant decrease of transcriptional activity occurred for MolHap2 (SaOs-2: 0.07-fold activity over the wt, p=0.0027; U2Os: 0.08-fold activity over the wt, p<0.0001) and MolHap4 (SaOs-2: 0.34-fold activity over the wt, p=0.0097; U2Os: 0.51-fold activity over the wt, p=0.0006). This isolated promoter portion comprising the three MolHaps, seemed to be poorly involved in the transcriptional momentum of *OPG* (0.5-fold induction over mock vector). Likewise, a 275 bp portion (-287/-13) of the 5'-flanking region, harboring the either -159T or -159C allele was linked to the promoter-less reporter gene vector pGL3basic and transient transfections were performed. In both cell lines, the reporter gene construct OPG-159T displayed a weak transcriptional activity at the level of the empty vector. The construct carrying the -159C allele (OPG-159C) revealed a significant increased activity (SaOs-2: 12.7-fold activity over OPG-159T, p=0.0001; U2Os: 2-fold activity over OPG-159T, p=0.0002) (Figure 28*B*).

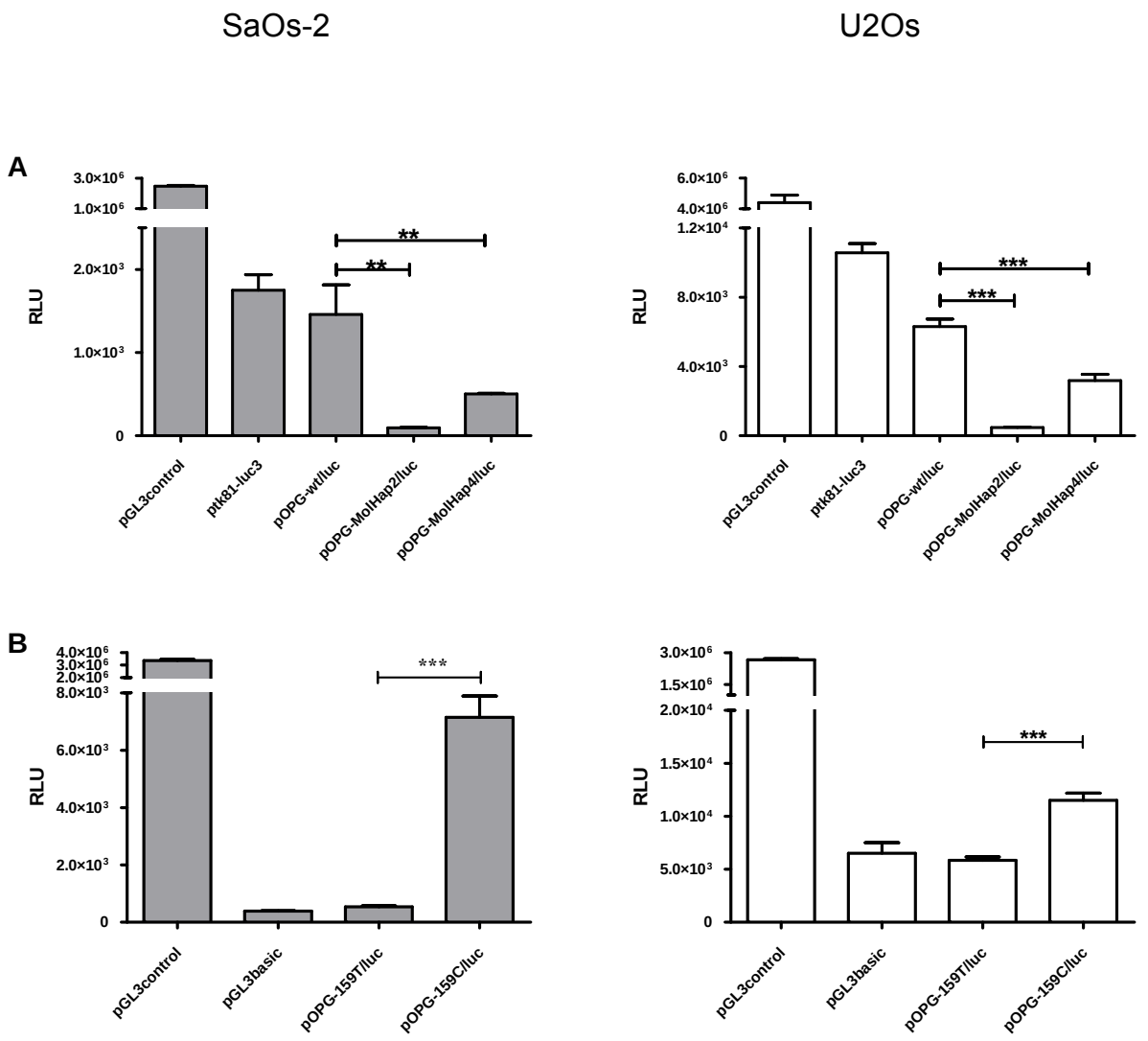

Figure 28 Reporter gene assays in SaOs-2 and U2Os. (A) Isolated MolHaps (pOPG-wt/luc, pOPG-MolHap2/luc, and pOPG-MolHap4/luc). In both cell lines, OPG-wt displayed a weak basal activity, less than the empty vector ptk81-luc3. Transcriptional activities were again significantly lower for MolHap2 (SaOs-2: 0.07-fold activity over wt, p=0.0027; U2Os: 0.08-fold activity over wt, p<0.0001) and MolHap4 (SaOs-2: 0.34-fold activity over wt, p=0.0097; U2Os: 0.51-fold activity over wt, p=0.0006). (B) Transient transfections with constructs carrying either the -159T or -159C allele. In both cell lines, presence of the -159C allele significantly increased transcriptional activity of the -287/-13 portion (SaOs-2: p=0.0001, U2Os: p=0.0002) (***, $p \leq 0.001$; **, $p \leq 0.01$; *, $p \leq 0.05$; *ns*, not significant).

4.7. Electrophoretic Mobility Shift Assays (EMSA)

To investigate DNA:protein interactions of the *OPG* promoter fragments, EMSAs were performed with SaOs-2 and U2Os nuclear protein extracts. Either PCR amplicons (154 bp, 3'-biotinylated) harboring OPG-wt, OPG-MolHap2, or OPG-MolHap4, or oligonucleotides (30 bp, 3'-biotinylated) containing the T-159C variant, served as probes, and were competed with an unlabeled PCR fragment in a 200-fold molar excess. In case, probes were competed with oligonucleotides harboring consensus sites for Sp1, NF-1, or Egr1 with a 200-fold molar excess.

4.7.1. SaOs-2 and U2Os nuclear extracts interact with OPG MolHaps

SaOs-2 nuclear extracts revealed a specific shift for all three MolHaps, being less pronounced for MolHap2 and MolHap4 (Figure 29, black arrow). In addition, a weak band was visible for MolHap2 and MolHap4, being competed with the unlabeled PCR fragment (Figure 29, open arrows). A similar binding pattern was observed with U2Os nuclear extracts. A distinct, specific shift for OPG-wt and OPG-MolHap4, being less intense for the latter was detected (Figure 29, open arrows).

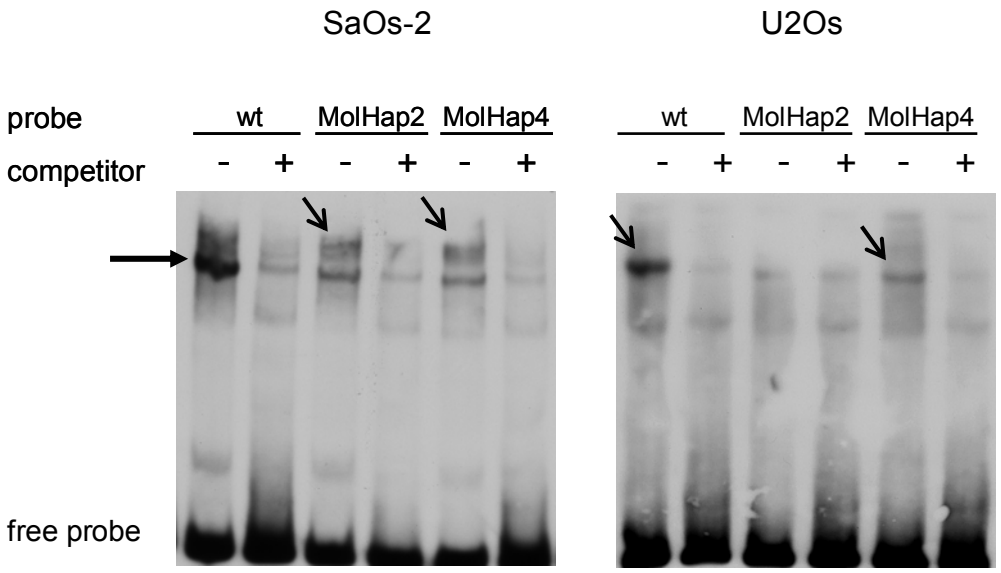

Figure 29 SaOs-2 and U2Os nuclear extracts interact with *OPG* MolHaps. Binding was competed with an unlabeled PCR fragment. In SaOs-2, specific shifts were detected for all three MolHaps (black arrow). Further, a semi allele-specific shift was detected for MolHap2 and MolHap4 (open arrow). In U2Os a semi allele-specific shift was detected for OPG-wt and MolHap4 (open arrow).

There was no specific binding pattern for MolHap2. The additional binding for MolHap2 and MolHap4 found in SaOs-2 cells was lost. Since *in silico* analyses predicted altered binding sites for transcription factors Sp1 and NF-1 (Figure 17), we performed EMSAs using the respective consensus sites as competitors. In SaOs-2, the prominent band (Figure 30, black arrow) was completely competed for all three MolHaps by NF-1, but not by Sp1 consensus oligonucleotides. The above described binding pattern for MolHap2 and MolHap4 was completely competed by a Sp1 consensus site (Figure 30, open arrows). In U2Os, the specific shift for OPG-wt and OPG-MolHap4 was completely competed with NF-1, but not by Sp1 consensus oligonucleotides (Figure 30, black arrow).

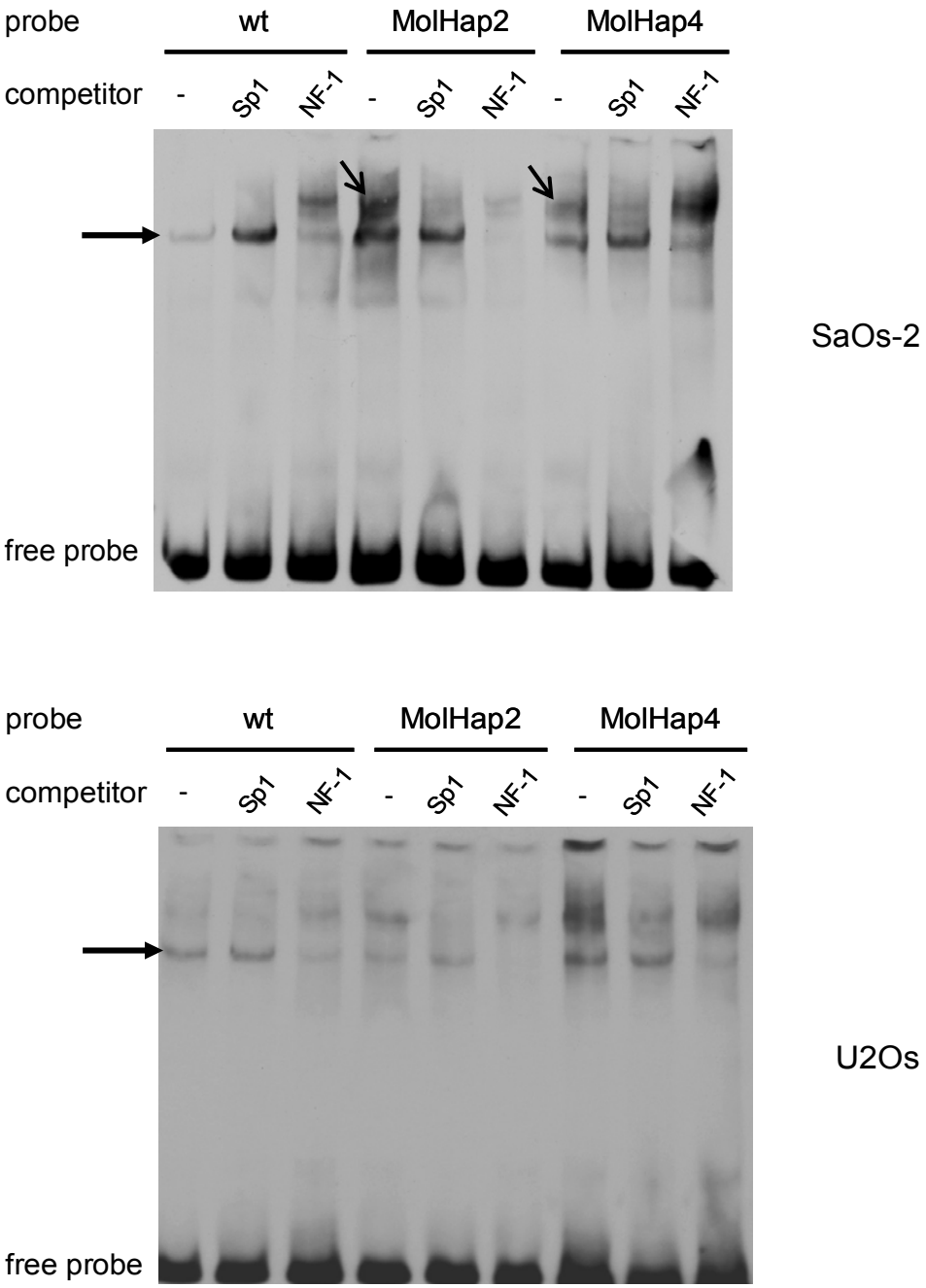

Figure 30 NF-1 and Sp1 interact with *OPG* MolHaps. Binding was competed with unlabeled consensus sites for Sp1 and NF-1 in a 200-fold molar excess. Free probe, specific binding of the three MolHaps (black arrow), and semi allele-specific binding of MolHap2 and MolHap4 (open arrows) are indicated.

4.7.2. The -159T allele is specifically bound by nuclear proteins from SaOs-2 and U2Os cells

EMSAs performed with nuclear extracts from unstimulated SaOs-2 cells resulted in an allele-specific shift for the major -159T allele, which was specifically competed with unlabeled

oligos. This binding pattern was lost, when EMSAs were performed with oligonucleotides bearing the -159C allele. In fact, we could not detect any specific protein binding pattern for the OPG -159C allele, the same being observed with nuclear extracts from U2Os cells (Figure 31, black arrows).

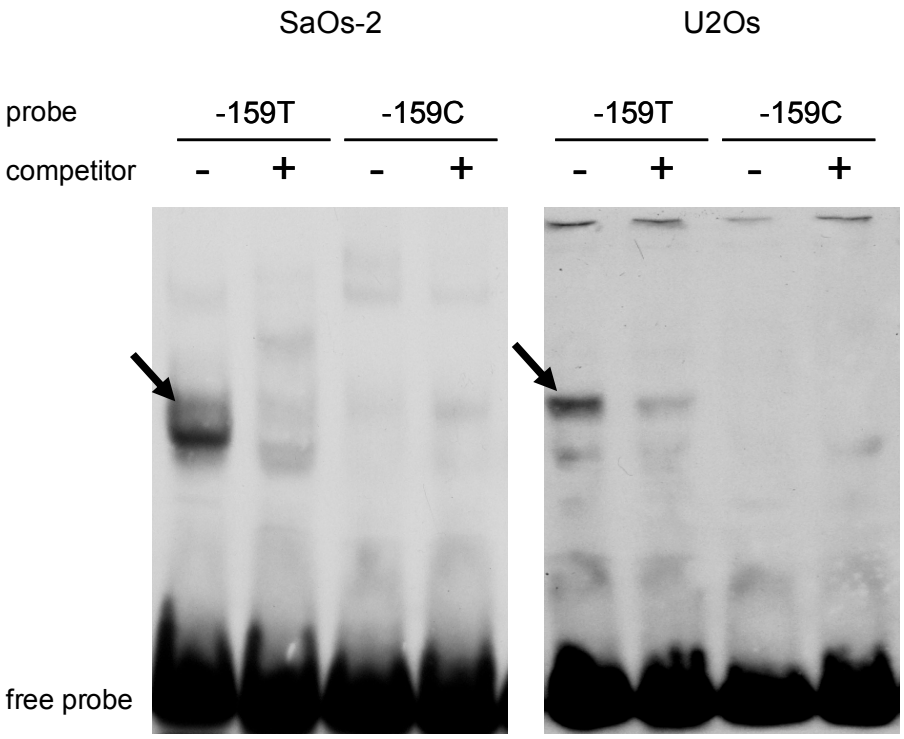

Figure 31 The -159T allele is specifically bound by nuclear proteins from SaOs-2 and U2Os cells. EMSAs with 30 bp oligonucleotides containing T-159C were performed with 5 µg of nuclear protein extracts from SaOs-2 and U2Os. The -159T allele displayed an allele-specific shift in both cell lines (black arrow).

Even though *in silico* analyses (Figure 18) did not predict altered TFBS for T-159C, EMSAs were performed using Sp1 and Egr1 consensus sites as competitor. These transcription factors are grouped in “clusters” of TFBS 68 bp upstream of T-159C. The prominent -159T binding pattern was competed with an Egr1 consensus site in SaOs-2 and U2Os cells, but not with a Sp1 consensus site (Figure 32*A*). Additionally, we incubated probes with recombinant Egr1 binding domain and detected specific binding exclusively to the -159T allele. A biotinylated Egr1 consensus site served as control (Figure 32*B*).

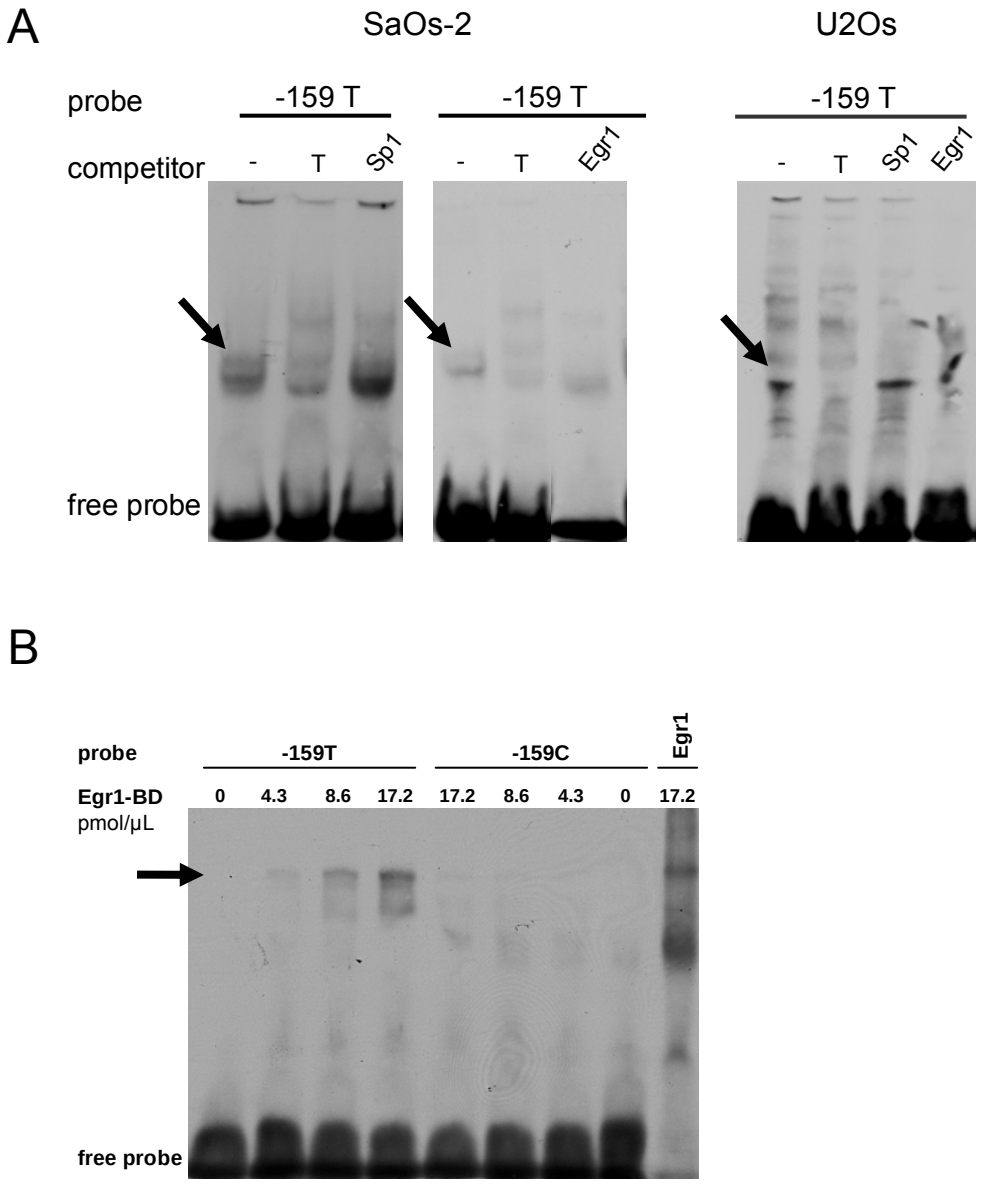

Figure 32 Egr1 binds specifically to the -159T allele. (A) EMSA was performed with -159T using Sp1 and Egr1 consensus sites for competition. The allele-specific band was competed with an Egr1, but not with a Sp1 consensus site (black arrow). (B) EMSA performed with labeled oligonucleotides harboring either the -159T or -159C allele and purified Egr1 binding domain (Egr1-BD). Egr1 binds exclusively to the -159T, not to the -159C allele (black arrow).

4.7.3. Co-transfections and ChIP

4.7.3.1. *OPG* MolHaps

Using an unlabeled NF-1 consensus site in EMSA experiments, a specific interaction of NF-1 with the OPG-MolHaps was observed. To identify the interacting individual members of the

NF-1 family of transcription factors, co-transfections with expression vectors for NF-1/A1.1, NF1/B2, NF1/C2, and NF1/X2 were performed.

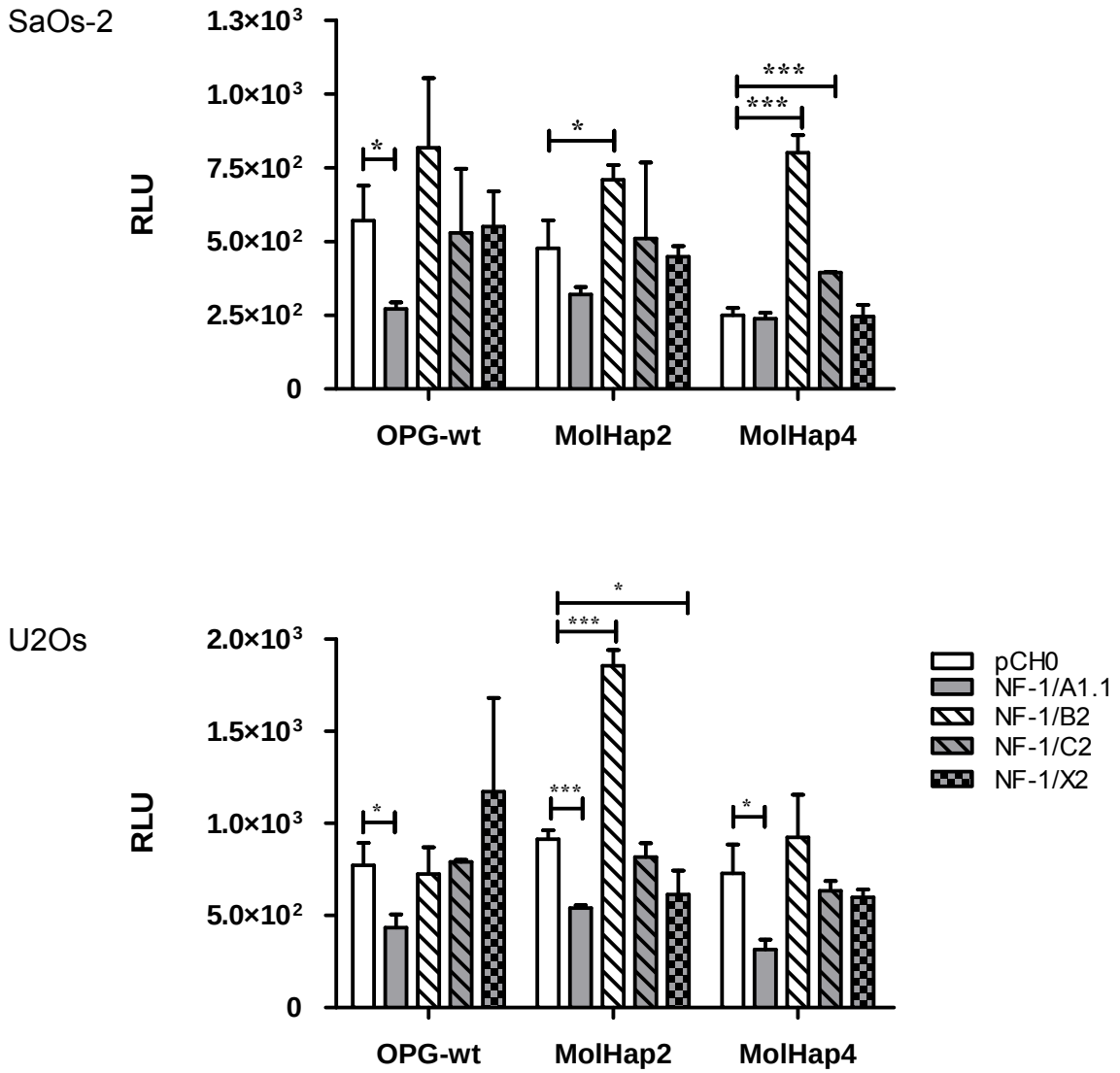

Figure 33 MolHaps in the context of the full length construct co-transfected with expression vectors of the NF-1 protein family. NF-1/A1.1 reduced transcriptional activity significantly for all three MolHaps in U2Os, and for OPG-wt in SaOs-2. NF-1/B2 increased transcriptional activity in both cell lines, significantly for MolHap2 and MolHap4 in SaOs-2, and MolHap2 in U2Os (***, $p \leq 0.001$; **, $p \leq 0.01$; *, $p \leq 0.05$; *ns*, not significant).

Co-transfection with NF-1/A1.1 revealed significant decreases of transcriptional activities of OPG-wt, MolHap2, and MolHap4 in U2Os cells (p=0.0138, p=0.0002, p=0.012, respectively). In SaOs-2 cells, only OPG-wt displayed a significantly decreased transcriptional activity when co-transfected with NF-1/A1.1 (p=0.013). Co-transfection with NF-1/B2 resulted in increased transcriptional activities, significantly for MolHap2 (p=0.02) and MolHap4

(*p*=0.0001) in SaOs-2 cells, and MolHap2 (*p*<0.0001) in U2Os cells. NF-1/C2 and NF-1/X2 did not alter transcriptional activity in any cell line (Figure 33).

Further, we performed ChIP assays with specific antibodies against Sp1, Egr1, and NF-1. In U2Os cells, we found transcription factor NF-1 bound to the sequence spanning SNPs T-960C, A-946G, G-900A, T-864G; this binding was completely absent for this promoter portion in SaOs-2 cells (Figure 34).

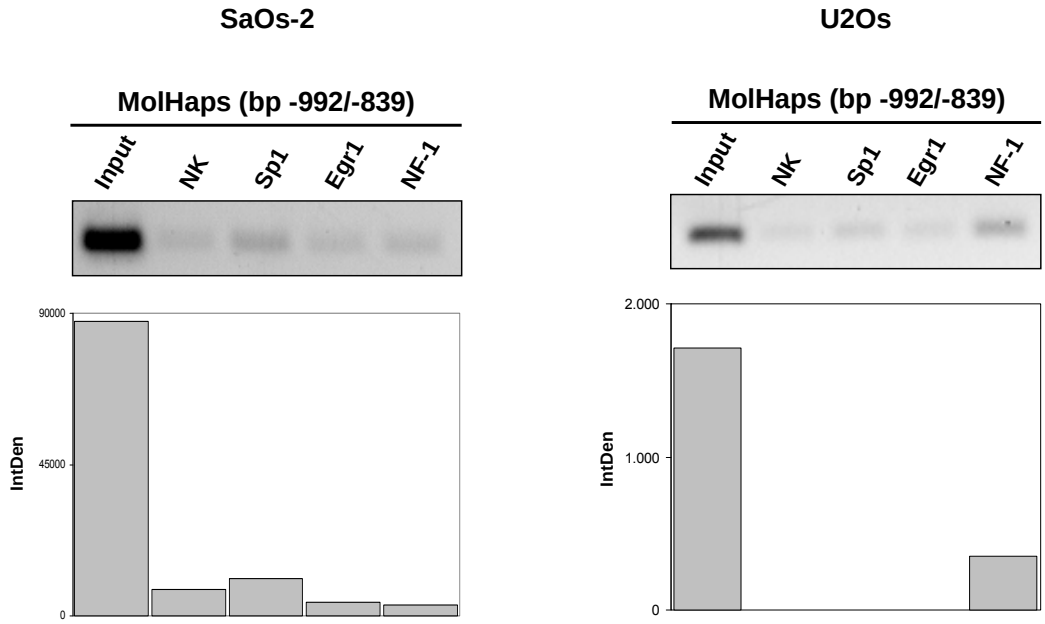

Figure 34 ChIP assay performed in SaOs-2 and U2Os cells. Precipitated DNA was amplified with specific primers covering T-960C, A-946G, G-900A, T-864G (bp -992/-839). In SaOs-2 cells, we could not detect any binding of Sp1, NF-1, or Egr1 to the distal -992/-839 portion. In U2Os cells, binding of transcription factor NF-1 was slightly detectable.

4.7.3.2. *OPG* T-159C

Since *in silico* analyses predicted combined binding sites for Sp1 and Egr1 68 bp upstream the T-159C (Figure 18), co-transfection analyses with expression vectors for Sp1 and Egr1 were performed (Figure 35*A*). Overexpression of Sp1 resulted in significantly increased transcriptional activities for OPG-Del1 (SaOs-2: 13.3-fold induction over empty expression vector, *p*<0.0001; U2Os: 18.14-fold induction over empty expression vector, *p*<0.0001) and OPG-D1-159c (SaOs-2: 7.5-fold induction over empty expression vector, *p*=0.0002; U2Os: 21.17-fold induction over empty expression vector, *p*<0.0001).

By contrast, overexpression of Egr1 resulted in significantly decreased transcriptional activities for both constructs, supporting the suggested repressing effect of Egr1 in *OPG*

gene regulation (OPG-Del1, SaOs-2: 0.43-fold induction over empty expression vector, p=0.0011; U2Os: 0.36-fold induction over empty expression vector, p=0.0003). Remarkably, this repressive effect was less pronounced for the -159C allele (OPG-Del1-159c, SaOS-2: 0.6-fold induction over empty expression vector, p=0.0014; U2Os: 0.46-fold induction over empty expression vector, p=0.0148). In addition, and as described above, ChIP assays with specific antibodies were performed. In SaOs-2, binding of Sp1 and a weak interaction of NF-1 with the T-159C spanning sequence (-288/-38) was detected. Similar results were obtained, when ChIP was performed in U2Os; Egr1 and NF-1 were found to bind -288/-38 portion of the *OPG* 5'-flanking region (Figure 35*B*).

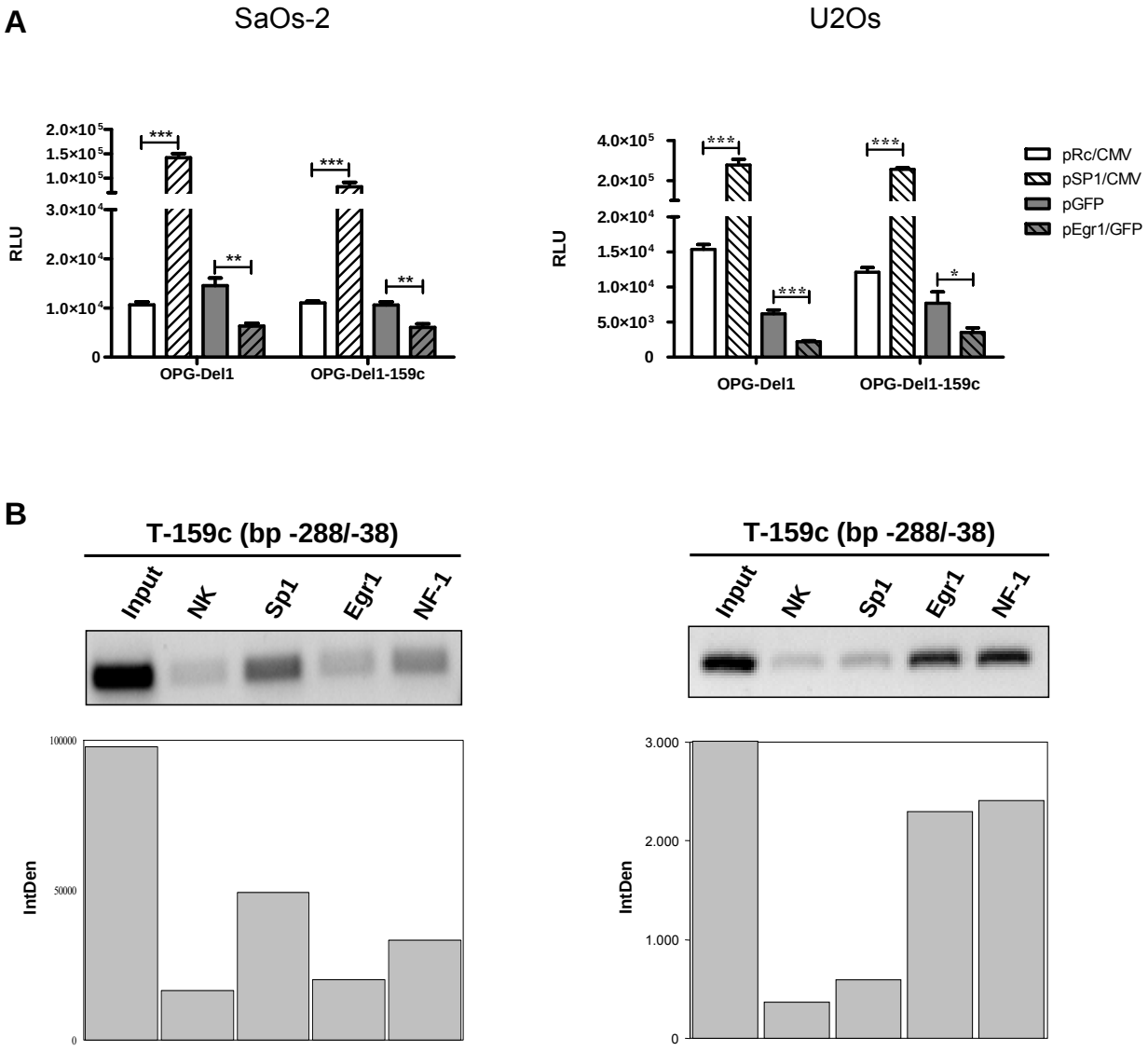

Figure 35 Egr1 interacts with the -288/-38 *OPG* promoter portion. (A) Co-transfection analyses of the full length construct harboring either the -159T allele (OPG-Del1) or the -159C allele (OPG-Del1-159C) with expression vectors for Sp1 and Egr1. Sp1 increased transcriptional activity of both constructs (white dashed bar). Overexpression of Egr1 resulted in a significant decreased transcriptional activity for OPG-Del1 (-159T allele), being less intense for -159C allele carrying full length construct (grey dashed bar) (***, $p \leq 0.001$; **, $p \leq 0.01$; *, $p \leq 0.05$; *ns*, not significant). (B) Precipitated DNA was amplified with specific primers located in the 5'-flanking region of the *OPG* gene promoter, covering the proximal variant T-159C (bp -288/-38). In SaOs-2 cells, binding of Sp1 was slightly detectable, while in U2Os cells binding of transcription factors Egr1 and NF-1 was detectable.

5. Discussion

In the present study, 5 genetic variants within the 5'-flanking region of the human *OPG* gene were analyzed: T-960C, A-946G, G-900A, T-864G, and T-159C. Sequences relevant for transcriptional regulation were analyzed as well as individual transcriptional consequences of the respective variants. Only few studies aimed at characterizing the *OPG* promoter region and very little is known about the molecular basis of its transcriptional regulation. Therefore, the focus was set on promoter analyses. In this study, a portion of 1008 bp was found to be sufficiently active and used for further promoter studies. A series of truncated promoter constructs was generated for both the identification and characterization of regulatory elements. A portion of 84 bp (bp -1020/-936) was found to be essential for transcriptional activity in tested osteosarcoma cell lines SaOs-2 and U2Os.

5.1. Alternative TSS of the OPG gene

Transcription of the *OPG* gene was shown to start at multiple TSS [Morinaga et al, 1998]. As known so far, the usage of alternative TSS in the *OPG* gene results in varying lengths of the transcripts, of the 5' untranslated region (5'UTR). In the present study, we first analyzed the transcriptional organization of the *OPG* promoter by 5' RACE, which led to the identification of one novel TSS 225 bp upstream of the ATG codon (TSS2, position 948 in Acc# AB008822). We then defined a TSS 64 bp upstream of the ATG codon (TSS1, position 1109 in Acc# AB008822) very close to the major TSS described by Morinaga *et al.* Authors reported a major TSS 67 bp upstream of the ATG codon, by primer extension with [γ-^{32}P]dCTP end-labeled primers. Given the very short difference (3 bp) between these two major TSS (67 bp and 64 bp upstream of the ATG codon), a technical inaccuracy rather than the actual presence of two separate TSS is presumable. In this respect, radioactive end-labeling of oligonucleotides often causes decompositions of the probe by radiation, leading to a possibly imprecise mapping of the TSS. Transcription from TSS1 and TSS2 results in a 2.4 kb transcript, which is the major transcript detectable in all OPG expressing tissues [Morinaga et al, 1998]. We further mapped a third TSS (TSS3, 667 bp upstream of the ATG codon, position 506 in Acc# AB008822) by use of diacritic PCR, which has been described previously. Transcription from TSS3 results in a 3.0 kb transcript, found in brain, placenta, spleen, and prostate [Yasuda et al, 1998]. Since the 3.0 kb transcript is tissue-specific, it is possible that transcription of the *OPG* gene is under control of two alternative promoters, activated by tissue-specific transcription factors. Alternative promoter usage is a common phenomenon, and on average 3.1 promoters are suggested per gene [Cheong et al, 2006]. *In silico* analyses of the *OPG* 5'-flanking region predicted two promoter regions, each harboring a TATA box in spatial vicinity of TSS1 and TSS3 (data not shown) [Center for

Information Technology]. As mentioned above, transcription started from the different TSS of the *OPG* gene will not alter the generated protein, but result in mRNA isoforms with heterogeneous 5'UTR, which may influence transcript stability and/or translation efficiency.

5.2. Genetic variants alter OPG promoter performance

Genetic variants within the promoter region may influence promoter activity when located in or near *cis*-active elements [Telgmann et al, 2008]. Quantification of differential transcriptional activities of a given DNA sequence by reporter gene assays depends on three items. Firstly, the basic transcription machinery needs to assemble. Secondly, variances within the provided sequence (wt or variant) may result in differential transcriptional activity, and thirdly, the introduction or presence of a Kozak-sequence or one or more TSS might lead to differences in transcript stability or expression [Heintzman and Ren, 2006; Ross, 1995]. Specific expression patterns are defined by *cis*-active elements that direct transcription by interplay with the core promoter [Lemon and Tjian, 2000]. Genetic variants within these regulatory regions may alter binding affinity of TF to their consensus DNA sequence, thereby affecting gene transcription and expression patterns.

Potential effects of the detected promoter variants were analyzed within a 1008 bp portion of the *OPG* promoter (-1020/-13) by measuring transcriptional activities under basal conditions. As expected, this promoter portion was sufficiently transcriptionally active. In bone, the relative expression of OPG and RANKL is critical for osteoclastogenesis and therefore critical for the regulation of skeletal mass, structure, and strength. Hence, a moderate transcriptional activity of the *OPG* gene under basic conditions, to not disequilibrate the osteoclast-osteoblast ratio, seems conceivable. Over the past years, there has been an emerging awareness that gene transcription can be regulated by *cis*-acting elements located at considerable distances, up to 1000 kb, from the gene they control [Higgs et al, 2008]. Therefore, the analyzed 1008 bp *OPG* promoter portion may not be considered as the entire *OPG* promoter, rather as a part of it, but being sufficient for *OPG* gene transcription in osteosarcoma cells. Nevertheless, transcriptional activities of MolHap2 and MolHap4 either in the context of the full length construct, or separately were significantly decreased when compared to the wt. In contrast to haplotypes estimated by maximum likelihood (ML) method of inference [Tregouet et al, 2002] or other tools, MolHaps are inferred from subcloning procedures of individual DNA providing the exact allelic constellations in a given DNA strand, which might be crucial information with respect to differential haplotypic function [Duan et al, 2003; Dördelmann et al, 2008]. In addition, introduction of the -159C allele into the respective full length construct further decreased transcriptional activities. As mentioned above, genetic variants within regulatory sequences may alter TFBS, or rather the binding

affinity for TFs. Altered binding affinities of TFs caused by the *OPG* promoter variants may cause the observed differences in transcriptional activities of the *OPG* promoter constructs.

5.3. Alterations of DNA:protein binding patterns

TFs act as transcriptional modules consisting of at least two proteins. Primarily, binding of TFs depends on the interaction/recognition of the electrostatic environment of the DNA sequence/TFBS they bind to, and on the stoichiometric availability of the TFs participated in the module. Other than in coding regions, TFBS are composed of a DNA sequence in which each position is of different importance and relevance for the molecular function of the entire site. Therefore, alterations of TFBS by SNPs may cause an altered affinity of the respective TF binding, rather than a complete loss of the binding performance. Further, the preference to recruit a certain TF to a given module depends on the affinity of the recruiting factor. Since computational predictions cannot integrate the physiological state of a cell and neither the impact of protein:protein binding affinities on the recruitment of factors to a transcriptional module, they fail to comprehensively predict protein binding for MolHap constellations.

5.3.1. OPG MolHaps

In silico analyses of the sequence spanning the *OPG* MolHaps revealed a binding site for Sp1 for the major -946A allele. This binding pattern is lost with the occurrence of the minor -946G allele, in MolHap2 and MolHap4. EMSA experiments revealed an allele-specific interaction of MolHaps 2 and 4 with Sp1 in SaOs-2. In U2Os no interaction of Sp1 with the *OPG* MolHaps was detectable. Sp1 represents a sequence specific protein, interacting specifically with GC-box promoter elements [Briggs et al, 1986]. In case of TATA-less promoters, activators, such as Sp1, are proposed to associate physically with TBP and thereby recruit the TFIID complex [Pugh and Tjian, 1991].

Further, occurrence of the -960C allele of MolHap4 generates a putative binding site for NF-1, whose interaction was detectable with all three MolHaps in EMSA experiments in both cell lines, and could be confirmed with ChIP in U2Os cells. Sequence analysis led to the identification of NF1/A, NF1/B, NF1/C, NF1/L and NF1/X [Rupp et al, 1990; Kruse et al, 1991]. This diversity is further increased by differential RNA splicing [Santoro et al, 1988]. In co-transfection analyses family members NF-1/A (repressing) and NF-1/B (activating) were identified as potential interaction partners. While the repressing effect of NF-1/A was nearly equal for all three MolHaps, the activating effect of NF-1/B was most pronounced for MolHap2, suggesting an increased affinity of NF-1/B for that haplotype constellation. As shown for other activating proteins, NF-1 family members can also mediate repression at

some promoters. The glutathione transferase P promoter contains a consensus NF-1 site that acts as a silencer and is bound by NF-1/A [Osada et al, 1997]. The mechanism by which NF-1 represses genes is not clearly understood, but results indicate that direct repression may work either through recruitment of co-repressors or interaction with the basal transcription machinery [Osada et al, 1997]. NF1/X, for example, was shown to specifically interact with Sp1 via its subtype-specific domain and block Sp1 induction of the PDGF A-chain promoter [Rafty et al, 2002].

5.3.2. OPG T-159C

In silico analyses predicted clustered binding sites of Egr1 and Sp1 at the T-159C polymorphic site. Indeed, Sp1 and Egr1 share very similar cognate binding sites; hence at many promoters, Sp1 sites overlap with binding sites for Egr1, but binding of Sp1 and Egr1 is often mutually exclusive [Hsu et al, 2009]. Both TF compete, dependent of the physiological state of a cell, for binding at the cognate sites. For the platelet-derived growth factor A-chain promoter, containing overlapping Sp1 and Egr1 sites, Sp1 mediates basal transcription, while PMA-induced Egr1 displaces Sp1 and stimulates gene expression [Khachigian et al, 1995]. While Sp1 is an activating transcription factor, it has been shown that Egr1 can also act as a repressor, e.g. of a constitutively expressed collagen gene, by preventing interactions between Sp1 and the general transcriptional machinery [Tan et al, 2003]. EMSA experiments revealed protein binding exclusively to the -159T allele and competition assays defined Egr1, not Sp1, as the protein binding to -159T allele. In ChIP assays, Egr1 as well as Sp1 were detected. Hence, it is quite conceivable that both proteins compete for binding at this cognate site, and bind context-specific with different affinities to the respective allele. Further, in both cell lines binding of NF-1 to this promoter portion was shown (ChIP). Since NF-1 was found to interact with the sequence spanning the MolHaps, an interaction of the MolHap-portion (NF-1) with the T-159C site (Egr1/Sp1) seems possible. Interaction of Sp1 and NF-1 has already been described [Rafty et al, 2002].

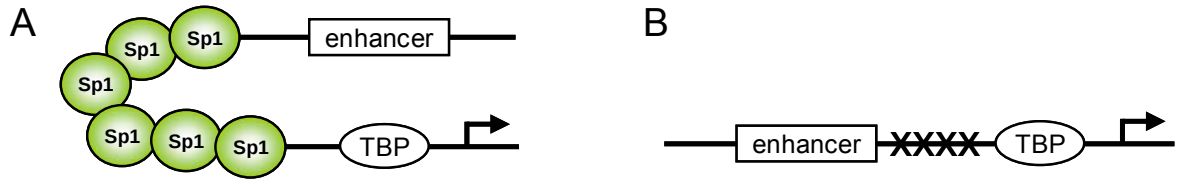

Figure 36 Sp1 alters DNA structure. (A) Sp1 mediated DNA bending brings enhancer elements close to the basal promoter complex. (B) Mutation of Sp1 binding sites (indicated by the Xs) reduces DNA bending and transcriptional activation [Fry and Farnham, 1999].

Sp1 can also achieve context-dependent transcriptional activation by altering the structure of DNA. As shown for the T-159C spanning sequence, the SV40 early promoter is composed of clustered binding sites for Sp1, and robust transcriptional activity from this promoter also requires an upstream enhancer that binds a number of different transcription factors. The clustered repeats contain an intrinsic DNA bend that can be stabilized by binding of Sp1 [Sun and Hurley, 1994]. It has been proposed that Sp1-stabilized bending activates transcription by bringing the factors bound to the upstream enhancer closer to the basal promoter (Figure 36). Courey et al demonstrated that Sp1 proteins bound 1.8 kb downstream of a promoter can cooperate with Sp1 bound at the basal promoter region to synergistically activate transcription [Courey et al, 1989].

Further hints of an interaction of the MolHap-site with the T-159C site were obtained by generating and analyzing serial deletion constructs (see below).

5.4. Identification of a cis-active element by serial deletion constructs

To define regions being involved in transcriptional activity of *OPG*, serial deletion constructs of the 5'-flanking region were generated and transiently transfected. Deletion construct analyses are also useful to mimic the impact of physical inactivation of DNA portions by nuclear histone packaging. The full length construct Del1 (-1020 to -13) displayed a sufficient transcriptional activity in both cell lines, while 5'-truncation of 84 bp (Del2 [-936 to -13]) resulted in a completely abrogated transcriptional activity, even below the level of the empty vector, strongly indicating a *cis*-active element within the truncated 84 bp (-1020/-936). The loss of transcriptional activity was also seen for the further truncated constructs (Del3 [-677 to -13] and Del4 [-287 to -13]). Interestingly, and controversially to the full length constructs,

introduction of the -159C allele into the respective deletion constructs resulted in a highly significant increase of transcriptional activity, supporting the idea of a *cis*-active element within the 84 bp (bp -1020/-936) interacting with the T-159C site. The obtained results further indicate that this supposed interaction triggers Egr1 to activate or repress *OPG* transcription depending on the accessibility of the -1020/-936 promoter portion (e.g. in case of concealing by histone binding).

Egr1 belongs to the family of zinc finger transcription factors, consisting of a DNA-binding domain (with 3 zinc finger motifs), an activation domain, and an inhibitory domain, located between the activation and the DNA-binding domain [Russo et al, 1995; Gashler et al, 1993]. Egr1 is a master regulator controlling the expression of a variety of genes, including transcription factors, signaling factors, growth factors, and cytokines [Fu et al, 2003]. Gene expression depending on Egr1 involves a functional cooperativity between Egr1 and a growing number of other regulatory factors, including among others the glucocorticoid receptor and AP-2 [Wong et al, 1998], RelA (p65) [Cogswell et al, 1997; Chapman and Perkins, 2002], p300 [Mouillet et al, 2004], and Sp1 [Srivastava et al, 1998]. Therefore, it seems likely that Egr1 does not act alone, but in concert with other transcription factors. Transcription factor modules, in which participation of Erg1 facilitates assembly and function of the complex, may either not form or be destabilized by the absence of Egr1 [Yan et al, 2000].

The variants T-960C and A-946G are located within the truncated 84 bp, and *in silico* analyses predicted a NFκB binding site within (Figure 17). Interactions of Egr1 with members of the NFκB family have already been described. In many NFκB responsive promoters, NFκB-proteins alone are insufficient to activate transcription [Baldwin, 1996]. Egr1 and RelA (p65) cooperatively stimulate transcription of the NFκB1 (p50) gene [Cogswell et al, 1997], and Chapman and Perkins reported an interaction of RelA (p65), similar to its interaction with Sp1, with the zinc-finger domain of Egr1. But contrary to Sp1, Egr1 represses transcriptional activity of RelA, possibly by sequestering RelA from its target promoter [Chapman and Perkins, 2002]. Taken these results together, it seems to be likely that Egr1 is capable of interacting cooperatively with NFκB in some promoter contexts, while sequestering and inhibiting in others.

The NFκB pathway is important for the expression of a variety of genes involved in immune and inflammatory response, cellular proliferation, and survival. The NFκB protein family members are ubiquitously expressed transcription factors: p65 (RelA), RelB, c-Rel, p50 (NFκB1, precursor p105), and p52 (NFκB2, precursor p100) [Yamamoto and Gaynor, 2004]. Signaling is primarily regulated by inhibitor κB proteins (IκB) and the IκB kinase complex (IKK) through two main pathways. In the canonical pathway, NFκB dimers (e.g. p50/RelA)

are located in the cytoplasm, bound to an IκB protein. Binding of a ligand to a cell surface receptor (e.g. TNFα to its receptor TNFR) leads to the recruitment of adaptor proteins (e.g. TRAF or RIP), which in turn recruit the IKK complex (consisting of the α and β catalytic subunit and two regulatory units [NEMO]). The IKK then phosphorylates the IκB leading to proteasomal degradation, while the NFκB dimer enters the nucleus and binds to its target sequence. The non-canonical pathway is for the p100/RelB activation during B- and T-cell organ development. Receptor binding leads to the activation of the NFκB inducing kinase (NIK) which phosphorylates and activates the IKKα complex (containing two α subunits, but no NEMO). IKKα in turn phosphorylates two serine residues of p100 leading to its partial proteolysis and the release of the p52/RelB complex, entering the nucleus [Gilmore, 2006].

5.5. A model of transcriptional regulation of OPG

Cis-active elements concert transcriptional activity by interaction with TFs that assemble at the promoter as modules rather than acting alone. The composition of an individual module and the composition of several modules is dependent on the genomic context and proteomic conditions, hence is cell type- and physiologically specific. Taking all results, as well as previous reports into account, the following model of transcriptional regulation of the *OPG* gene is conceivable: Based on the sufficiently active full length construct (1008 bp) harboring the wt sequence, transcription may be regulated by transcription factors Sp1, NF-1, NFκB, and Egr1 acting in concert and achieving sufficient transcriptional activity (Figure 37*A*). This interaction is possibly mediated by a Sp1 stabilized DNA bend [Fry and Farnham, 1999]. Introduction of the -159C allele (Figure 37*B*, black bar) leads to an altered TFBS to which Egr1 is not capable to bind and stimulate transcription in cooperation with Sp1, NF-1, and NFκB. This results in a decreased activity, indicating that Egr1 is adequate but not essential for transcriptional activity in the context of the full length. Altered transcriptional activities of the *OPG* MolHaps, seen in the full length construct, may be caused by an altered protein binding pattern of the TFs, as shown for Sp1 and NF-1. But occurrence of the haplotype constellations wt, MolHap2, and MolHap4 may not cause the loss of one TFBS, rather an attenuated binding affinity of a TF to its respective TFBS, resulting in a decreased transcriptional activity as observed. Indeed, binding affinity can be that attenuated, being below the detection limit of an EMSA.

Truncation of the 1008 bp full length construct about 84 bp resulted in a completely abrogated transcriptional activity, caused, following this model, by the truncation of TFBS for Sp1, NF-1, and NFκB (Figure 37, red dashed box). Binding of Egr1 alone seems to repress transcriptional activity (Figure 37*C*, dotted arrow), because in case of the -159C allele and a not-binding of Egr1, transcriptional activity is partial restored (Figure 37*D*), possibly reflecting

the activity of the basal transcription machinery. Truncation of a full length construct is a good tool to mimic the impact of physical inactivation of DNA portions, e.g. by nuclear histone packaging. This indicates that the *cis*-active element (-1020/-936; TFBS for Sp1, NF-1, and NFκB), more precisely the accessibility of the *cis*-active element, is essential for a sufficient transcriptional activity. Moreover, both, the T-159C site and the MolHap spanning sequence, require one another to facilitate a sufficient transcriptional activity of the *OPG* gene promoter. As also seen in transient transfection analyses, with both polymorphic sites (MolHaps and T-159C) separated, transcriptional activities at the level of the shuttle vector were detected. Besides further evidence that transcription factors act as modules, within this model it is also shown that an altered composition of the module has differential consequences for transcriptional activity, and that factors in a module do have different weightings for the stimulation of transcription.

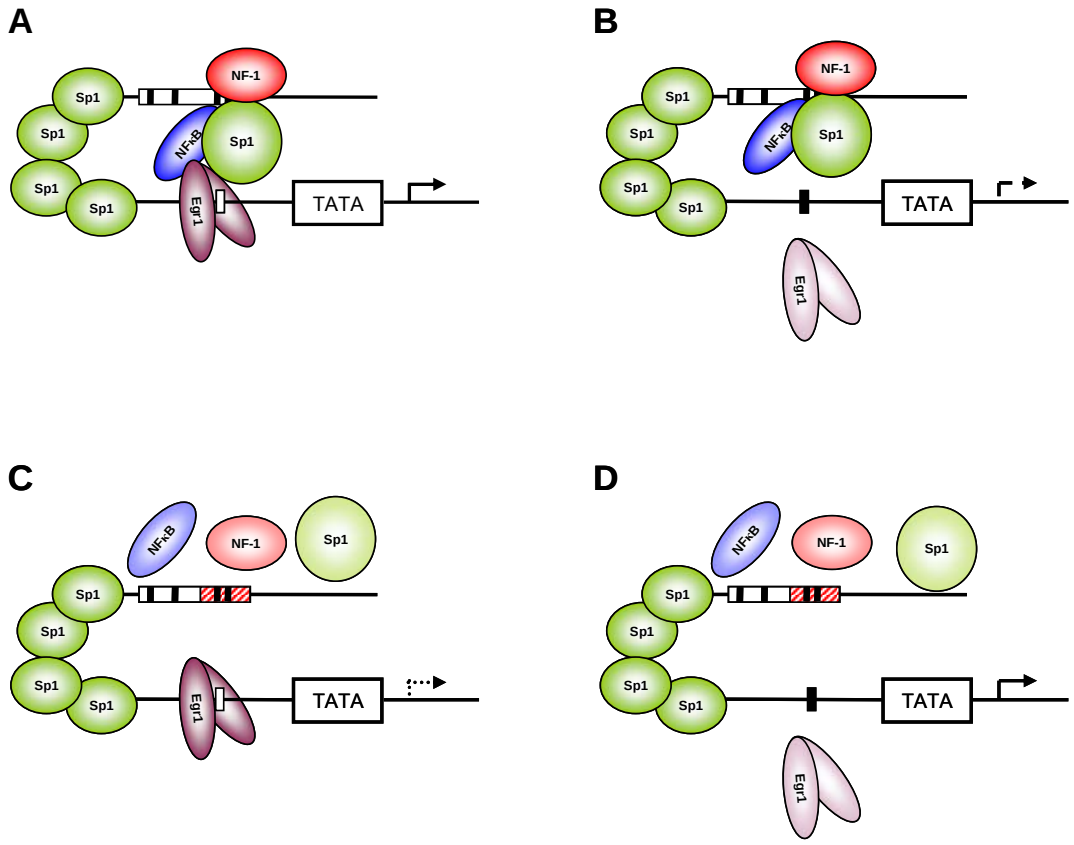

Figure 37 Proposed transcriptional regulation of *OPG*. (A) Sp1 (green), NF-1 (red), and NFκB (blue) bind to the distal promoter portion harboring the MolHap constellations (white box with black bars), and interact with Egr1 (violet), bound to the -159T allele (white bar), to cooperatively stimulate transcription (black arrow). (B) Introduction of the -159C allele leads to an attenuated binding-affinity of Egr1; as a consequence, the transcriptional module is altered in its composition and transcriptional activity is decreased (interrupted arrow). (C) Truncation (red dashed bar) leads to a loss of TFBS for Sp1 (green), NF-1 (red), and NFκB (blue), while Egr1 (violet) alone seems to act as a repressor (dotted arrow). (D) Additional introduction of the -159C allele (black bar) into to the truncated constructs results in a partial restoration of transcriptional activity.

Certainly, the provided hypothesis for the transcriptional regulation of the *OPG* gene needs to be further confirmed in continuative experiments. Projects involving studying the protein:protein interactions and the precise composition, as well as additional TF of the suggested module are conceivable. Therefore, functional-identificatory methods (e.g. co-immunoprecipitations, Yeast-One-Hybrid) and biophysical approaches (mass spectrometry, multiple isotope labeling, multiple reaction monitoring) are useful. Further, it would be quite interesting to study the transcriptional regulation and the module composition under stimulatory conditions (e.g. TNFα, TGFβ, 17β-Estradiol).

5.6. Conclusion

The clinical progression of arteriosclerosis and cardiovascular outcome is influenced by environmental and lifestyle factors, and strongly determined by individual genetic predispositions [Marenberg et al, 1994]. Identification of genetic variants with whole-genome approaches and consequently functional analyses may therefore help gaining a better understanding of the pathophysiology and aetiology of arteriosclerosis [Cambien and Tiret, 2007]. DNA micro array technologies in genome-wide association studies enable genotyping of large study cohorts. Nevertheless, it is mandatory to profile the functional basis of the identified genetic variants [Brand-Herrmann, 2008]. Only 3% of the human genome are coding regions, while the remaining 97% represent introns, regulatory regions, and intergenic regions. These intergenic regions, former described as “junk DNA”, play an emerging role in understanding gene regulatory mechanisms. As a result of the HapMap project, genetic variants associated with a certain disease were detected within these regions, with no idea of their functionality. Thus, the role of intergenic regions is not yet clarified. One presumption is that they represent a bank of advantageous new genes, but they may also be evolutionary artefacts encoding for proteins that are no longer expressed (pseudo-genes). It becomes more and more evident that pseudo-genes may have gene regulatory properties. It is supposed that every 10^{th} pseudo-gene is transcribed, and it was already shown that RNA of a pseudo-gene can silence transcription of its “regular” gene [Korneev et al, 1999]. Genetic variants located in regulatory regions of a gene do not affect the resulting protein directly, but may have profounding transcriptional consequences. Since not only single genetic variants but also alternative promoter usage and epigenetic events can be associated with a certain disease, the entire structure of candidate gene promoters needs to be investigated.

Single genetic variants within regulatory regions may cause alterations in the function of TFBS. But, as mentioned before, a physical TFBS requires the cellular and genomic context to be functional. For that reason, analyses of naturally occurring, molecular haplotype constellations are reasonable. As shown in this study, single genetic variants (T-159C) and haplotype constellations do have sufficient cell type-specific effects on transcriptional regulation of the analyzed *OPG* gene. These effects were more or less pronounced depending on the accessibility of a newly identified *cis*-active region, which in turn may depend on histone modifications, e.g. acetylation of lysine. Alterations of TFBS may cause altered binding affinities of a respective TF (e.g. Egr1 for the -159C allele). As a consequence, an increased stoichiometric availability of the TF is needed to sustain the biologic function. This in turn depends, amongst other factors, on the individual genetic background of the respective transcription factor.

Environmental factors may influence the epigenetic signature of an individual, and depending on its genetic background, the analyzed variants in the *OPG* promoter region may have different consequences for OPG expression and thus for the individual risk of vascular calcification and arteriosclerosis. As OPG is assumed to have protective role in CVD and vascular calcification, patients carrying MolHap2 and MolHap4, as well as the -159C allele, may have an additional risk factor for the incidence of vascular calcification and/or arteriosclerosis.

6. Outlook

The genetic predisposition for complex diseases such as CAD is undisputed, but escapes comprehensive explanation of its development, progression, and severity. With the help of genome-wide association studies and candidate gene approaches, single-genetic variants were identified with a highly significant association with progression and severity of CAD. Since the molecular functionality of these variants in their genomic context is not understood yet, findings are not sufficiently valuable for risk stratification. Therefore, it is mandatory to understand the modularly functionality of human gene promoters. Currently, a change of concept of the understanding of how the human genome works emerges. Erstwhile, the nature of the human genome was considered to be a collection of individual programs (genes), while the modern concept is rather that of an interconnected, dynamic data-processing system software with the capability to interact and "learn" by e.g. epigenetic events. Modern promoter concepts also consider flexible adjustments to change circumstances, comprising transcriptional modules, selection and utilization of alternative promoters, and epigenetics.

Functional SNPs, like those *OPG* haplotypes identified and characterized in this study, may serve as a valuable tool for differentiation- and cell type-specific gene activation, and for analyzing the impact of *cis*-regulatory elements, acting in concert in the natural context of the human genome; molecular haplotypes may be realized as "*in situ* deletions". The understanding of the stated function of individual haplotypes offer for a better risk stratification than any individual SNP. Advantageous concepts support the idea of an individual genome.

New approaches no longer focus on single candidate genes or one genetic predisposition. Based on large-scale gene expression data and linkage analyses, altered transcriptional modules and deflected pathways with a potential role in the pathophysiology of arteriosclerosis, or other complex disease, are identified and functionally analyzed. Therefore, it should further be analyzed whether the TF module, identified within this work and supposedly involved in *OPG* gene regulation, is involved in pro-inflammatory or inflammation-response pathways. Highly associated genetic variants identified in linkage analyses may fail to display any effects in functional analyses. Meanwhile, it is assumed that these variants may play an important role during differentiation processes, and thus are "silent" in differentiated tissues. In future, body's own cells might be de-differentiated into pluri-potent stem cells, and subsequently re-differentiated into cardiomyocytes. Understanding of the complexity of the individuality of each single human genome, based on the individuality of the composing haplotypes has just begun.

7. Bibliography

"MatInspector: Too many matches" Genomatix tutorial. www.genomatix.de

Allison MA, Criqui MH, Wright CM. (2004) Patterns and risk factors for systemic calcified atherosclerosis. *Arterioscler Thromb Vasc Biol.* 24,33133-33136.

Arko B, Prezelj J, Komel R, Kocijancic A, Hudler P, Marc J. (2002) Sequence variations in the osteoprotegerin gene promoter in patients with postmenopausal osteoporosis. *J Clin Endocrinol Metab.* 87,4080-4084.

Arnett DK, Baird AE, Barkley RA, Basson CT, Boerwinkle E, Ganesh SK, Herrington DM, Hong Y, Jaquish C, McDermott DA, O'Donnell CJ. (2007) Relevance of genetics and genomics for prevention and treatment of cardiovasculardisease. *Circulation.* 115,2878-2901.

Ayoubi TA, Van De Ven WJ. (1996) Regulation of gene expression by alternative promoters. *FASEB J.* 10,453-460. Review.

Bajic VB, Choudhary V, Hock CK. (2004) Content analysis of the core promoter region of human genes. *In Silico Biol.* 4,109-125.

Baldwin AS, Jr. (1996) The NF-kappa B and I kappa B proteins: new discoveries and insights. *Annu Rev Immunol*. 14,649-683.

Bennett BJ, Scatena M, Kirk EA, Rattazzi M, Varon RM, Averill M, Schwartz SM, Giachelli CM, Rosenfeld ME. (2006) Osteoprotegerin inactivation accelerates advanced atherosclerotic lesion progression and calcification in older ApoE-/- mice. *Arterioscler Thromb Vasc Biol.* 26,2117-2124.

Bird A. (2002) DNA methylation patterns and epigenetic memory. *Genes Dev*. 16,6-21.

Birnboim HC, Doly J. (1979) A rapid alkaline extraction procedure for screening recombinant plasmid DNA. *Nucleic Acids Res.* 7,1513-1523.

Bondarenko VA, Liu YV, Jiang YI, Studitsky VM. (2003) Communication over a large distance: enhancers and insulators. *Biochem Cell Biol.* 81,241-251. Review.

Bostrom K, Watson KE, Horn S, Wortham C, Herman IM, Demer LL. (1993) Bone morphogenetic protein expression in human atherosclerotic lesions. *J Clin Invest.* 91,1800–1809.

Boyd KE, Wells J, Gutman J, Bartley S M, Farnham P J. (1998) c-Myc target gene specificity is determined by a post-DNAbinding mechanism. *Proc Natl Acad Sci.* 95,13887-13892.

Brand-Herrmann SM. (2008) Where do we go for atherothrombotic disease genetics? *Stroke.* 39,1070-1075.

Brändström H, Jonsson KB, Ohlsson C, Vidal O, Ljunghall S, Ljunggren Ö. (1998) Regulation of osteoprotegerin mRNAlevels by prostaglandin E2 in human bone marrow stroma cells. *Biochem Biophys Res Com.* 247,338–341.

Brandstrom H, Stiger F, Lind L, Kahan T, Melhus H, Kindmark A. (2002) A single nucleotide polymorphism in the promoter region of the human gene for osteoprotegerin is related to vascular morphology and function. *Biochem Biophys Res Commun.* 293,13-17.

Brändström H, Stiger F, Lind L, Kahan T, Melhus H, Kindmark A. (2002) A single nucleotide polymorphism in the promoter region of the human gene for osteoprotegerin is related to vascular morphology and function. *Biochem Biophys Res Commun.* 293,13-17.

Briggs MR, Kadonaga JT, Bell SP, Tjian R. (1986) Purification and biochemical characterization of the promoter-specific transcription factor, Sp1. *Science.* 234,47-52.

Browner WS, Lui LY, Cummings SR. (2001) Associations of serum osteoprotegerin levels with diabetes, stroke, bone density, fractures, and mortality in elderly women. *J Clin Endocrinol Metab.* 86,631-637.

Bucay N, Sarosi I, Dunstan CR, Morony S, Tarpley J, Capparelli C, Scully S, Tan HL, Xu W, Lacey DL, Boyle WJ, Simonet WS. (1998) Osteoprotegerin-deficient mice develop early onset osteoporosis and arterial calcification. *Genes Dev.* 12,260-1268.

Burgess TL, Qian Y, Kaufman S, Ring BD, Van G, Capparelli C, Kelley M, Hsu H, Boyle WJ, Dunstan CR, Hu S, Lacey DL. (1999) The ligand for osteoprotegerin (OPGL) directly activates mature osteoclasts. *J Cell Biol.* 145,527-538.

Cambien F, Poirier O, Lecerf L, Evans A, Cambou JP, Arveiler D, Luc G, Bard JM, Bara L, Ricard S, Tiret L, Amouyel P, Alhenc-Gelas F, Soubrier F. (1992) Deletion polymorphism in the gene for angiotensin-converting enzyme is a potent risk factor for myocardial infarction. *Nature.* 359,641-644.

Cambien F, Tiret L. (2007) Genetics of cardiovascular diseases: from single mutations to the whole genome. *Circulation.* 116,1714-1724.

Center for Information Technology, National Instituts of Health. http://www-bimas.cit.nih.gov/molbio/proscan/

Chapman NR, Perkins ND. (2002) Inhibition of the RelA(p65) NF-kappaB subunit by Egr-1. *J Biol Chem*. 275,4719-4725.

Cheong J, Yamada Y, Yamashita R, Irie T, Kanai A, Wakaguri H, Nakai K, Ito T, Saito I, Sugano S, Suzuki Y. (2006) Diverse DNA methylation statuses at alternative promoters of human genes in various tissues. *DNA Res.* 13,155-167.

Cogswell PC, Mayo MW, Baldwin AS, Jr. (1997) Involvement of Egr-1/RelA synergy in distinguishing T cell activation from tumor necrosis factor-alpha-induced NF-kappa B1 transcription. *J Exp Med*. 185,491–497.

Courey AJ, Holtzman DA, Jackson SP, Tjian R. (1989) Synergistic activation by the glutamine-rich domains of human transcription factor Sp1. *Cell.* 59,827-836.

Dai G, Kaazempur-Mofrad MR, Natarajan S, Zhang Y, Vaughn S, Blackman BR, Kamm RD, García-Cardeña G, Gimbrone MA Jr. (2004) Distinct endothelial phenotypes evoked by arterial waveforms derived from atherosclerosis-susceptible and -resistant regions of human vasculature. *Proc Natl Acad Sci U S A.* 101,14871-14876.

Dempsey PW, Doyle SE, He JQ, Cheng G. (2003) The signaling adaptors and pathways activated by TNF superfamily. *Cytokine Growth Factor Rev.* 14,193-209.

Dhore CR, Cleutjens JP, Lutgens E, Cleutjens KB, Geusens PP, Kitslaar PJ, Tordoir JH, Spronk HM, Vermeer C, Daemen MJ. (2001) Differential expression of bone matrix regulatory proteins in human atherosclerotic plaques. *Arterioscler Thromb Vasc Biol.* 21,1998–2003.

Don RH, Cox PT, Wainwright BJ, Baker K, Mattick JS. (1991) 'Touchdown' PCR to circumvent spurious priming during gene amplification. *Nucleic Acids Res.* 19,4008.

Dördelmann C, Telgmann R, Brand E, Hagedorn C, Schröer B, Hasenkamp S, Baumgart P, Kleine-Katthöfer P, Paul M, Brand-Herrmann SM. (2008) Functional and structural profiling of the human thrombopoietin gene promoter. *J Biol Chem.* 283,24382-24391.

Dorsett D. (1999) Distant liaisons: long-range enhancer-promoter interactions in Drosophila. *Curr Opin Genet Dev.* 9,505-514. Review.

Duan J, Wainwright MS, Comeron JM, Saitou N, Sanders AR, Gelernter J, Gejman PV. (2003) Synonymous mutations in the human dopamine receptor D2 (DRD2) affect mRNA stability and synthesis of the receptor. *Hum Mol Genet.* 12,205-216.

Eckhardt F, Lewin J, Cortese R, Rakyan VK, Attwood J, Burger M, Burton J, Cox TV, Davies R, Down TA, Haefliger C, Horton R, Howe K, Jackson DK, Kunde J, Koenig C, Liddle J, Niblett D, Otto T, Pettett R, Seemann S, Thompson C, West T, Rogers J, Olek A, Berlin K, Beck S. (2006) DNA methylation profiling of human chromosomes 6, 20 and 22. *Nat Genet.* 38,1378-1385.

Frohman MA, Dush MK, Martin GR. (1988) Rapid production of full-length cDNAs from rare transcripts: amplification using a single gene-specific oligonucleotide primer. *Proc Natl Acad Sci U S A.* 85,8998-9002.

Frostegård J, Ulfgren AK, Nyberg P, Hedin U, Swedenborg J, Andersson U, Hansson GK. (1999) Cytokine expression in advanced human atherosclerotic plaques: dominance of pro-inflammatory (Th1) and macrophage-stimulating cytokines. *Atherosclerosis.* 145,:33-43.

Fry CJ, Farnham PJ. (1999) Context-dependent transcriptional regulation. *J Biol Chem.* 274,29583-29586.

Fu M, Zhu X, Zhang J, Liang J, Lin Y, Zhao L, Ehrengruber MU, Chen YE. (2003) Egr-1 target genes in human endothelial cells identified by microarray analysis. *Gene*. 315,33-41.

Gashler AL, Swaminathan S, Sukhatme VP. (1993) A novel repression module, an extensive activation domain, and a bipartite nuclear localization signal defined in the immediate-early transcription factor Egr-1. *Mol Cell Biol.* 13,4556-4571.

Geyer PK, Corces VG. (1992) DNA position-specific repression of transcription by a Drosophila zinc fingerprotein. *Genes Dev.* 6,1865-1873.

Giachelli C, Bae N, Lombardi D, Majesky M, Schwartz S. (1991) Molecular cloning and characterization of 2B7, a rat mRNA which distinguishes smooth muscle cell phenotypes in vitro and is identical to osteopontin (secreted phosphoprotein I, 2aR). *Biochem Biophys Res Commun.* 177,867–873.

Giachelli CM, Bae N, Almeida M, Denhardt DT, Alpers CE, Schwartz SM. (1993) Osteopontin is elevated during neointima formation in rat arteries and is a novel component of human atherosclerotic plaques. *J Clin Invest.* 92,1686–1696.

Gilmore TD. (2006) Introduction to NF-kappaB: players, pathways, perspectives. *Oncogene.* 25,6680-6684. Review.

Grabe N. (2002) AliBaba2: context specific identification of transcription factor binding sites. *In Silico Biol.* 2,1-15.

Hansson GK. (2001) Immune mechanisms in atherosclerosis. Arterioscler Thromb Vasc Biol. 21,1876-1890.

Hehlgans T, Pfeffer K. (2005) The intriguing biology of the tumour necrosis factor/tumour necrosis factor receptor superfamily: players, rules and the games. *Immunology.* 115,1-20.

Heintzman ND, Ren B. (2006) The gateway to transcription: identifying, characterizing and understanding promoters in the eukaryotic genome. *Cell Mol Life Sci.* 64,386-400.

Higgs DR, Vernimmen D, Wood B. (2008) Long-range regulation of alpha-globin gene expression. *Adv Genet.* 61,143-173. Review.

Hillebrand U, Lang D, Telgmann R, Hagedorn C, Stock CM, Wilhelmi M, Oberleithner H, Hausberg M. (2009) Nebivolol increases endothelial cell size and elasticity via the estrogen receptor – a Nano-Imaging Study. *J Hypertens.* In press.

Hofbauer LC, Dunstan CR, Spelsberg TC, Riggs BL, Khosla S. (1998) Osteoprotegerin production by human osteoblast lineage cells is stimulated by vitamin D, bone morphogenetic protein-2, and cytokines. *Biochem Biophys Res Commun.* 250,776-781.

Hofbauer LC, Khosla S, Dunstan CR, Lacey DL, Spelsberg TC, Riggs BL. (1999) Estrogen stimulates gene expression and protein production of osteoprotegerin in human osteoblastic cells. *Endocrinology.* 140,4367–4370.

Hsu H, Huang J, Shu HB, Baichwal V, Goeddel DV. (1996) TNF-dependent recruitment of the protein kinase RIP to the TNF receptor-1 signaling complex. *Immunity.* 4,387-396.

Hsu HH, Duning K, Meyer HH, Stölting M, Weide T, Kreusser S, van Le T, Gerard G, Telgmann R, Brand-Herrmann SM, Pavenstädt H, Bek MJ. (2009) Hypertension in mice lacking the CXCR3 chemokine receptor. *Am J Physiol Renal Physiol.* [Epub ahead of print].

Hunt JL, Fairman R, Mitchell ME, Carpenter JP, Golden M, Khalapyan T, Wolfe M, Neschis D, Milner R, Scoll B, Cusack A, Mohler ER 3rd. (2002) Bone formation in carotid plaques: a clinicopathological study. *Stroke.* 33,1214–1219.

Ikeda T, Shirasawa T, Esaki Y, Yoshiki S, Hirokawa K. (1993) Osteopontin mRNA is expressed by smooth muscle-derived foam cells in human atherosclerotic lesions of the aorta. *J Clin Invest.* 92,2814–2820.

Jenuwein T, Allis CD. (2001) Translating the histone code. *Science.* 293,1074-1080.

Jones KA, Kadonaga JT, Rosenfeld PJ, Kelly TJ, Tjian R. (1987) A cellular DNA-binding protein that activates eukaryotic transcription and DNA replication. *Cell.* 48,79-89.

Jono S, Ikari Y, Shioi A, Mori K, Miki T, Hara K, Nishizawa Y. (2002) Serum osteoprotegerin levels are associated with the presence and severity of coronary artery disease. *Circulation.* 106,1192-1194.

Katzen F. (2007) Gateway® recombinational cloning: a biological operating system. *Expert Opin Drug Discov.* 2,571-589.

Khachigian LM, Williams AJ, Collins T. (1995) Interplay of Sp1 and Egr-1 in the proximal platelet-derived growth factor A-chain promoter in cultured vascular endothelial cells. *J Biol Chem.* 270,27679-27686.

Khosla S. (2001) Minireview: the OPG/RANKL/RANK system. *Endocrinology.* 142,5050-5055.

Kiechl S, Schett G, Wenning G, Redlich K, Oberhollenzer M, Mayr A, Santer P, Smolen J, Poewe W, Willeit J. (2004) Osteoprotegerin is a risk factor for progressive atherosclerosis and cardiovascular disease. *Circulation.* 109,2175-2180.

Kornberg RD. (2007) The molecular basis of eucaryotic transcription. *Cell Death Differ.* 14,1989-1997.

Kornblihtt AR. (2006) Chromatin, transcript elongation and alternative splicing. *Nat Struct Mol Biol.* 13,5-7.

Korneev SA, Park JH, O'Shea M. (1999) Neuronal expression of neural nitric oxide synthase (nNOS) protein is suppressed by an antisense RNA transcribed from an NOS pseudogene. *J Neurosci.* 19,7711-7720.

Kruse U, Qian F, Sippel AE. (1991) Identification of a fourth nuclear factor I gene in chicken by cDNA cloning: NFI-X. *Nucleic Acids Res.* 19,6641.

Landy A. (1989) Dynamic, structural, and regulatory aspects of lambda site-specific recombination. *Ann Rev Biochem.* 58,913-949.

Langdahl BL, Carstens M, Stenkjaer L, Eriksen EF. (2002) Polymorphisms in the osteoprotegerin gene are associated with osteoporotic fractures. *J Bone Miner Res.* 17,1245-1255.

Lemon B, Tjian R. (2000) Orchestrated response: a symphony of transcription factors for gene control. *Genes Dev.* 14,2551-2569.

Lin SL, Kim H, Ying SY. (2008) Intron-mediated RNA interference and microRNA (miRNA). *Front Biosci.* 13,2216-2230.

Liu S, Spinner DS, Schmidt MM, Danielsson JA, Wang S, Schmidt J. (2000) Interaction of MyoD family proteins with enhancers of acetylcholine receptor subunit genes in vivo. *J Biol Chem.* 275,41364-41368.

Mackey R, Venkitachalam L, Sutton-Tyrrell K. (2007) Calcifications, Arterial Stiffness and Atherosclerosis. *Adv Cardiol.* 44,234-244.

Marenberg ME, Risch N, Berkman LF, Floderus B, de Faire U. (1994) Genetic susceptibility to death from coronary heart disease in a study of twins. *N Engl J Med.* 330,1041-1046.

Massberg S, Brand K, Grüner S, Page S, Müller E, Müller I, Bergmeier W, Richter T, Lorenz M, Konrad I, Nieswandt B, Gawaz M. (2002) A critical role of platelet adhesion in the initiation of atherosclerotic lesion formation. *J Exp Med.* 196,887-896.

Matsuzaki K, Udagawa N, Takahashi N, Yamaguchi K, Yasuda H, Shima N, Morinaga T, Toyama Y, Yabe Y, Higashio K, Suda T. (1998) Osteoclast differentiation factor (ODF) induces osteoclast-like cell formation in human peripheral blood mononuclear cell cultures. *Biochem Biophys Res Commun.* 246,199-204.

McNally JG, Müller WG, Walker D, Wolford R, Hager GL. (2000) The glucocorticoid receptor: rapid exchange with regulatory sites in living cells. *Science.* 287,1262-1265.

Medscape General Medicine http://www.medscape.com/content/2000/00/40/89/408911/art-wh0308.aubi.fig2.gif

Merkel KD, Erdmann JM, McHugh KP, Abu-Amer Y, Ross FP, Teitelbaum SL. (1999) Tumor necrosis factor-α mediates orthopedic implant osteolysis. *Am J Pathol.* 154,203–210.

Mohler ER 3rd, Gannon F, Reynolds C, Zimmerman R, Keane MG, Kaplan FS. (2001) Bone formation and inflammation in cardiac valves. *Circulation.* 103,1522–1528.

Montecucco F, Steffens S, Mach F. (2007) The immune response is involved in atherosclerotic plaque calcification: could the RANKL/RANK/OPG system be a marker of plaque instability? *Clin Dev Immunol.* 2007,75805-75813.

Morinaga T, Nakagawa N, Yasuda H, Tsuda E, Higashio K. (1998) Cloning and characterization of the gene encoding human osteoprotegerin/osteoclastogenesis-inhibitory factor. *Eur J Biochem.* 254,685-691.

Morony S, Tintut Y, Zhang Z, Cattley RC, Van G, Dwyer D, Stolina M, Kostenuik PJ, Demer LL. (2008) Osteoprotegerin inhibits vascular calcification without affecting atherosclerosis in ldlr(-/-) mice. *Circulation.* 117,411-420.

Mouillet JF, Sonnenberg-Hirche C, Yan X, Sadovsky Y. (2004) p300 regulates the synergy of steroidogenic factor-1 and early growth response-1 in activating luteinizing hormone-beta subunit gene. *J Biol Chem.* 279,7832-7839.

Mullis K, Faloona F, Scharf S, Saiki R, Horn G, Erlich H. (1986) Specific enzymatic amplification of DNA in vitro: the polymerase chain reaction. *Cold Spring Harb Symp Quant Biol.* 51,263-273.

Murakami T, Yamamoto M, Yamamoto M, Ono K, Nishikawa M, Nagata N, Motoyoshi K, Akatsu T. (1998) Transforming growth factor-b1 increases mRNA levels of osteoclastogenesis inhibitory factor in osteoblastic/stromal cells and inhibits the survival of murine osteoclast-like cells. *Biochem Biophys Res Com.* 252,747–752.

Nagata K, Guggenheimer RA, Enomoto T, Lichy JH, Hurwitz J. (1982) Adenovirus DNA replication in vitro: identification of a host factor that stimulates synthesis of the preterminal protein-dCMP complex. *Proc Natl Acad Sci U S A.* 79,6438-6442.

Nitta K, Akiba T, Uchida K, Otsubo S, Takei T, Yumura W, Kabaya T, Nihei H. (2004) Serum osteoprotegerin levels and the extent of vascular calcification in haemodialysis patients. *Nephrol Dial Transplant.* 19,1886-1889.

Ogbourne S, Antalis TM. (1998) Transcriptional control and the role of silencers in transcriptional regulation in eukaryotes. *Biochem J.* 331,1-14.

Ohler U, Liao GC, Niemann H, Rubin GM. (2002) Computational analysis of core promoters in the Drosophila genome. *Genome Biol.* 3, RESEARCH0087.

Olesen P, Nguyen K, Wogensen L, Ledet T, Rasmussen LM. (2007) Calcification of human vascular smooth muscle cells: associations with osteoprotegerin expression and acceleration by high-dose insulin. *Am J Physiol Heart Circ Physiol.* 292,H1058-1064.

Osada S, Daimon S, Ikeda T, Nishihara T, Yano K, Yamasaki M, Imagawa M. (1997) Nuclear factor 1 family proteins bind to the silencer element in the rat glutathione transferase P gene. *J Biochem.* (Tokyo) 121,355-363.

Osada S, Ikeda T, Xu M, Nishihara T, Imagawa M. (1997) Identification of the transcriptional repression domain of nuclear factor 1-A. *Biochem Biophys Res Commun.* 238,744-747.

Peiser L, Mukhopadhyay S, Gordon S. (2002) Scavenger receptors in innate immunity. *Curr Opin Immunol.* 14,123-128.

Plutzky J. (2003) The vascular biology of atherosclerosis. *Am J Med.*115,55S-61S. Review.

Pugh BF, Tjian R. (1991) Transcription from a TATA-less promoter requires a multisubunit TFIID complex. *Genes Dev.* 5,1935-1945.

Rafty LA, Santiago FS, Khachigian LM. (2002) NF1/X represses PDGF A-chain transcription by interacting with Sp1 and antagonizing Sp1 occupancy of the promoter. *The EMBO Journal.* 21,334–343.

Rasmussen LM, Tarnow L, Hansen TK, Parving HH, Flyvbjerg A. (2006) Plasma osteoprotegerin levels are associated with glycaemic status, systolic blood pressure, kidney function and cardiovascular morbidity in type 1 diabetic patients. *Eur J Endocrinol.* 154,75-81.

Rhee EJ, Oh KW, Jung CH, Lee WY, Oh ES, Yun EJ, Baek KH, Kang MI, Kim SW. (2006) The relationship between four single nucleotide polymorphisms in the promoter region of the osteoprotegerin gene and aortic calcification or coronary artery disease in Koreans. *Clin Endocrinol.* 64,689-697.

Rittenhouse J, Marcus F. (1984) Peptide mapping by polyacrylamide gelelectrophoresis after cleavage at aspartyl-prolyl peptide bonds in sodiumdodecyl sulfate-containing buffers. *Anal Biochem.* 138,442-448.

Roseman RR, Pirrotta V, Geyer PK. (1993) The su(Hw) protein insulates expression of the Drosophila melanogaster white gene from chromosomal position-effects. *EMBO J.* 12,435-442.

Ross FP. (2000) RANKing the importance of measles virus in Paget's disease. *J Clin Invest.* 105,555-558.

Ross J. (1995) mRNA stability in mammalian cells. *Microbiol Rev.* 59,423-450.

Ross R. (1995) Cell biology of atherosclerosis. *Annu Rev Physiol.* 57,791-804.

Rumberger JA, Simons DB, Fitzpatrick LA, Sheedy PF, Schwartz RS. (1995) Coronary artery calcium area by electron-beam computed tomography and coronary atherosclerotic plaque area. A histopathologic correlative study. *Circulation.* 92,2157-2162.

Rupp RA, Kruse U, Multhaup G, Gobel U, Beyreuther K, Sippel AE. (1990) Chicken NFI/TGGCA proteins are encoded by at least three independent genes: NFI-A, NFI-B and NFI-C with homologues in mammalian genomes. *Nucleic Acids Res.* 18,2607–2616.

Russo MW, Sevetson BR, Milbrandt J. (1995) Identification of NAB1, a repressor of NGFI-A- and Krox20-mediated transcription. *Proc Natl Acad Sci U S A.* 92,6873-6877.

Sambrook J, Russell DW. (2001) Molecular Cloning: A Laboratory Manual, 3rd Ed. *Cold Spring Harbor Laboratory Press*, Cold Spring Harbor, NY.

Santoro C, Mermod N, Andrews PC, Tjian R. (1988) A family of human CCAAT-box-binding proteins active in transcription and DNA replication: cloning and expression of multiple cDNAs. *Nature.* 334,218–224.

Schoppet M, Preissner KT, Hofbauer LC. (2002) RANK ligand and osteoprotegerin: paracrine regulators of bone metabolism and vascular function. *Arterioscler Thromb Vasc Biol.* 22,549-553.

Schreiber E, Matthias P, Muller MM, Schaffner W. (1989) Rapid detection of octamer binding G proteins with 'mini-extracts', prepared from a small number of cells. *Nucleic Acids Res.* 17,6419.

Scott KS, Geyer PK. (1995) Effects of the su(Hw) insulator protein on the expression of the divergently transcribed Drosophila yolk protein genes. *EMBO J.* 14,6258-6267.

Shanahan CM, Cary NR, Metcalfe JC, Weissberg PL. (1994) High expression of genes for calcification-regulating proteins in human atherosclerotic plaques. *J Clin Invest.* 93,2393–2402.

Shioi A, Nishizawa Y, Jono S, Koyama H, Hosoi M, Morii H. (1995) ß-glycerophosphate accelerates calcification in cultured bovine vascular smooth muscle cells. *Arterioscler Thromb Vasc Biol.* 15,2003–2009.

Simonet WS, Lacey DL, Dunstan CR, Kelley M, Chang MS, Lüthy R, Nguyen HQ, Wooden S, Bennett L, Boone T, Shimamoto G, DeRose M, Elliott R, Colombero A, Tan HL, Trail G, Sullivan J, Davy E, Bucay N, Renshaw-Gegg L, Hughes TM, Hill D, Pattison W, Campbell P, Sander S, Van G, Tarpley J, Derby P, Lee R, Boyle WJ. (1997) Osteoprotegerin: a novel secreted protein involved in the regulation of bone density. *Cell.* 89,309-319.

Simonet WS, Lacey DL, Dunstan CR, Kelley M, Chang MS, Lüthy R, Nguyen HQ, Wooden S, Bennett L, Boone T, Shimamoto G, DeRose M, Elliott R, Colombero A, Tan HL, Trail G, Sullivan J, Davy E, Bucay N, Renshaw-Gegg L, Hughes TM, Hill D, Pattison W, Campbell P, Sander S, Van G, Tarpley J, Derby P, Lee R, Boyle WJ. (1997) Osteoprotegerin: a novel secreted protein involved in the regulation of bone density. *Cell.* 89,309-319.

Skålén K, Gustafsson M, Rydberg EK, Hultén LM, Wiklund O, Innerarity TL, Borén J. (2002) Subendothelial retention of atherogenic lipoproteins in early atherosclerosis. *Nature.* 417,750-754.

Smith CA, Farrah T, Goodwin RG. (1994) The TNF receptor superfamily of cellular and viral proteins: activation, costimulation, and death. *Cell.* 76,959-962.

Smith JD, Trogan E, Ginsberg M, Grigaux C, Tian J, Miyata M. (1995) Decreased atherosclerosis in mice deficient in both macrophage colony-stimulating factor (op) and apolipoprotein E. *Proc Natl Acad Sci U S A.* 92,8264-8268.

Soufi M, Schoppet M, Sattler AM, Herzum M, Maisch B, Hofbauer LC, Schaefer JR. (2004) Osteoprotegerin gene polymorphisms in men with coronary artery disease. *J Clin Endocrinol Metab.* 89,3764-3768.

Soufi M, Schoppet M, Sattler AM, Herzum M, Maisch B, Hofbauer LC, Schaefer JR. (2004) Osteoprotegerin gene polymorphisms in men with coronary artery disease. *J Clin Endocrinol Metab.* 89,3764-3768.

Srivastava S, Weitzmann MN, Kimble RB, Rizzo M, Zahner M, Milbrandt J, Ross FP, Pacifici R. (1998) Estrogen blocks M-CSF gene expression and osteoclast formation by regulating phosphorylation of Egr-1 and its interaction with Sp-1. *J Clin Invest.* 102,1850-1859.

Stanger BZ, Leder P, Lee TH, Kim E, Seed B. (1995) RIP: a novel protein containing a death domain that interacts with Fas/APO-1 (CD95) in yeast and causes cell death. *Cell.* 81,513-523.

Steitz SA, Speer MY, Curinga G, Yang HY, Haynes P, Aebersold R, Schinke T, Karsenty G, Giachelli CM. (2001) Smooth muscle cell phenotypic transition associated with calcification: upregulation of Cbfa1 and downregulation of smooth muscle lineage markers. *Circ Res.* 89,1147–1154.

Stemme S, Faber B, Holm J, Wiklund O, Witztum JL, Hansson GK. (1995) T lymphocytes from human atherosclerotic plaques recognize oxidized low densitylipoprotein. *Proc Natl Acad Sci U S A.* 92,3893-3897.

Sun D, Hurley LH. (1994) Cooperative bending of the 21-base-pair repeats of the SV40 viral early promoter by human Sp1. *Biochemistry.* 33,9578-9587.

Szabo SJ, Sullivan BM, Peng SL, Glimcher LH. (2003) Molecular mechanisms regulating Th1 immune responses. *Annu Rev Immunol*. 21,713-758.

Takai H, Kanematsu M,Yano K, Tsuda E, Higashio K, Ikeda K, Watanabe K, Yamada Y. (1998) Transforming growth factor-b stimulates the production of osteoprotegerin/osteoclastogenesis inhibitory factor by bone marrow stromal cells. *J Biol Chem.* 273,27091–27096.

Tan L, Peng H, Osaki M, Choy BK, Auron PE, Sandell LJ, Goldring MB. (2003) Egr-1 mediates transcriptional repression of COL2A1 promoter activity by interleukin-1beta. *J Biol Chem.* 278,17688-17700.

Tanimura A, McGregor DH, Anderson HC. (1983) Matrix vesicles in atherosclerotic calcification. *Proc Soc Exp Biol Med.* 172, 173–177.

Telgmann R, Dördelmann C, Brand E, Nicaud V, Hagedorn C, Pavenstädt H, Cambien F, Tiret L, Paul M, Brand-Herrmann SM. (2008) Molecular genetic analysis of a human insulin-like growth factor 1 promoter P1 variation. *FASEB J.* 2008 Dec 22.

Tjian R. http://www.hhmi.org/research/investigators/tjian.html

Towbin H, Staehlin T, Gordon J. (1979) Electrophoretic transfer of proteins polyacrylamid gels to nitrocellulose sheet: precodure and some applications. *Proc Natl Acad Sci USA.* 76,4350-4354.

Tregouet DA, Barbaux S, Escolano S, Tahri N, Golmard JL, Tiret L, Cambien F. (2002) Specific haplotypes of the P-selectin gene are associated with myocardial infarction. *Hum Mol Genet*. 11,2015-2023.

Tsuda E, Goto M, Mochizuki S, Yano K, Kobayashi F, Morinaga T, Higashio K. (1997) Isolation of a novel cytokine from human fibroblasts that specifically inhibits osteoclastogenesis. *Biochem Biophys Res Commun.* 234,137-142.

Vidal NOA, Brändström H, Jonsson KB, Ohlsson C. (1998) Osteoprotegerin mRNA is expressed in primary human osteoblast-like cells: Down-regulation by glucocorticoids. *J Endocrinol.* 159,191–195.

Wolffe AP. (1998) Packaging principle: how DNA methylation and histone acetylation control the transcriptional activity of chromatin. *J Exp Zool.* 282,239-244. Review.

Wong DL, Siddall BJ, Ebert SN, Bell RA, Her S. (1998) Phenylethanolamine N-methyltransferase gene expression: synergistic activation by Egr-1, AP-2 and the glucocorticoid receptor. *Brain Res Mol Brain Res.* 61,154-161.

World Health Organization, Cardiovascular Disease site (http://www.who.int/cardiovascular_diseases/en)

Yamaguchi K, Kinosaki M, Goto M, Kobayashi F, Tsuda E, Morinaga T, Higashio K. (1998) Characterization of structural domains of human osteoclastogenesis inhibitory factor. *J Biol Chem.* 273,5117-5123.

Yamamoto Y, Gaynor RB. (2004) IkappaB kinases: key regulators of the NF-kappaB pathway. *Trends Biochem Sci.* 29,72-79. Review.

Yan SF, Fujita T, Lu J, Okada K, Shan Zou Y, Mackman N, Pinsky DJ, Stern DM. (2000) Egr-1, a master switch coordinating upregulation of divergent gene families underlying ischemic stress. *Nat Med.* 6,1355-1361.

Yasuda H, Shima N, Nakagawa N, Mochizuki SI, Yano K, Fujise N, Sato Y, Goto M, Yamaguchi K, Kuriyama M, Kanno T, Murakami A, Tsuda E, Morinaga T, Higashio K. (1998) Identity of osteoclastogenesis inhibitory factor (OCIF) and osteoprotegerin (OPG): a mechanism by which OPG/OCIF inhibits osteoclastogenesis in vitro. *Endocrinology.* 139,1329-1337.

8. Appendix

8.1. SNPs identified in the OPG gene

Table 1. SNPs identified in the *OPG* gene with their according rs number and region of appearance.

SNP		region
T-960C	rs3134071	5´-flanking region
A-946G	rs3102735	5´-flanking region
G-900A	rs3134070	5´-flanking region
T-864G	rs3134069	5´-flanking region
T-159C	rs2073617	5´-flanking region
G+73C	rs2073618	exon 1
C1217T	rs3102734	intron 1
Ins/Del/ct 6533/34	rs10554146	intron 3
A+832G	rs7844577	exon 4
A8731C	rs7844539	intron 4

8.2. Oligonucleotide sequences by application

Table 2. Nucleotide sequences for diagnostic PCR. In general overlapping exon-intron-boundaries.

Name	Sequence 5'-3'	Position	Accession #/ Ref
OPGdiag SS	CTC GTG TTT CTG GAC ATC	bp 119	U94332
OPGdiag AS	ACA GGG TAA CAT CTA TTC C	bp 698	U94332
OPG TSS1 SS	GGA GAC GCA CCG GAG C	bp 1110	AB008822
OPG TSS2 SS	CTG GAG CTT TCT GCA CA	bp 952	AB008822
OPG TSS3 SS	ACT CCC CGA AAA GGG CTC AGA	bp 922	AB008822
OPG TSS4 SS	ACT CCC CGA AAA GGG CTC AGA	bp 506	AB008822
hRP27 SS	CCA GGA TAA GGA AGG AAT TCC TCC TG	bp 128	NM_002954.3
hRP27 AS	CCA GCA CCA CAT TCA TCA GAA GG	bp 424	NM_002954.3

Table 3. Nucleotide sequences for cloning. 5' added nucleotides for creating restriction sites for endonucleases are bold.

Name	Sequence 5'-3'	Position	Accession #/ Ref
OPG MolHap SS-SacI	A**GA GCT C**A ACC CGC GAA CTG TAA TCC ATG	bp 88	AB008822
OPG MolHap AS-NheI	A**GC TAG C**A TAA CCT TGC GGA GCA CTG	bp337	AB008822
OPG-159 SS	AGC CGC CTT GTT CCT CAG	bp 822	AB008822
OPG-159 AS	GAG AGA TCT CTC ATC ACG TTA TAT ATA GCG TCC	bp 1096	AB008822
OPG-Del1 SS-SacI	A**GA GCT C**A ACC CGC GAA CTG TAA TCC ATG	bp 88	AB008822
OPG-Del2 SS-SacI	A**GA GCT C**AC AGC GAA CCC TAG AGC	bp 173	AB008822
OPG-Del3 SS-SacI	A**GA GCT C**TA GGG CCA ATC AGA CAT TAG TTA G	bp 428	AB008822
OPG-Del4 SS-SacI	A**GA GCT C**AG CCG CCT TGT TCC TCA G	bp 822	AB008822
OPG Del AS-BglIII	GAG **AGA TCT** CTC ATC ACG TTA TAT ATA GCG TCC	bp 1096	AB008822

Table 4. Nucleotide sequences for EMSA sequencing reaction.

Name	Sequence 5'-3'	Position	Accession #/ Ref
OPG Seq SS	TAG GGC CAA TCA GAC ATT AGT TAG	bp 432	AB008822
OPG Seq AS	TTC ACT TCG GGT TCT GAA ACC TC	bp 582	AB008822
pGL3 SS	AGT GCA AGT GCA GGT GCC AG	bp 90	U47295
pGL3 AS	CTT TAT GTT TTT GGC GTC TTC C	bp4781	U47295

Table 5. Nucleotide sequences for site-directed mutagenesis.

Name	Sequence 5'-3'	Position	Accession #/ Ref
OPG mut-957	GTC ATC AAG TCT AAC TTC **C**AG ACC AGG GAA TTG ATG G	bp 131	AB008822
OPG mut-897	GCA AAG TGC CAA ACT TCT GTC **AA**T AGC TTG	bp 188	AB008822
OPG mut-861	GGA AAG ACC TCG AGG AGG C**G**A CTC CAG AAG TT	bp 226	AB008822

Table 6. Nucleotide sequences for RACE.

Name	Sequence 5'-3'	Position	Accession #/ Ref
RACE cDNA snth.	CGC TCT GGG GTT CCA GCT T	bp 507	U94332
RACE anchor	GAC CAC GCG TAT CGA TGT CGA $C(T)_{16}$		Kit #3353621001
RACE adaptor SS	GAC CAC GCG TAT CGA TGT CGA C		Kit #3353621001
RACE PCR AS	CCT GGG TGG TCC ACT TAA TGG A	bp 158	U94332
RACE Seq	CGA GCG CGC AGC ACA GCA A	bp 122	U94332

Table 7. Nucleotide sequences for sequencing reaction.

Name	Sequence 5'-3'	Position	Accession #/ Ref
OPG Seq SS	TAG GGC CAA TCA GAC ATT AGT TAG	bp 432	AB008822
OPG Seq AS	TTC ACT TCG GGT TCT GAA ACC TC	bp 582	AB008822
pGL3 SS	AGT GCA AGT GCA GGT GCC AG	bp 90	U47295
pGL3 AS	CTT TAT GTT TTT GGC GTC TTC C	bp4781	U47295

Table 8. Nucleotide sequences for EMSA probes.

Name	Sequence 5'-3'	Position	Accession #/ Ref
EMSA Oligo -156 SS	CCC TGA AAG CGT TAA **T/C** CCT GGA GCT TTC TGC	bp 935	AB008822
EMSA Oligo -156 AS	GCA GAA AGC TCC AGG **A/G** TTA ACG CTT TCA GGG	bp 965	AB008822
Egr-1 consensus	CCT CCC CCC GCC TTG CCC GGG GTT GTG G		Koyano-Nakagawa et al, 1994
NF-1 consensus	GGG CTA GAT GGC TGC CAG CCA AGG CTT CAT		
Sp1 consensus	ATT CGA TCG GGG CGG GGC GAG C		

Danksagung

Zunächst gilt mein Dank Herrn Prof. Dr. Dr. med. Brand-Herrmann für die Bereitstellung des sehr interessanten Themas und die Möglichkeit, die Ergebnisse meiner Arbeit auf verschiedenen nationalen und internationalen Kongressen vorzustellen. Ich möchte mich auch bei Prof. Dr. Bruno Moerschbacher, meinem Betreuer an der biologischen Fakultät der WWU Münster, bedanken.

Mein ganz besonderer Dank gilt der „Laborcrew“ der AG Prof. Dr. Dr. med. Brand-Herrmann. Ihr habt zum Gelingen der Arbeit wesentlich beigetragen und vieles wäre ohne Euch nicht möglich gewesen: Dr. Corinna Dördelmann, Boris Schmitz, Bianca Schröer, Friedericke Bruns, Dr. Ralph Telgmann, Christine Fabritius, Karin Tegelkamp, Margit Käse und insbesondere Frau Dr. Sandra Hasenkamp aus der AG Prof. Dr. Brand. Vielen, vielen Dank für die tolle Zusammenarbeit und das super Klima der letzten drei Jahre, sowie für viele anregende Diskussionen und Ideen. Ihr seid spitze. Besonders herzlich möchte ich an dieser Stelle Corinna Dördelmann danken, mit der ich von Anfang an alle Höhen und Tiefen gemeistert habe. Du wirst mir sehr fehlen. Mein ganz besonderer Dank gilt auch Dr. Ralph Telgmann, der immer an mich geglaubt hat, für seine stetige Bereitschaft für Diskussionen und seine Unterstützung jeglicher Art.

Meinen Freunden, die immer ein aufbauendes Wort mich hatten, sei ganz herzlichst für ihre Unterstützung in jeder Hinsicht und die nötige Ablenkung gedankt. Ich bin froh dass es euch gibt. Nicht zuletzt möchte ich mich bei meiner Familie, insbesondere meinen Eltern bedanken. Liebe Mama, lieber Papa, vielen Dank für die immerwährende Hilfe und Motivation, und dass ihr immer für mich da ward. Ohne Euch wäre ich nie so weit gekommen.

Publikationsliste

Hagedorn C, Telgmann R, Dördelmann C, Schmitz B, Hasenkamp S, Cambien F, Paul M, Brand E, Brand-Herrmann SM. (2009) Identification and functional analyses of molecular haplotypes of the human osteoprotegerin gene promoter. *Hum Mol Genet.* Submitted.

Schmidt-Petersen K, Brand E, Telgmann R, Nicaud V, Hagedorn C, Dördelmann C, Elbaz A, Gautier-Bertand M, Evans A, Kee F, Morrison C, Arveiler D, Stoll M, Amarenco P, Cambien F, Paul M, Brand-Herrmann SM. (2009) Osteopontin Gene variation and cardio/cerebrovascular disease phenotypes. *Atherosclerosis.* In press.

Hillebrand U, Lang D, Telgmann R, Hagedorn C, Stock CM, Wilhelmi M, Oberleithner H, Hausberg M. (2009) Nebivolol increases endothelial cell size and elasticity via the estrogen receptor – a Nano-Imaging Study. *J Hypertens.* In press.

Telgmann R, Dördelmann C, Brand E, Nicaud V, Hagedorn C, Pavenstädt H, Cambien F, Tiret L, Paul M, Brand-Herrmann SM. (2008) Molecular genetic analysis of a human IGF1 promoter P1 variation. *FASEB J.* Epub ahead of print.

Hasenkamp S, Telgmann R, Staessen JA, Hagedorn C, Dördelmann C, Bek M, Brand-Herrmann SM, Brand E. (2008) Characterization and functional analyses of the human G protein-coupled receptor kinase 4 gene promoter. *Hypertension.* 52,737-746.

Dördelmann C, Telgmann R, Brand E, Hagedorn C, Schröer B, Hasenkamp S, Baumgart P, Kleine-Katthöfer P, Paul M, Brand-Herrmann SM. (2008) Functional and structural profiling of the human thrombopoietin gene promoter. *J Biol Chem.* 283,24382-24391.

Kawamura A, Baitsch D, Telgmann R, Feuerborn R, Weissen-Plenz G, Hagedorn C, Saku K, Brand-Herrmann SM, von Eckardstein A, Assmann G, Nofer JR. (2007) Apolipoprotein E interrupts interleukin-1beta signaling in vascular smooth muscle cells. *Arterioscler Thromb Vasc Biol.* 27,610-1617.

Telgmann R, Brand E, Nicaud V, Hagedorn C, Beining K, Schönfelder J, Brink-Spalink V, Schmidt-Petersen K, Matanis T, Vischer P, Nofer JR, Hasenkamp S, Plouin PF, Drouet L, Cambien F, Paul M, Tiret L, Brand-Herrmann SM. (2007) SAH gene variants are associated with obesity-related hypertension in Caucasians: the PEGASE Study. *J Hypertens.* 25,557-564.

Kongressbeiträge

2006

Claudia Hagedorn, Eva Brand, Ralph Telgmann, Katrin Beining, Jacqueline Schönfelder, Klaus Schmidt-Petersen, Verena Brink-Spalink, Viviane Nicaud, Peter Vischer, François Cambien, Laurence Tiret, Martin Paul, Stefan-Martin Brand-Herrmann. SAH gene variants are associated with essential hypertension; the PEGASE Study. 37. Kongress der Gesellschaft für Nephrologie/ 39. Jahrestagung der Deutschen Arbeitsgemeinschaft für klinische Nephrologie, Essen 23.-25.September 2006

2007

Claudia Hagedorn, Ralph Telgmann, Eva Brand, Viviane Nicaud, Stefanie Kurtz, Jacqueline Schönfelder, Corinna Dördelmann, Barbara Knipper, Peter Baumgart, Peter Kleine-Katthöfer, François Cambien, Martin Paul, Stefan-Martin Brand-Herrmann. Identification and functional analyses of molecular haplotypes of the human osteoprotegerin gene promoter in SaOs-2 osteosarcoma cells. 48. Frühjahrstagung der DGPT, Mainz 13.-15. März 2007, Naunyn-Schmiedebergs Archive of Pharmacology 2007; 375, 535. Oral presentation

Claudia Hagedorn, Ralph Telgmann, Eva Brand, Viviane Nicaud, Stefanie Kurtz, Jacqueline Schönfelder, Corinna Dördelmann, Barbara Knipper, Peter Baumgart, Peter Kleine-Katthöfer, François Cambien, Martin Paul, Stefan-Martin Brand-Herrmann. Identification and functional analyses of molecular haplotypes of the human osteoprotegerin gene promoter in SaOs-2 osteosarcoma cells. 73. Jahrestagung der Deutschen Gesellschaft für Kardiologie, Mannheim 12.-14. April 2007. Oral presentation

Claudia Hagedorn, Ralph Telgmann, Eva Brand, Viviane Nicaud, Stefanie Kurtz, Jacqueline Schönfelder, Corinna Dördelmann, Barbara Knipper, Peter Baumgart, Peter Kleine-Katthöfer, François Cambien, Martin Paul, Stefan-Martin Brand-Herrmann. Identification and functional analyses of molecular haplotypes of the human osteoprotegerin gene promoter in SaOs-2 osteosarcoma cells. 17th European Meeting on Hypertension, Mailand 15-19. Juni 2007, Young Investigators' Accomodation Award

Claudia Hagedorn, Ralph Telgmann, Eva Brand, Viviane Nicaud, Stefanie Kurtz, Jacqueline Schönfelder, Corinna Dördelmann, Barbara Knipper, Peter Baumgart, Peter Kleine-Katthöfer,

François Cambien, Martin Paul, Stefan-Martin Brand-Herrmann. Identification and functional analyses of molecular haplotypes of the human osteoprotegerin gene promoter in SaOs-2 osteosarcoma cells. 38. Kongress der Gesellschaft für Nephrologie/ 40. Jahrestagung der Deutschen Arbeitsgemeinschaft für klinische Nephrologie, München 22.-25. September 2007

Claudia Hagedorn, Ralph Telgmann, Eva Brand, Viviane Nicaud, Stefanie Kurtz, Jacqueline Schönfelder, Corinna Dördelmann, Barbara Knipper, Peter Baumgart, Peter Kleine-Katthöfer, François Cambien, Martin Paul, Stefan-Martin Brand-Herrmann. Identification and functional analyses of molecular haplotypes of the human osteoprotegerin gene promoter in SaOs-2 osteosarcoma cells. 13th Annual Meeting of the ECCR, Nizza 10.-12. Oktober 2007, Young Investigators' Accomodation Award. Oral presentation

Claudia Hagedorn, Ralph Telgmann, Eva Brand, Viviane Nicaud, Stefanie Kurtz, Jacqueline Schönfelder, Corinna Dördelmann, Barbara Knipper, Peter Baumgart, Peter Kleine-Katthöfer, François Cambien, Martin Paul, Stefan-Martin Brand-Herrmann. Identification and functional analyses of molecular haplotypes of the human osteoprotegerin gene promoter in SaOs-2 osteosarcoma cells. 31. Wissenschaftlicher Kongress der Deutschen Liga zur Bekämpfung des Hochdrucks/ Deutsche Hypertoniegesellschaft, Bochum 22.-24. November 2007. Posterpreis der Session „Experimentelle Hypertonie-Forschung III, Genexpression"

2008

Claudia Hagedorn, Klaus Schmidt-Petersen, Eva Brand, Ralph Telgmann, Viviane Nicaud, Corinna Dördelmann, Alexis Elbaz, Marion Gautier-Bertrand, Alun Evans, Caroline Morrison, Dominique Arveiler, Monika Stoll, Pierre Amarenco, François Cambien, Martin Paul, Stefan-Martin Brand-Herrmann. Osteopontin gene variation and cardio/cerebrovasculat disease phenotypes. 49. Frühjahrstagung der DGPT, Mainz 11.-13. März 2008, Naunyn-Schmiedebergs Archive of Pharmacology 2008; 377, 482. Oral presentation

Claudia Hagedorn, Klaus Schmidt-Petersen, Eva Brand, Ralph Telgmann, Viviane Nicaud, Corinna Dördelmann, Alexis Elbaz, Marion Gautier-Bertrand, Alun Evans, Caroline Morrison, Dominique Arveiler, Monika Stoll, Pierre Amarenco, François Cambien, Martin Paul, Stefan-Martin Brand-Herrmann. Osteopontin gene variation and cardio/cerebrovasculat disease phenotypes. 18th European Meeting on Hypertension, Berlin 14-19. Juni 2008, Hypertension 2008; 26 Suppl 1

2009

Claudia Hagedorn, Ralph Telgmann, Corinna Dördelmann, Boris Schmitz, Sandra Hasenkamp, François Cambien, Martin Paul, Eva Brand, Stefan-Martin Brand-Herrmann. Identification and functional analyses of molecular haplotypes of the human osteoprotegerin gene promoter. 50. Frühjahrstagung der DGPT, Mainz 10.-12. März 2009, Oral presentation